

# **The role of teashirt 1 during motor neuron development**

Inaugural-Dissertation

to obtain the academic degree

Doctor rerum naturalium (Dr. rer. nat.)

submitted to the Department of Biology, Chemistry and Pharmacy

of Freie Universität Berlin

by

Charlotte Chaimowicz

from Paris, France

December 2015

This work was carried out at the Max-Delbrück Center for Molecular Medicine from December 2011 to December 2015 under the supervision of Prof. Dr. Carmen Birchmeier and Dr. Alistair Garratt.

1st Reviewer: Prof. Dr. Carmen Birchmeier

2nd Reviewer: Prof. Dr. Fritz Rathjen

Date of defense: 01/03/2016

## Acknowledgements

The work presented in this thesis would not have been possible without the help of the following persons.

I would first like to thank Prof. Dr. Carmen Birchmeier for giving me the opportunity to carry out my PhD in her research group. Her expertise and her critical supervision made me a better scientist and helped the project to move forward.

I am grateful to Dr. Alistair Garratt for trusting me with the Tshz1 project and for his valuable advices and support.

I thank Prof. Dr. Fritz Rathjen for being my thesis advisor and for constructive discussions during my PhD committees.

I thank my colleagues for their help, collaboration and feedback on my work, as well as, for the good times at the bench and outside of the lab. I am particularly thankful to Dr. Cyril Chéret for the help with the analysis and discussion of the data. I would also like to thank Dominique Bröhl for carefully reading and editing my thesis, and for helping me multiple times with German translations. I thank Petra Stallerow for her help with the animal husbandry and Carola Griffel for technical assistance at the end of my PhD.

Finally, I would like to thank my family and friends in Paris and in Berlin that supported me through these 4 years of PhD.

## Table of content

|  |           |
|--|-----------|
| <b>1. INTRODUCTION</b>   | <b>1</b>  |
| <b>1.1. FUNCTION OF MOTOR NEURONS</b>  | <b>1</b>  |
| 1.1.1. MOTOR NEURONS CONTROL MUSCLE CONTRACTION                              | 1         |
| 1.1.2. MOTOR NEURON DIVERSITY IN THE SPINAL CORD                             | 1         |
| 1.1.3. INNERVATION OF LIMB MUSCLES   | 3         |
| 1.1.4. INNERVATION OF THE DIAPHRAGM BY PHRENIC NERVES                        | 4         |
| 1.1.5. SPECIFICITY OF CRANIAL MOTOR NERVE INNERVATION                        | 5         |
| 1.1.6. INNERVATION OF THE TONGUE BY THE HYPOGLOSSAL NERVE                    | 7         |
| <b>1.2. DEVELOPMENT OF MOTOR NEURONS</b>                                     | <b>10</b> |
| 1.2.1. SPECIFICATION OF NEURAL TISSUE AND ANTERO-POSTERIOR PATTERNING        | 10        |
| 1.2.2. DORSO-VENTRAL SIGNALS AND THE GENERATION OF THE MOTOR NEURON IDENTITY | 10        |
| 1.2.3. <i>HOX</i> GENES AND SPECIFICATION OF MOTOR NEURON SUBTYPES           | 12        |
| 1.2.4. HINDBRAIN MOTOR NEURON SPECIFICATION                                  | 14        |
| 1.2.5. MOTOR AXON PATHFINDING AND ESTABLISHMENT OF NEUROMUSCULAR JUNCTION    | 14        |
| <b>1.3. THE <i>TEASHIRT</i> GENE FAMILY</b>                                  | <b>15</b> |
| 1.3.1. ROLE OF <i>TSH</i> IN <i>DROSOPHILA</i>                               | 15        |
| 1.3.2. <i>TEASHIRT</i> ORTHOLOGUES IN MICE                                   | 17        |
| 1.3.3. TSHZ1 FUNCTIONS IN VERTEBRATES  | 18        |
| <b>1.4. AIM OF THE STUDY</b>   | <b>19</b> |
| <br>   |           |
| <b>2. MATERIALS AND METHODS</b>  | <b>21</b> |
| <b>2.1. MATERIALS</b>  | <b>21</b> |
| 2.1.1. CHEMICALS   | 21        |
| 2.1.2. BACTERIAL STRAINS   | 21        |
| 2.1.3. ANTIBODIES  | 22        |
| 2.1.4. MOUSE STRAINS   | 23        |
| 2.1.5. SOLUTIONS AND BUFFERS   | 24        |
| 2.1.5.1. Solutions   | 24        |
| 2.1.5.2. Commonly used buffers   | 25        |
| 2.1.5.3. Bacterial culture   | 26        |
| 2.1.5.4. Buffers used for whole-mount <i>in situ</i> hybridization           | 26        |
| 2.1.5.5. Buffers for X-gal staining  | 27        |
| 2.1.5.6. Buffers for immunostaining  | 28        |
| 2.1.5.6.1. Immunohistochemistry on sections                                  | 28        |
| 2.1.5.6.2. Whole-mount diaphragm staining                                    | 28        |
| 2.1.5.6.3. Whole-mount staining of tongues                                   | 29        |
| <b>2.2. METHODS</b>  | <b>29</b> |
| 2.2.1. EXTRACTION AND PURIFICATION OF NUCLEIC ACIDS                          | 29        |
| 2.2.1.1. Isolation of plasmid DNA  | 29        |

## Table of contents

---

|             |  |           |
|-------------|--|-----------|
| 2.2.1.2.    | Isolation of genomic DNA from mouse tissue   | 30        |
| 2.2.1.3.    | Polymerase chain reaction (PCR)  | 30        |
| 2.2.2.      | GENERATION OF RIBOPROBES FOR <i>IN SITU</i> HYBRIDIZATION  | 35        |
| 2.2.3.      | WHOLE-MOUNT <i>IN SITU</i> HYBRIDIZATION   | 35        |
| 2.2.4.      | DISSECTION AND FIXATION OF MOUSE TISSUE  | 37        |
| 2.2.5.      | PREPARATION OF FROZEN SECTIONS   | 37        |
| 2.2.6.      | HEMATOXYLIN-EOSIN STAINING   | 38        |
| 2.2.7.      | X-GAL STAINING   | 39        |
| 2.2.8.      | IMMUNOCHEMISTRY ON SECTION   | 39        |
| 2.2.9.      | WHOLE-MOUNT DIAPHRAGM STAINING   | 39        |
| 2.2.10.     | WHOLE-MOUNT TONGUE STAINING  | 40        |
| 2.2.11.     | IMAGING AND ANALYSIS   | 41        |
| 2.2.11.1.   | Imaging of <i>in situ</i> hybridization, X-gal and HE staining   | 41        |
| 2.2.11.2.   | Confocal imaging   | 41        |
| 2.2.11.3.   | Counting of motor neuronal populations   | 41        |
| 2.2.11.4.   | Branching analysis   | 42        |
| <b>3.</b>   | <b>RESULTS</b>   | <b>43</b> |
| <b>3.1.</b> | <b><i>TSHZ1</i> EXPRESSION IN MOTOR NEURONS</b>  | <b>43</b> |
| 3.1.1.      | RNA EXPRESSION OF <i>TSHZ1</i>   | 43        |
| 3.1.2.      | ANALYSIS OF <i>TSHZ1</i> EXPRESSION IN MOTOR NEURONS   | 45        |
| <b>3.2.</b> | <b>MUTATION OF <i>TSHZ1</i> IN MOTOR NEURONS LEADS TO NEONATAL LETHALITY</b>   | <b>51</b> |
| 3.2.1.      | CONDITIONAL MUTATION OF <i>TSHZ1</i> IN MOTOR NEURONS USING <i>OLIG2<sup>CRE</sup></i> ALLELE                        | 51        |
| 3.2.2.      | <i>TSHZ1<sup>MNA</sup></i> MUTANTS DIE ON THE FIRST DAY AFTER BIRTH  | 53        |
| 3.2.3.      | <i>TSHZ1<sup>MNA</sup></i> MUTANTS DO NOT HAVE MALFORMATION OF THE ORAL CAVITY                                       | 54        |
| 3.2.4.      | THE HYPOGLOSSAL NUCLEUS IS SMALLER AND HYPOGLOSSAL NERVE BRANCHING IS IMPAIRED IN <i>TSHZ1<sup>MNA</sup></i> MUTANTS | 56        |
| 3.2.5.      | THE PHRENIC MOTOR COLUMN IS REDUCED AND PHRENIC NERVE BRANCHING IS IMPAIRED IN <i>TSHZ1<sup>MNA</sup></i> MUTANTS    | 59        |
| 3.2.6.      | OTHER MOTOR COLUMNS ARE NOT AFFECTED IN <i>TSHZ1<sup>MNA</sup></i> MUTANTS   | 63        |
| <b>4.</b>   | <b>DISCUSSION</b>  | <b>65</b> |
| <b>4.1.</b> | <b>IDENTIFICATION OF <i>TSHZ1</i>-EXPRESSING MOTOR NEURONS</b>   | <b>65</b> |
| <b>4.2.</b> | <b><i>TSHZ1</i> EXPRESSION IN MOTOR NEURONS IS REQUIRED FOR FEEDING AND NORMAL BREATHING</b>                         | <b>67</b> |
| <b>4.1.</b> | <b><i>TSHZ1</i> IS NECESSARY FOR SURVIVAL OF HYPOGLOSSAL MOTOR NEURONS AND CORRECT INNERVATION OF THE TONGUE</b>     | <b>68</b> |
| <b>4.2.</b> | <b><i>TSHZ1</i> IS NECESSARY FOR THE SURVIVAL OF PHRENIC MOTOR NEURONS AND CORRECT DIAPHRAGM INNERVATION</b>         | <b>69</b> |
| <b>4.3.</b> | <b>SPECIFIC ROLE OF <i>TSHZ1</i> IN HYPOGLOSSAL AND PHRENIC MOTOR NEURONS</b>  | <b>71</b> |
| <b>4.4.</b> | <b>PERSPECTIVES</b>  | <b>71</b> |

## Table of contents

---

|                                     |           |
|-------------------------------------|-----------|
| <b>5. SUMMARY</b>                   | <b>73</b> |
| <b>6. ZUSAMMENFASSUNG</b>           | <b>74</b> |
| <b>7. REFERENCES</b>                | <b>76</b> |
| <b>8. EIDESSTATTLICHE ERKLÄRUNG</b> | <b>85</b> |

---

## Abbreviations

|                               |                                      |
|-------------------------------|--------------------------------------|
| °C                            | degree Celsius                       |
| AP                            | alkaline phosphatase                 |
| BABB                          | benzyl alcohol / benzyl benzoate     |
| BCIP                          | 5-Bromo-4-chloro-3-indolyl-phosphate |
| Bp                            | base pair                            |
| BSA                           | bovine serum albumin                 |
| BTX                           | bungarotoxin                         |
| cDNA                          | complementary DNA                    |
| ChAT                          | choline acetyltransferase            |
| CNS                           | central nervous system               |
| DAB                           | 3,3'-diaminobenzidine                |
| DAPI                          | 4',6-diamidino-2-phenylindole        |
| DIG                           | digoxigenin                          |
| DMSO                          | dimethylsulfoxide                    |
| DNA                           | deoxyribonucleic acid                |
| dNTP                          | deoxyribonucleotide triphosphate     |
| DTT                           | dithiothreitol                       |
| E                             | embryonic day                        |
| EDTA                          | ethylene diamine tetraacetic acid    |
| <i>et al.</i>                 | <i>et altera</i>                     |
| fw                            | forward                              |
| g                             | gram                                 |
| GFP                           | green fluorescent protein            |
| h                             | hour                                 |
| H <sub>2</sub> O <sub>2</sub> | hydrogen peroxide                    |
| HCl                           | hydrochloric acid                    |
| HMC                           | hypaxial motor column                |
| HRP                           | Horseshoe radish peroxidase          |
| HS                            | horse serum                          |
| Igepal                        | Octylphenoxypolyethoxyethanol        |
| l                             | liter                                |
| LacZ                          | β-galactosidase coding sequence      |
| LB                            | Luria-Bertani medium                 |
| LMCm/l                        | lateral motor column medial/lateral  |

---

|                       |   |
|-----------------------|---|
| M                     | molar   |
| MgCl <sub>2</sub>     | magnesium chloride  |
| min                   | minute  |
| ml                    | milliliter  |
| mM                    | millimolar  |
| MMC                   | medial motor column   |
| MN                    | motor neuron  |
| mRNA                  | messenger ribonucleic acid                                    |
| mQ-H <sub>2</sub> O   | milliQ H <sub>2</sub> O (Millipore)                           |
| NaCl                  | sodium chloride   |
| NaOH                  | sodium hydroxide  |
| NBT                   | nitro blue tetrazolium chloride                               |
| NJM                   | neuromuscular junction  |
| nm                    | nanometer   |
| NTMT                  | alkaline phosphatase buffer                                   |
| nX                    | dorsal motor nucleus of the vagus                             |
| nXII                  | hypoglossal nucleus   |
| ON                    | overnight   |
| P                     | postnatal day   |
| PBS                   | phosphate buffered saline                                     |
| PCR                   | polymerase chain reaction                                     |
| PFA                   | paraformaldehyde  |
| PGC                   | preganglionic column  |
| pH                    | potentium hydrogenii  |
| rev                   | reverse   |
| RNA                   | ribonucleic acid  |
| RNase                 | ribonuclease  |
| rpm                   | rotations per minutes   |
| RT                    | room temperature  |
| SDS                   | sodium dodecyl sulfate  |
| Sp5                   | spinal trigeminal nucleus                                     |
| SSC                   | saline sodium citrate   |
| Tris                  | 2-Amino-2-(hydroxymethyl)-propane-1,3-diol                    |
| Triton X100           | polyethylene glycol p-(1,1,3,3-tetramethylbutyl)-phenyl ether |
| tRNA                  | transfer ribonucleic acid                                     |
| Tshz1 <sup>NULL</sup> | Tshz1 $\Delta/\Delta$   |

---

|                      |  |
|----------------------|--|
| Tshz1 <sup>ΔMN</sup> | Olig2 <sup>Cre/+</sup> ; Tshz1 <sup>flox/Δ</sup> |
| Tween-20             | polyoxyethylene (20) sorbitan monolaurate        |
| U                    | unit   |
| UTR                  | untranslated region                              |
| X-Gal                | 5-bromo-4-chloro-3-indolyl-β-D-galactopyranoside |
| μm                   | microliter                                       |

---

# 1. Introduction

## 1.1. Function of motor neurons

### 1.1.1. Motor neurons control muscle contraction

Movement is essential for the life of animals and humans. There is a broad range of movements: from the simple and vital breathing movements, to the more complex movements such as locomotion or grasping. However, all movements rely on the same physiological process: muscle contraction.

In vertebrates, movement is controlled by several structures in the central nervous system (CNS), i.e. the motor cortex, basal ganglia, the cerebellum, parts of the brainstem and spinal cord. Motor neurons (MNs) relay between the other parts of the CNS and the muscles and are the only neurons able to directly trigger muscle contraction. MNs reside in the CNS, i.e. the brainstem and spinal cord, and send their axons to the periphery to form highly specialized synapses – neuromuscular junctions (NMJ) – on muscle fibers (Kanning et al., 2010). When a motor neuron generates an action potential, the electrical impulse travels quickly along its axon and leads to the release of a neurotransmitter, acetylcholine, in the synaptic cleft. Acetylcholine molecules bind their receptors, which are ligand-gated ion channels, on the postsynaptic muscle fiber. This causes the opening of the ion channel and a sodium ion influx into the muscle fiber, which starts a chain of events that eventually leads to muscle contraction (Kanning et al., 2010).

### 1.1.2. Motor neuron diversity in the spinal cord

Despite the similar output, i.e. muscle contraction, motor neurons are diverse. Motor neurons locate in the ventral part of the spinal cord and innervate different muscle groups. They cluster into motor columns and settle in different medio-lateral positions along the spinal cord according to the muscles they innervate (Fig. 1.1). MNs of the medial motor column (MMC) locate near the midline at all axial levels and innervate axial muscles. MNs that innervate limb muscles cluster in the lateral motor column (LMC) in brachial and lumbar spinal cord. In the thoracic spinal cord, MNs of the hypaxial (HMC) and the preganglionic motor columns (PGC) are positioned, and

innervate the body wall muscles and sympathetic ganglia, respectively. MNs located in these different motor columns express distinct set of transcription factors and therefore have a distinct molecular identity (Table 3 in §1.2.3)(Dasen and Jessell, 2009; Kanning et al., 2010).

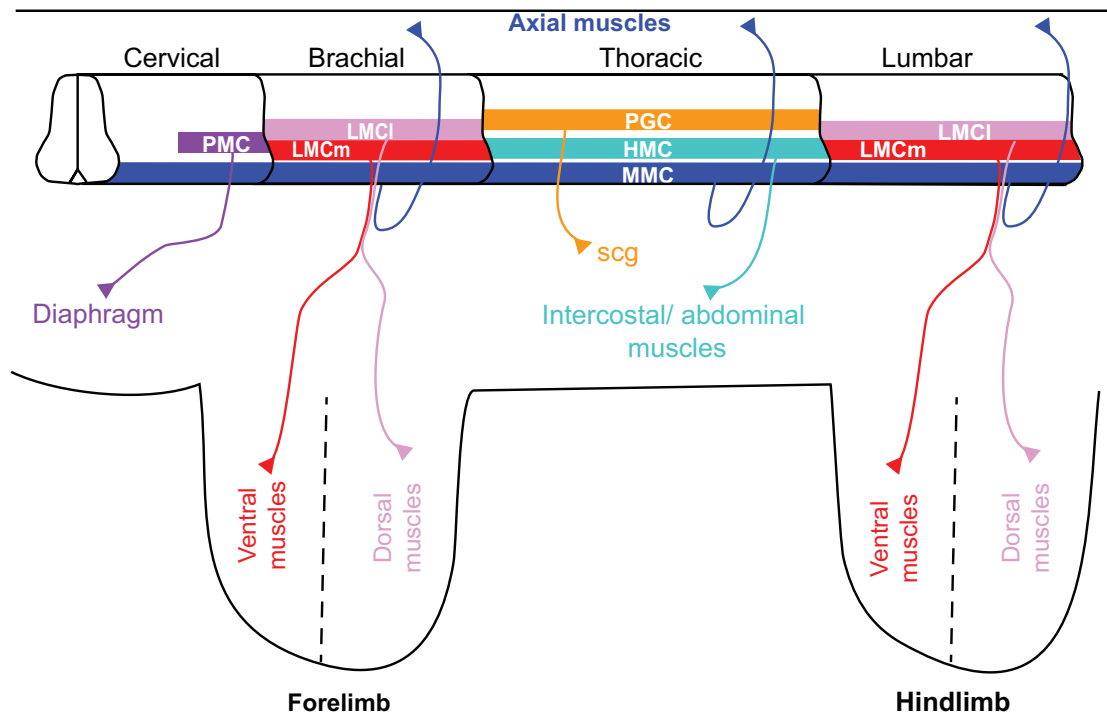


**Figure 1.1 | Motor neuron columnar organization in the spinal cord and muscle targets**

Spinal motor neurons cluster into motor columns (colored boxes) according to the group of muscles they innervate.

At all spinal levels, motor neurons of the medial motor column (MMC, dark blue) innervate the axial muscles of the back. MNs that innervate the diaphragm locate in the phrenic motor column (PMC, purple) in the cervical spinal cord. Motor neurons that innervate the fore- and hindlimbs cluster at brachial and lumbar level in the lateral motor column (LMC). The LMC is further divided into a medial (LMCm, red) and a lateral (LMCI, pink) component that innervate ventral and dorsal muscles of the limbs, respectively. In the thoracic spinal cord, the hypaxial motor column (HMC, cyan) innervate abdominal and intercostal muscles. The preganglionic chain motor column (PGC) innervates neurons of the sympathetic chain ganglia (scg).

### 1.1.3. Innervation of limb muscles

Locomotion is a fundamental motor behavior that allows movement of animals and humans. Walking relies on the activation of several groups of limb muscles in a rhythmic and coordinated manner. Timing, rhythmicity and coordination of movement are controlled by neuronal networks in the spinal cord (central pattern generators) that contact and regulate MN firing (Goulding, 2009; Kiehn, 2006).

Motor neurons that control the contraction of limb muscles locate in the ventro-lateral spinal cord in the brachial and lumbar LMCs. The LMC is further divided into a medial and lateral column, and the corresponding MNs innervate ventral and dorsal limb muscles, respectively. There is an even higher degree of spatial organization: MNs that innervate one skeletal muscle cluster to form a motor pool. Motor pools located in the rostral and caudal LMC innervate proximal and distal limb muscles, respectively, as illustrated in Figure 1.2 (Dasen and Jessell, 2009; Kanning et al., 2010; Rousso et al., 2008; Sürmeli et al., 2011).

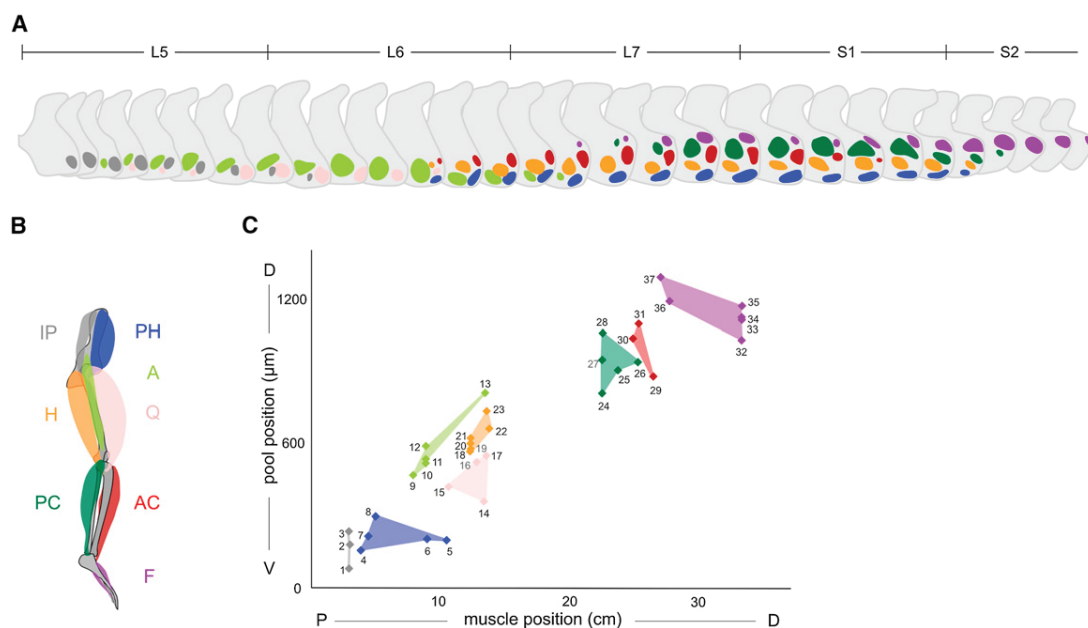


**Figure 1.2 | Motor neuron pool organization in the lumbar spinal cord**

*Taken from Sürmeli et al. 2011*

In this figure, hindlimb muscles and their innervating motor pools are color coded as follows: in dark blue, proximal hip (PH); in gray, iliopsoas (IP); in light green, adductors (A); in pink, quadriceps (Q); in orange, hamstring (H); in red, anterior crural (AC); in dark green, posterior crural (PC); in purple, foot (F).

---

**(A)** Motor pools in cat lumbar (L) and sacral (S) spinal cord. **(B)** The proximodistal organization of muscles in cat hindlimb. **(C)** The dorsoventral (DV,  $\mu\text{m}$ ) positions of motor pools in cat lumbar spinal cord and the proximodistal (PD, cm) positions of muscles in cat hindlimb. Colored fields represent synergy groups, and individual points mark specific motor pools and limb muscles.

#### 1.1.4. Innervation of the diaphragm by phrenic nerves

Mammals use their lungs for breathing. Rhythmicity and coordination of the inspiratory and expiratory phases are controlled by the preBötzinger complex and additional neuron types in the brainstem, that control respiratory muscles via MNs (Bianchi et al., 1995; Garcia et al., 2011). Normal inhalation relies on the diaphragm muscle. When the diaphragm contracts, the thoracic cage expands leading to an influx of air inside the lungs; this is the inspiratory phase. When the diaphragm relaxes, air is exhaled from the lungs; this is the expiratory phase that is passive under normal conditions. However, under high demand like exercise, expiratory muscles in the abdomen actively control expiration.

MNs innervating the diaphragm locate to the phrenic motor column of the cervical spinal cord. Phrenic MN axons exit the spinal cord in cervical nerves on C3 to C5 levels and are then bundled in the phrenic nerve, which projects posteriorly between the lungs and heart to innervate the diaphragm. The phrenic nerve divides into three branches when it reaches the diaphragm: a dorsal, a ventral and one that innervates the crus (Laskowski et al., 1991; Machado et al., 2014) (Fig. 1.3).

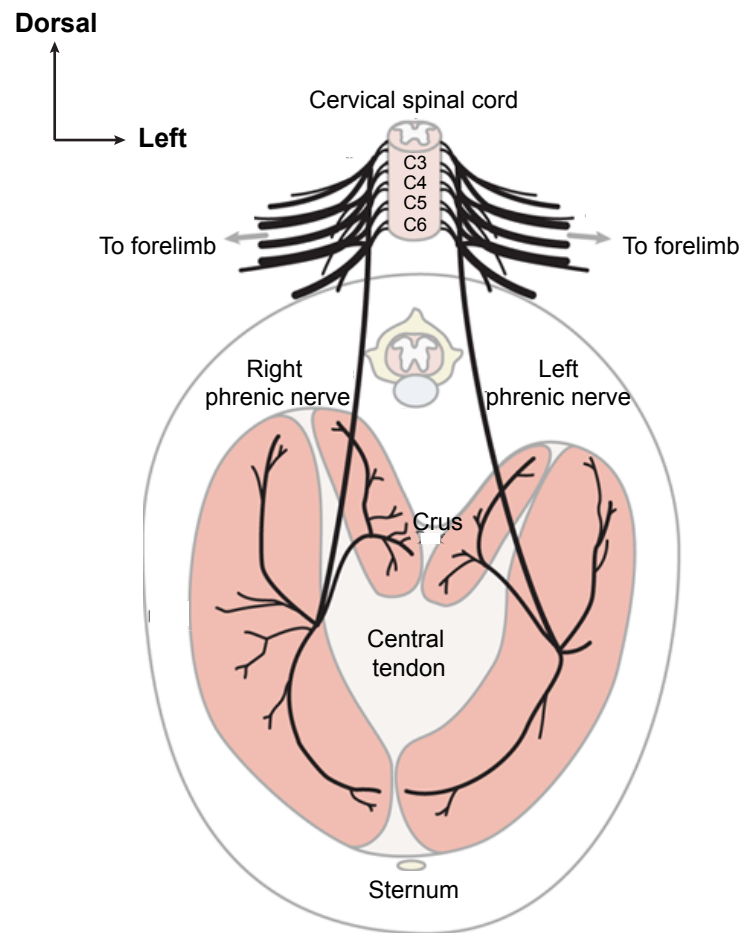


**Figure 1.3 | Diaphragm innervation by the phrenic nerve**

*Adapted from Burgess et al. 2006*

Phrenic nerves contain axons of motor neurons whose cell bodies are located in the cervical spinal cord (C3-C5). When reaching the diaphragm, phrenic nerves divide into three main branches: one ventral branch, one dorsal branch and one branch that innervates the crus of the diaphragm that is located dorsally.

### 1.1.5. Specificity of cranial motor nerve innervation

Cranial motor nerves innervate muscles from the head and the neck and thus control movements of the eyes, tongue, head and neck, which are essential for behaviors like feeding and speech. Cranial motor neurons cluster into different nuclei in the brainstem (Table 1). Cranial motor neurons comprise three subtypes: (1) branchiomotor neurons, which innervate the muscle that derive of the branchial arches; (2) visceromotor neurons, which innervate visceral (i.e. non-striated) muscles

located for instance around the pharynx and (3) somatic motor neurons, which innervate striated voluntary muscles of the face. Cell bodies of viscer- and branchiomotor neurons locate dorsally in the brainstem and their axons exit the brainstem dorsally in large common exit points. In contrast, cell bodies of somatic MNs locate ventrally and their axons exit the brainstem ventrally in small bundles (Fig. 1.4) (Cordes 2001; Guthrie 2007). Cranial nerves often have several motor components as indicated in Table 1. I focused my work on somatic motor neurons and therefore highlighted the somatic motor components of cranial nerves (in orange).

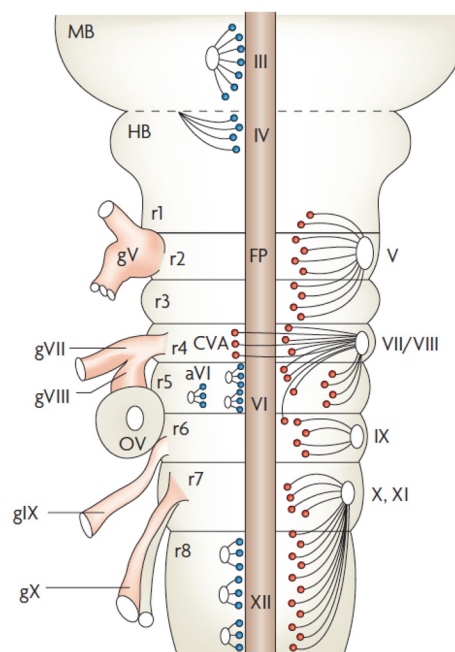


**Figure 1.4 | Motor neuron organization in the mouse hindbrain**

*Taken from Guthrie 2007*

The scheme represents the organization of motor neurons in a flat-mounted mouse brainstem at E11.5. Rhombomere (r) levels are indicated; branchio- and visceromotor neurons are shown in red; somatic motor neurons in blue. Roman numerals alone denote the cranial nerves: III, oculomotor; IV, trochlear; V, trigeminal; VI, accessory abducens; VII/VIII, facial/vestibuloacoustic; IX, glossopharyngeal; X, vagus; XI, cranial accessory; XII, hypoglossal. Roman numerals with the letter g denote the cranial ganglia: gV, trigeminal ganglion; gVII, geniculate ganglion; gVIII, vestibuloacoustic ganglion; gIX, petrosal ganglion; gX, nodose ganglion.

**Table 1 | Motor components of cranial nerves and their targets**

| Nerve      | Subtype       | Nucleus                                 | Target  |
|------------|---------------|---|---|
| III        | Somatic motor | Oculomotor                              | Superior, inferior and medial recti muscles; inferior oblique, levator palpebrae superioris (eye, eyelid) |
|            | Visceromotor  | Edinger-Westphal                        | Ciliary ganglion  |
| IV         | Somatic motor | Trochlear                               | Superior oblique (eye)  |
| V          | Branchiomotor | Trigeminal motor                        | Muscles of mastication, tensor tympani, anterior belly digastric, etc                                     |
| VI         | Somatic motor | Abducens                                | Lateral rectus muscle (eye)   |
| VII        | Branchiomotor | Facial motor                            | Muscles of facial expression, stapedius, posterior belly digastric  |
|            | Visceromotor  | Superior salivatory                     | Pterygopalatine/sphenopalatine ganglion, submandibular ganglion   |
| IX         | Branchiomotor | Nucleus ambiguus                        | Stylopharyngeus muscle  |
|            | Visceromotor  | Inferior salivatory                     | Otic ganglion   |
| X          | Branchiomotor | Nucleus ambiguus                        | Laryngeal and pharyngeal muscles  |
|            | Visceromotor  | Dorsal motor                            | Non-striated muscles of thoracic and abdominal viscera  |
| Cranial XI | Branchiomotor | Nucleus ambiguus                        | Laryngeal and pharyngeal muscles  |
| Spinal XI  | Branchiomotor | Accessory nucleus, cervical spinal cord | Sternocleidomastoid and trapezius muscles   |
| XII        | Somatic motor | Hypoglossal                             | Tongue muscles  |

Adapted from Guthrie, 2007

### 1.1.6. Innervation of the tongue by the hypoglossal nerve

In mammals, the tongue is necessary for vital behaviors like breathing, sound production, suckling, food manipulation and swallowing. Tongue musculature is composed of four extrinsic muscles, which attach the tongue to bony structures – genioglossus, hyoglossus, palatoglossus and styloglossus – and four intrinsic muscles, which locate inside the tongue and have no bone attachment – inferior longitudinalis, superior longitudinalis, transversus and verticalis (McLoon and

Andrade, 2013) (Fig. 1.5). Unlike other striated skeletal muscles, contraction of tongue muscles leads to changes in tongue shape, rigidity or position but not volume. Extrinsic muscles have been associated with movement of the tongue, whereas intrinsic muscles mainly change of the shape of the tongue and participate in tongue protrusion or retrusion (Table 2). However, tongue function is complex and at the end requires the combined action of all eight muscles (McLoon and Andrade, 2013).

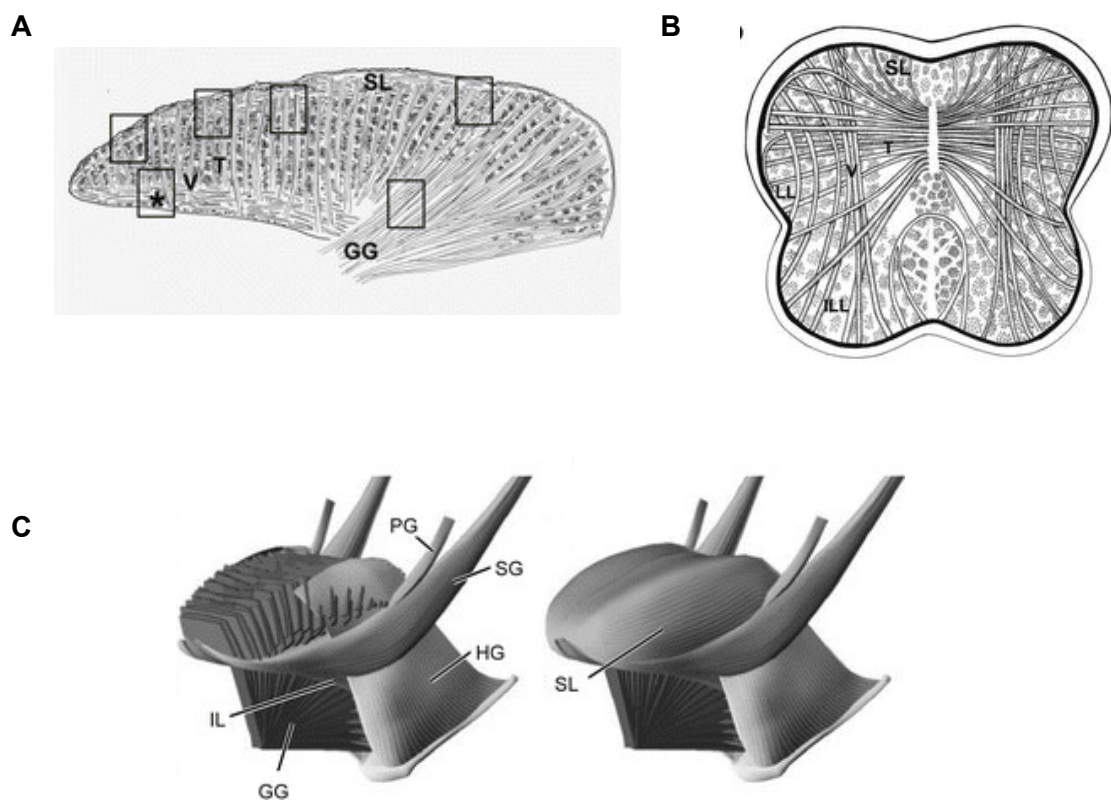


**Figure 1.5 | Tongue musculature**

*Taken from McLoon & Andrade 2013*

Sagittal **(A)** and coronal **(B)** sections of murine tongue showing fiber orientations of different tongue muscles. Extrinsic muscles: *Styloglossus (SG)*, *Genioglossus (GG)*, *Hyoglossus (HG)*, *Palatoglossus (PG)*. Intrinsic muscles: *Verticalis (V)*, *Transversus (T)*, *Inferior longitudinalis (IL)*, *Superior longitudinalis (SL)*. **(C)** Scheme of the organization of muscles at the base of the human tongue.

**Table 2 | Tongue muscles and movements**

|                                 |                         |                                   |
|---------------------------------|-------------------------|-----------------------------------|
| <b>Extrinsic tongue muscles</b> | Genioglossus            | Pulls the tongue forward and down |
|                                 | Hyoglossus              | Pulls the tongue back and down    |
|                                 | Palatoglossus           | Pulls the tongue up and back      |
|                                 | Styloglossus            | Retracts the tongue               |
| <b>Intrinsic tongue muscles</b> | Inferior longitudinalis | Retrusion                         |
|                                 | Superior longitudinalis | Retrusion                         |
|                                 | Transversus             | Protusion                         |
|                                 | Verticalis              | Protusion                         |

The hypoglossal nerve (the cranial nerve number XII) innervates all tongue muscles except the palatoglossus that is innervated by the vagus nerve (cranial nerve X). The hypoglossal nucleus consists of somatic motor neurons, whose cell bodies are located near the midline in rhombomeres 7/8 of the hindbrain. Axons of hypoglossal MNs exit the brainstem ventrally and form the hypoglossal nerve. The hypoglossal nerve projects under the tongue and then branches to innervate the tongue muscles (Guthrie, 2007; Lowe, 1980).

Similarly to spinal MNs, hypoglossal MNs display a precise myotopic organization. MNs of the hypoglossal nucleus cluster according to three criteria: (1) MNs located dorsally supply axons that form the lateral branch of the hypoglossal nerve and innervate the tongue retrusor muscles, while MNs located ventrally supply axons that form the medial branch of the hypoglossal nerve and innervate protrusor muscles. (2) MNs that innervate extrinsic and intrinsic muscles are located in the lateral and medial part of the nucleus, respectively. (3) There is an inverse rostro-caudal topography: rostral hypoglossal MNs project to caudal tongue muscles, while the caudal MNs project toward rostral muscles (Aldes, 1995; Dobbins and Feldman, 1995; McClung and Goldberg, 2002).

## 1.2. Development of motor neurons

### 1.2.1. Specification of neural tissue and antero-posterior patterning

Neural tissue is induced during early embryonic development: after gastrulation, the neural plate becomes morphologically distinct as a thickened layer of epithelial cells. Patterning of the central nervous system is initiated by signaling events that occur during neural plate formation. The anterior neural fate is the 'default' state of ectodermal cells. Neural-inducing proteins (follistatin, chordin and noggin) are expressed by the dorsal mesoderm, bind to proteins of the TGF- $\beta$  (transforming growth factor  $\beta$ ) family (e.g. BMP4, BMP7) and antagonize their epidermal-inducing action. Additionally, in the posterior neural plate, secreted FGF (fibroblast growth factor) ligands induce a posterior neural fate, independently of TGF- $\beta$  signals. Retinoic acid secreted primarily by the caudal paraxial mesoderm and then by the somites is crucial for the specification of spinal cord and of hindbrain rhombomeres 5 to 8 identity. Hence, the rostro-caudal identity of neural tissue is established by the coordinated actions of these different signals. Thus, neural cells in the most anterior part of the neural plate give rise to forebrain structures, and further posterior cells give rise to midbrain, hindbrain and spinal cord (Cowan et al., 1997; Gouti et al., 2015; Harland, 2000).

### 1.2.2. Dorso-ventral signals and the generation of the motor neuron identity

Cells of the neural tube (at the brainstem and spinal cord levels) receive information from gradients of diffusible molecules. The patterning of cell types is organized as Cartesian coordinates along the rostro-caudal and dorso-ventral axes: the position a progenitor cell occupies along these axes defines the amount of inductive signals it will receive, and thus its fate (Alaynick et al., 2011; Cohen et al., 2013; Cowan et al., 1997).

Along the dorso-ventral axis, the spinal cord is divided into six dorsal (pd1-pd6) and five ventral (p0-p3, pMN) progenitor domains. The specification of the most dorsal progenitor domains, pd1-pd3, depends on TGF- $\beta$  and Wnt signals emanating from the roof plate (Alaynick et al., 2011; Helms and Johnson, 2003).

The specification of the ventral progenitor domains results from the gradient of the morphogen Sonic Hedgehog (Shh). Shh protein is primarily secreted by the notochord and then by the floor plate from where it diffuses dorsally and establishes a gradient of activity. According to their distance from the floor plate, progenitor cells receive different concentrations of Shh molecules, which regulate different sets of transcription factors in the progenitor domains that in turn specify distinct neuron types (Fig. 1.6). Transcription factors responding to Shh signaling are classified as class I proteins (Pax7, Dbx1, Dbx2, Irx3 and Pax6) that are repressed by Shh at different concentration thresholds, and class II proteins (Nkx6.1, Nkx6.2, Nkx2.2 and Olig2) that are activated by Shh at different thresholds. Pairs of class I and class II proteins that require similar Shh thresholds for their repression/activation, cross-repress each other and thus establish discrete boundaries between their expression territories. Dorsal and ventral limits of expression of class I and class II transcription factors define the limits of progenitor domains. Hence, each progenitor domain expresses a unique transcription factor code, which determines the identity of differentiating neurons. For instance, motor neuron progenitors (pMNs) that express *Olig2*, *Pax6*, *Nkx6.1* and *Nkx6.2* sequentially generate MNs (E9.5-E13) and oligodendrocyte progenitors (from E12.5)(Briscoe and Ericson, 2001; Cowan et al., 1997; Dessaud et al., 2007; Dias et al., 2014; Jessell, 2000).

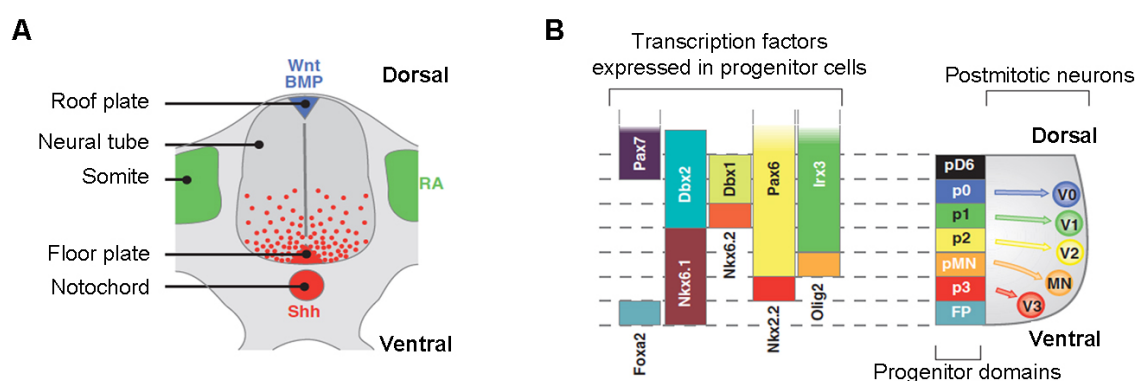


**Figure 1.6 | Secreted signal regulates the spatial expression of transcription factors to establish the dorsal-ventral pattern of progenitors**

*Taken from Dessaud et al. 2008*

In the neural tube, distinct postmitotic neurons are generated in a spatially segregated manner in response to signals emanating within the neural tube and from surrounding tissues. The key signals are represented in (A): Shh (red) is secreted by the notochord and floor plate and spreads from ventral to dorsal to establish a gradient of activity within the ventral neural

tube (red dots); retinoic acid (RA, green) is produced by the somites that flank the neural tube and BMP and Wnt family members (blue) are produced dorsally. **(B)** In the ventral spinal cord, the gradient of Shh activity controls position identity by regulating the expression of a set of transcription factors in neural progenitors. Shh signaling represses class I genes (i.e. *Dbx1*, *Dbx2*, *Pax6* and *lrx3*) and activates class II genes (i.e. *Nkx6.1*, *Olig2*, *Nkx2.2* and *Foxa2*). Selective repressions between pairs of class I and II genes establish distinct ventral and dorsal boundaries in their expression (e.g. *Pax6* and *Nkx2.2*). Each progenitor domain (p0-p3, pMN) is identified by its transcription factor code, and this code determines the neuronal progeny generated. Each progenitor domain generates different ventral interneuron subtypes (V0-V3) or motor neurons (MN).

In pMNs, *Nkx6.1* induces the expression of the homeodomain transcription factor *Hb9*. *Hb9* consolidates the motor neuronal fate and induces the expression of downstream transcription factors which are initially common to all spinal motor neuron subtypes (i.e. *Isl1*, *Isl2*, *Lhx3* and *Hb9*) but that later are expressed only in distinct motor columns. *Isl1* expression is switched on when motor neuron progenitors exit the cell cycle and become postmitotic (Jessell, 2000).

### 1.2.3. *Hox* genes and specification of motor neuron subtypes

Motor neuron progenitors receive signals from the somites (FGF and retinoic acid) and from the floor plate (gradient of Shh) which are necessary to define a general motor neuron identity. However, motor neurons are diverse: motor neurons of different motor columns express distinct sets of transcription factors (Table 3). For instance, phrenic motor neurons express high levels of *Oct6*, *Isl1/2* and low levels of *Hb9* whereas the medial motor column expresses *Lhx3*, *Isl1/2*, low levels of *Oct6* and high levels of *Hb9* (Dasen and Jessell, 2009; Philippidou and Dasen, 2013; Rousso et al., 2008).

*Hox* genes represent a family of homeodomain transcription factors crucial for body patterning. Differential expression of *Hox* genes is responsible for the motor neuron diversity along the rostro-caudal axis. In mice and humans, 39 *Hox* genes exist that are organized in four clusters (*HoxA* to *HoxD*), and the four clusters are located on different chromosomes. There are 13 distinct *Hox* gene paralogues (*Hox1* to *Hox13*), and paralogues are found in each of the four clusters, but no cluster contains all 13 genes. In the central nervous system, *Hox* genes are induced by a gradient of FGF, and their pattern of expression correlates with their position inside a *Hox* cluster: genes located at the 3' end of the cluster are expressed more anteriorly (high FGF)

than genes at the 5' end (low FGF). As a consequence, *Hox1-Hox5* paralogues are expressed in the hindbrain, and *Hox4-Hox8* in brachial, *Hox8-Hox9* in thoracic and *Hox10-Hox13* in lumbar spinal cord (Dasen and Jessell, 2009; Philippidou and Dasen, 2013). Hence combinatorial expression of *Hox* genes in postmitotic MNs can contribute to distinct columnar and motor pool fate. Cross-repressive interactions between *Hox* genes specify rostro-caudal boundaries of motor columns and, at a same axial level, motor pool formation (Dasen and Jessell, 2009; Dasen et al., 2003; Dasen et al., 2005). For instance, cross-repressive actions between *Hox6* and *Hox9* are the key to specify brachial LMC versus thoracic preganglionic motor neuron fate. Cross-repression between *Hox9* and *Hox10* specifies the boundary between preganglionic and lumbar LMC motor neurons (Dasen et al., 2003). In the brachial spinal cord, *Pea3*-expressing MNs require *Hoxc8* and *Hoxc6* to form a defined motor pool.

**Table 3 | Molecular markers of motor neuron subtypes**

| Motor neuron subtype | Molecular markers  |
|----------------------|--|
| MMC                  | Lhx3, Hb9, Isl1, Isl2, Oct6 <sup>low</sup>   |
| Phrenic MNs          | Oct6 <sup>high</sup> , Isl1, Isl2, Hb9 <sup>low</sup>                              |
| LMCm                 | Foxp1, Isl1, Isl2, Hb9 <sup>low</sup> , Raldh2, Oct6 (only in a caudal motor pool) |
| LMCI                 | Foxp1, Isl2, Hb9, Raldh2   |
| PGC                  | Foxp1, Isl1, Hb9 <sup>low</sup> , nNOS   |

*Hox* gene expression in the CNS is not confined to motor neurons and, therefore, co-factors such as *Foxp1* (forkhead protein 1) are necessary to restrict their role in MNs. *Foxp1* is required to specify preganglionic and lateral motor columns that are *Hox*-dependent: in *Foxp1* mutants, LMC and PGC motor neurons acquire a MMC identity and innervate MMC muscle targets (Rousso et al., 2008).

#### 1.2.4. Hindbrain motor neuron specification

The specification of hindbrain and spinal motor neurons share similarities. First, a Shh gradient emanating from the notochord and the floor plate establishes distinct progenitor domains. In the hindbrain, the p3 domain that flanks the floor plate expresses the transcription factors *Nkx2.2*, *Nkx2.9*, *Nkx6.1* and *Nkx6.2*, and gives rise to branchiomotor and visceromotor neurons. The pMN domain expresses *Pax6*, *Olig2*, *Nkx6.1* and *Nkx6.2*, and gives rise to somatic motor neurons. Branchiomotor and visceromotor neurons are characterized by the expression of the transcription factors *Isl1*, *Phox2b*, *Phox2a* and *Tbx20*. In contrast, somatic MNs express the transcription factors *Hb9*, *Isl1*, *Isl2*, *Lhx3* and *Lhx4* (Cordes, 2001; Guthrie, 2007).

In the hindbrain, *Hox* genes control segmentation and rhombomere identity. The anterior limits of *Hox* gene expression domains correspond to rhombomere (r) boundaries: *Hox2*, 3 and 4 expression domains end at the limit between r2-r3, r4-r5 and r6-r7, respectively (Guthrie, 2007). *Hox5* paralogues are also expressed in rhombomere 8. In addition, *Hox* genes play a role in hindbrain motor neuron specification, and in the acquisition of the expression of characteristic transcription factors. For instance, *Hox3* genes regulate the differentiation of the somatic abducens MNs (r5); in *Hoxa3/Hoxb3* double mutant, abducens MNs are lost (Gaufo et al., 2003; Guthrie, 2007).

#### 1.2.5. Motor axon pathfinding and establishment of neuromuscular junction

Somatic motor axons exit the brainstem and spinal cord ventrally and travel a long way to contact muscle fibers. The motor axon senses guidance cues provided by intermediate targets that lie on the way to the muscle. Guidance mechanisms involved in motor axon pathfinding are similar to the ones described for other neuron types (e.g. GDNF/Ret, Ephrin/eph, Cxcl12/Cxcr4) (Bonanomi and Pfaff, 2010). For instance, the cytokine ligand Cxcl12, expressed by mesenchymal cells flanking the hindbrain and spinal cord, guides *Cxcr4*-expressing motor axons to exit the neural tube ventrally (Lieberam et al., 2005). Recent work highlighted that motor axons need to reach their intermediate targets on time, and are programmed to die otherwise. Indeed, in *Fz3* mutant mice axonal growth defects observed in several MN populations (hypoglossal, phrenic and LMCI motor neurons) led to programmed cell

death (i.e. apoptosis) two days before motor axons reach their muscle (Hua et al., 2013).

When reaching the target muscle, the motor axon releases the protein Agrin. Agrin molecules bind to the tyrosine kinase receptor MuSK, which activates signaling pathways leading to clustering of synaptic proteins (e.g. AchR, rapsin) and formation of the neuromuscular junction (Bloch-Gallego, 2015; Burden, 1998; Wu et al., 2010).

Muscle fibers are primarily contacted by several motor axons. However, to be functional, one muscle fiber must form a neuromuscular junction with only one motor axon. Therefore, some neuromuscular junctions are consolidated and others eliminated. Motor neurons whose axon does not contact a muscle fiber are eliminated by programmed cell death. The developmental apoptosis wave occurs around E13-E14 in mouse embryos and eliminates up to 50% of motor neurons (Dekkers et al., 2013; Yamamoto and Henderson, 1999).

### 1.3. The *teashirt* gene family

*Teashirt* genes encode an evolutionarily conserved family of zinc finger transcription factors. They contain three atypical zinc finger motifs (*teashirt* zinc finger motif, CX<sub>2</sub>CX<sub>12</sub>HMX<sub>4</sub>H) that are characterised by a five amino acid spacing between histidine residues; the typical spacing consists of three amino acids. Additionally, *teashirt* zinc fingers are widely spaced, which is unusual for zinc fingers. Teashirt proteins possess in the N-terminus an acidic domain and a five amino acid consensus sequence for recruitment of the co-repressor CtBP (C-terminal binding protein, motif: PLDLS in drosophila, PIDLT in vertebrates) (Caubit et al., 2000; Fasano et al., 1991; Manfroid et al., 2004; Santos et al., 2010). *Teashirt* zinc finger motifs are also found in a more recently discovered gene in Drosophila called *Tiptop* (Santos et al., 2010).

#### 1.3.1. Role of *Tsh* in Drosophila

*Tsh*, founding member of the *teashirt* family, was discovered in Drosophila by random integration of a reporter element in the *teashirt* locus (enhancer trap strategy). The reporter was expressed during embryogenesis in the thoracic part of the trunk,

---

internal tissues, central and peripheral nervous systems and the somatic mesoderm (Fasano et al., 1991). Subsequent loss- and gain-of-function studies in *Drosophila* established that *Tsh* is as key regulator of trunk patterning (Fasano et al., 1991) and is required for midgut morphogenesis (Mathies et al., 1994) and development of the proximal part of the adult appendages (Erkner et al., 1999). In addition, *Tsh* induces eye formation when ectopically expressed (Pan and Rubin, 1998).

*Tsh* acts as a homeotic gene during *Drosophila* development: loss-of-function mutation induced the thorax and abdomen to acquire an anterior head identity (Röder et al., 1992). *Tsh* cooperates with the Hox protein Sex combs reduced (*Scr*, which is the homologue of *Hoxa5* in mice) to repress head identity and thus establish prothorax identity. *Tsh* directly interacts with *Scr* via its N-terminal acidic domain (de Zulueta et al., 1994; Taghli-Lamalle et al., 2007). The *Tsh/Scr* complex represses transcription of the *modulo* gene by directly binding of *Tsh* to a cis-regulatory element of *modulo* (Alexandre et al., 1996; Taghli-Lamalle et al., 2007).

*Tsh* also modulates *wingless* (*Wg*, homologue of *Wnt* in mouse) signalling during establishment of cuticles in the trunk of *Drosophila* (Gallet et al., 1998; Gallet et al., 1999). *Tsh* is necessary to maintain late target genes of *Wg* signalling in the trunk, including *Wg* itself. Armadillo (*Arm*, homologue of the mammalian  $\beta$ -catenin gene) is a central player in *Wg* signalling. In absence of *Wg*, *Arm* locates in the cytoplasm, can be ubiquitinated and is then degraded by the proteasome. Upon *Wg* signalling, *Arm* is stabilized, translocates to the nucleus where it binds to the transcription factor pangolin (also known as Tcf, T-cell factor in mammals) to activate downstream genes (Kühl, 2003). *Wg* signalling induces *Tsh* phosphorylation and its subsequent nuclear accumulation. In the nucleus, *Tsh* binds the C-terminal end of *Arm* protein and the complex directly regulates expression of specific trunk target genes of *Wg* signalling (Gallet et al., 1998; Gallet et al., 1999). Another study established that *ultrabithorax* repression upon *Wg* signalling in the midgut requires *Tsh*. Indeed, high *Wg* levels induce local expression of *Tsh*, *Tsh* protein is recruited in a complex with Brinker and the co-repressor CtBP to the promoter of *ultrabithorax* (Saller et al., 2002; Waltzer et al., 2001).

### 1.3.2. *Teashirt* orthologues in mice

Three orthologues of *Drosophila Tsh* (*Tshz1*, *Tshz2* and *Tshz3*) have been identified by sequence homology in the mouse (Caubit et al., 2000; Manfroid et al., 2004). In addition to the *teashirt* zinc finger motifs, murine *teashirt* proteins contain a homeodomain and two classical zinc fingers in their C-termini. Despite a conservation in amino acid sequence of only 35% between *Drosophila* and mouse *teashirt* genes (the homology is limited to the *teashirt* zinc finger and acidic domains), the expression of any murine *teashirt* protein rescues *Tsh* loss-of-function in *Drosophila*. This indicates that murine *teashirt* proteins are functionally equivalent to *Drosophila Tsh* (Caubit et al., 2000; Manfroid et al., 2004).

During mouse development, expression patterns of *Tshz1*, *Tshz2* and *Tshz3* are similar but not entirely overlapping. For instance, all *Tshz* genes are expressed in the dorsal spinal cord during embryonic development and in the forebrain. However, only *Tshz1* is expressed in the first and second branchial arches and in interdigit areas of the paw (Caubit et al. 2000; Manfroid et al. 2004; Caubit et al. 2005; personal observations). Mutant alleles of all three *Tshz* genes have been developed to investigate their roles in vertebrate development. Several essential functions of *Tshz1* have been described and since my thesis concentrates on the analysis of *Tshz1* mutants I devote to these an entire chapter (§1.3.3). *Tshz2* mutant mice are viable and fertile but were not studied further (unpublished observations from Prof. Garratt and Dr. Rocca). As yet, *Tshz3* is the most intensely studied member of the *teashirt* family in mice.

*Tshz3* mutant mice fail to initiate breathing due to a major loss of motor neurons of the nucleus ambiguus and an altered rhythmogenesis in the embryonic parafacial respiratory group (Caubit et al., 2010). In addition, *Tshz3* mutant mice have hydronephrosis i.e. too much urine in the bladder, that results in a swollen kidney. This is due to an incomplete differentiation of smooth muscle cells of the ureter. During smooth muscle differentiation, *Tshz3* acts downstream of Shh and BMP4 and is required for *myocardin* expression (Caubit et al., 2008). *Tshz3* physically interacts with Sox9 via its N-terminal acidic domain. The *Tshz3*/Sox9 complex binds to *myocardin* protein and reduces its activity to regulate the timing of smooth muscle differentiation (Martin et al., 2013). *Tshz3* is also involved in skeletal muscle differentiation. *Tshz3* is expressed in quiescent and activated satellite cells, and overexpression of *Tshz3* in C2C12 cells leads to an inhibition of myogenic

differentiation, a downregulation of *myogenin* and a subsequent upregulation of *Pax7* expression. *Tshz3* interacts with BAF57, a protein of the chromatin remodelling complex SWI/SNF, and this interaction is required for *myogenin* inhibition (Faralli et al., 2011).

### 1.3.3. *Tshz1* functions in vertebrates

Mutation of *Tshz1* in mice (*Tshz1*<sup>NULL</sup>) leads to perinatal lethality and causes multiple developmental defects. *Tshz1*<sup>NULL</sup> animals do not feed, gasp and have their intestines filled with air bubbles (aerophagia). Coré and her colleagues explained the aerophagia and the absence of milk in the pups' stomach by malformations of the oral cavity. The soft palate of *Tshz1*<sup>NULL</sup> mice is absent and the epiglottis appears malformed. Hence, such animals have a premature and enlarged entrance to the pharynx. *Tshz1*<sup>NULL</sup> animals also display skeletal abnormalities, such as defects of middle ear elements (i.e. a shorter tympanic ring and the malleus bone lacking manubrium and processus brevis components) and a fusion phenotype of cervical vertebrae that is not fully penetrant (Coré et al., 2007).

A study conducted in our laboratory established that *Tshz1* is necessary for the development of the olfactory bulb and for olfaction (Ragancokova et al., 2014). A conditional mutation of *Tshz1* (*coTshz1*) specifically in the central and peripheral nervous system (recombination induced by *Nestin*<sup>Cre</sup>) allows survival of 30% of *coTshz1* animals to adulthood and allowed examination of *Tshz1* functions in olfactory bulb neurogenesis during development and the adult. In *coTshz1* mice, neuroblasts are generated and able to migrate tangentially in the rostral migratory stream. However, in the olfactory bulb, the rostral migratory stream is enlarged, neuroblasts retain *doublecortin* expression and fail to switch on *NeuN*, a postmitotic marker. Hence, neuroblasts are not able to exit the rostral migratory stream, initiate radial migration and differentiate into postmitotic neurons. Multiple olfactory tests revealed that the defects observed in the olfactory bulb of *coTshz1* mice lead to a deficient sense of smell. Microarray and chromatin immunoprecipitation experiments showed that *Tshz1* activates *PKR2* (prokinesin receptor 2) expression via direct binding of *Tshz1* to an intronic sequence of *PKR2* (Ragancokova et al., 2014).

A recent study also found a role of *Tshz1* in the maturation of pancreatic  $\beta$ -cells. *Tshz1* is a direct target of *Pdx1*, a homeodomain transcription factor that is essential

for pancreas organogenesis,  $\beta$ -cell specification and their postnatal function. Endocrine precursor cells are specified in *Tshz1*<sup>NULL</sup> embryos, however critical regulators for formation and function of  $\beta$ - (*Pdx1* and *Nkx6.1*) and  $\alpha$ - (*MafB* and *Arx*) cells are downregulated. Adult animals heterozygous for *Tshz1* develop glucose intolerance due to deficits in glucose-stimulated insulin secretion (Raum et al., 2015).

Haploinsufficiency of the *TSHZ1* gene was observed in human patients and causes phenotypes that resemble those observed in *Tshz1*<sup>NULL</sup> mice. Indeed, *TSHZ1* was associated with congenital aural atresia (absence of an ear canal leading to deafness) and intellectual disabilities (Feenstra et al., 2011). These patients display in addition a deficit in olfaction (Ragancokova et al., 2014). More recently, *TSHZ1* haploinsufficiency was associated with cleft palate formation in the context of Peters plus syndrome (congenital condition characterized by eye abnormalities, short stature, opening in the lip and the roof of the mouth, distinctive facial features, and intellectual disability) (Conte et al., 2015).

#### 1.4. Aim of the study

*Tshz1* is strongly expressed in the central nervous system of the mouse during development and into adulthood. A previous study compiled in the laboratory stated a role of *Tshz1* for neuroblast radial migration and differentiation during adult neurogenesis in the olfactory bulb. However, other functions of *Tshz1* in the CNS remained unknown. During my PhD thesis, I aimed to define a potential role of *Tshz1* during motor neuron development.

I determined a precise spatio-temporal expression pattern of *Tshz1* in motor neurons of the hindbrain and the spinal cord during embryonic and fetal development. I performed *in situ* hybridization with a probe against *Tshz1* mRNA and co-localization studies of GFP expressed from the *Tshz1*<sup>GFP</sup> allele with several motor neuron markers (i.e. *Isl1*, *Oct6*, *ChAT*, *Lhx3*, *Foxp1*, *Phox2b*).

To investigate the role of *Tshz1* in somatic motor neurons, I induced *Tshz1* loss-of-function mutation and introduced recombination using *Olig2*<sup>Cre</sup> (*Tshz1*<sup>MN $\Delta$</sup> ). I verified *Olig2*<sup>Cre</sup> recombination pattern by introducing a *Rosa26R-LacZ* reporter allele and detecting  $\beta$ -galactosidase (the protein product of *LacZ*) by immunohistology and the use of a colorimetric reaction with its substrate X-Gal.

---

To understand the role of *Tshz1* in motor neuron development, I first observed the behavior and analyzed the anatomy of *Tshz1*<sup>MNΔ</sup> animals at birth. I examined their oral cavity by histological stainings (hematoxylin-eosin). Next, I assessed the integrity of several motor nuclei/columns in *Tshz1*<sup>MNΔ</sup> animals: I stained for motor neurons (Isl1, ChAT and for phrenic motor neurons Oct6) and counted them. Countings of motor neurons in E12.5 mice determined whether MNs were generated in appropriate number. Motor neuron counts at E14.5 and analysis of activated caspase-3 staining determined whether MNs were undergoing cell death. And finally, counts at P0.5 determined the extent of the loss of motor neurons at birth. In addition, I used immunohistological staining with neurofilament (NF200) antibodies and an *Hb9-GFP* allele to visualize and analyze the branching pattern of the hypoglossal and the phrenic nerve that innervate the tongue and the diaphragm, respectively. The data that I collected indicate that hypoglossal and phrenic motor neurons require *Tshz1* to survive and to innervate correctly tongue and diaphragm muscles.

---

## 2. Materials and methods

### 2.1. Materials

#### 2.1.1. Chemicals

All chemicals, enzymes, materials, oligonucleotides and kits for molecular biology were purchased from following companies: Ambion (Austin, USA), Biochrom (Berlin), BD Biosciences (Franklin Lakes, USA), DakoCytomation (Glostrup, DK), Dianova (Hamburg), Gibco (Darmstadt), Invitrogen (Karlsruhe), Marienfeld (Lauda-Königshofen), Molecular Research Center (Cincinnati, USA), MWG Eurofins (Ebersberg), New England Biolabs (Ipswich, USA), PAN-Biotech (Aidenbach), Partec (Münster), PerkinElmer Life Sciences (Boston, USA), Promega (Madison, USA), Roche (Basel, CH), Roth (Karlsruhe), R&D Systems (Minneapolis, USA), Sakura Finetek (Torrance, USA), Serva (Heidelberg), Sigma-Aldrich (St. Louis, USA), Thermo Scientific (Waltham, USA), Qiagen (Hilden), Vector Laboratories (Burlingame, USA).

#### 2.1.2. Bacterial strains

*Escherichia coli* DH10B F- endA1 recA1 galE15 galK16 nupG rpsLΔlacX74  
Φ80lacZΔM15 araD139 Δ(ara,leu)7697 mcrAΔ (mrr-hsdRMS-mcrBC) λ-

Oligonucleotides were synthesized by MWG Eurofins, Ebersberg. All sequences are given in the 5'-3' direction.

| <b>Name</b>              | <b>Sequence 5'-3'</b>         |
|--------------------------|-------------------------------|
| Cre new 1                | GAACGCACTGATTTTCGACCA         |
| Cre new 2                | AACCAGCGTTTTTCGTTCTGC         |
| Tshz1_genot1_sense       | GTTGAGGTGGCCTTGTAAGC          |
| Tshz1_genot1_mut_anti    | AAGTCGTGCTGCTTCATGTG          |
| Tshz1_genot1_wt_anti     | ATTCGCTCTCCTGAATGTCC          |
| Tshz1F_homo_up           | TCCATTCAGTCACTGAGTGGAGTAC     |
| Flox_recomb_anti         | GCTCCAGTGTCAACCTTCAGCCCAA     |
| Flox_homotyping_sense 5' | GAGGATCGAGAGTTCAAAGCCAGCC     |
| flox_alistai_an 5'       | CTTTAGAGCAAGCCAGGGAGTCATC     |
| SAM_wt_up                | ATGCGGTACCTCTTTGGTGCTGTCCCTGC |
| SAM_wt_lw                | CAGACTGTGCTCCACTGTG           |
| SAM_mut_fw               | GAACAAAGCAGCCACTCTC           |
| SAM_mut_rev              | CGACCTGCAGCCCAAGCTGATCC       |
| GFP 1                    | AAGTTCATCTGCACCACCG           |
| GFP 2                    | TCCTTGAAGAAGATGGTGCG          |
| LacZ a                   | TCCCAACAGTTGCGCAGCCTGAATG     |
| LacZ b                   | ATATCCTGATCTTCCAGATAACTGCCG   |

### 2.1.3. Antibodies

| <b>Antigen</b>         | <b>Host animal</b> | <b>Dilution</b> | <b>Source</b>                   |
|------------------------|--------------------|-----------------|---------------------------------|
| GFP                    | rat                | 1:1500          | Nacalai Tesque                  |
| NF200                  | chicken            | 1:5000          | Millipore                       |
| Isl1 (39.4D5 & 40.2D6) | mouse              | 1:400           | DSHB                            |
| Isl1                   | guinea pig         | 1:5000          | T. Jessell (Columbia Univ., NY) |
| Lhx3 (67.4E12)         | mouse              | 1:300           | DSHB                            |
| FoxP1                  | rabbit             | 1:500           | Abcam                           |
| Oct6                   | rabbit             | 1:500           | Abcam                           |
| Olig2                  | rabbit             | 1:500           | Millipore                       |
| ChAT                   | goat               | 1:300           | Chemicon                        |
| Caspase-3, cleaved     | rabbit             | 1:300           | Cell signaling                  |
| $\beta$ -Galactosidase | rabbit             | 1:20000         | Cappell                         |
| Phox2b                 | rabbit             | 1:4000          | J.F. Brunet (ENS, Paris)        |
| Phox2b                 | guinea pig         | 1:2000          | J.F. Brunet (ENS, Paris)        |
| Tshz1                  | guinea pig         | 1:4000          | A.Garratt (MDC, Berlin)         |
| Digoxigenin Fab-AP     | sheep              | 1:2000          | Roche                           |

Secondary antibodies were conjugated with Cy2, Cy3, Cy5 or HRP (Dianova, 0.5mg/ml) or Alexa Fluor 488, 555 and 648 (1:500) (Invitrogen).

DAPI was used at a concentration of 1µg/ml (Roche).

Alexa Fluor 555 conjugated- BTX (Invitrogen) was used at 1:1000.

#### 2.1.4. Mouse strains

##### **Olig2<sup>Cre</sup>**

Olig2<sup>tm1<sup>(cre)</sup>Tmj</sup> (Thomas M. Jessell, Columbia University, New York, USA)

The exon 2 of *Olig2* was replaced with the Cre open reading frame.

(Dessaud et al., 2007)

##### **Tshz1<sup>GFP</sup>**

Tshz1<sup>tm1<sup>Garr</sup></sup> (Alistair Garratt, Charité, Berlin, Germany)

The second exon of *Tshz1* was replaced by the Gap43-GFP coding sequence. This is a null allele.

(Ragancokova et al., 2014)

##### **Tshz1<sup>flox</sup>**

Tshz1<sup>tm2.1<sup>Garr</sup></sup> (Alistair Garratt, Charité, Berlin, Germany)

The second exon of *Tshz1* gene is flanked by loxP sites. Upon expression of Cre recombinase, the exon is deleted and *Tshz1* protein is not produced.

(Ragancokova et al., 2014)

##### **Tshz1 $\Delta$**

Tshz1<sup>tm2.2<sup>Garr</sup></sup> (Alistair Garratt, Charité, Berlin, Germany)

Tshz1<sup>flox</sup> mice were paired a cre-deleter strain to obtain a germline deletion and generate the *Tshz1 $\Delta$*  allele.

(Ragancokova et al., 2014)

##### **Tau-GFP (SAM)**

Mapt<sup>tm2<sup>Arbr</sup></sup> (Silvia Arber, Biowentrum University of Basel, Basel, Switzerland)

A cassette containing loxP-STOP-loxP-mGFP-IRES-NLS-lacZ-pA was inserted into exon 2 of the locus. mGFP consists of the first 40 amino acids of the protein MARCKS, a plasmalemmal targeting sequence, fused to enhanced GFP (eGFP).

(Hippenmeyer et al., 2005)

**Hb9-GFP**

Tg(Hlx9-GFP) (Thomas M. Jessell, Columbia University, New York, USA)

The transgenic construct contains a 9kb sequence of the 5' portion of the mouse *Hb9* gene, a Green Fluorescent Protein (GFP) open reading frame, and a bovine growth hormone polyadenylation site sequence.

(Wichterle et al., 2002a)

**Rosa26R-LacZ**

Gt(ROSA)26Sor<sup>tm1Sor</sup> (Philippe Soriano, Mount Sinai, New York, USA)

A targeting vector was designed from the original gene trap strain, ROSA beta-geo26, to include a splice acceptor sequence (SA), a neo expression cassette flanked by loxP sites, a lacZ gene, and a polyadenylation (bpA) sequence inserted at a unique Xba1 site approximately 300-bp 5' of the original gene-trap integration site. In addition, a triple polyadenylation sequence was added to the 3' end of the neo expression cassette to prevent transcriptional read-through. Presence of the floxed neo cassette prevents lacZ expression. When crossed with a cre transgenic strain, lacZ is expressed in all cells/tissue where Cre is expressed.

(Soriano, 1999)

**2.1.5. Solutions and buffers****2.1.5.1. Solutions****PBS**

8 g NaCl  
0.2 g KCl  
1.44 g Na<sub>2</sub>HPO<sub>4</sub>  
0.24 g KH<sub>2</sub>PO<sub>4</sub>  
mQ-H<sub>2</sub>O to 1000 ml

**PBT**

0.1% Tween-20 in PBS

**PBX**

0.1% Triton-X in PBS

**1M Na<sub>2</sub>HPO<sub>4</sub>**177.95 g in 1000 ml mQ-H<sub>2</sub>O**1M NaH<sub>2</sub>PO<sub>4</sub>**156.01 g in 1000 ml mQ-H<sub>2</sub>O**4M NaOH**160 g NaOH in 1000 ml mmQ-H<sub>2</sub>O**0.5M EDTA pH 8.0**146.1 g EDTA in 1000 ml mQ-H<sub>2</sub>O, pH adjusted with NaOH**1M MgCl<sub>2</sub>**203.3 g MgCl<sub>2</sub> in 1000 ml mQ-H<sub>2</sub>O**5M NaCl**292.2 g NaCl in 1000 ml mQ-H<sub>2</sub>O**1M Tris pH 7.4/ pH 7.5/ pH 8.0/ pH 8.5/ pH 9.5**211.9 g Tris in 1000 ml mQ-H<sub>2</sub>O**10% SDS**10 g SDS in 100 ml mQ-H<sub>2</sub>O**2.1.5.2. Commonly used buffers****0.2M Sodium phosphate buffer (2x)**1M Na<sub>2</sub>HPO<sub>4</sub> .....154.8 ml1M NaH<sub>2</sub>PO<sub>4</sub> .....45.0 mlmQ-H<sub>2</sub>O to 1000 ml (**pH 7.4**)**4% Paraformaldehyde (PFA)**

paraformaldehyde (Roth) .....20 g

0.2M sodium phosphate buffer .....250 ml

mQ-H<sub>2</sub>O to 500 ml (**pH 7.4**, adjusted with NaOH)

**Tail lysis buffer**

|                               |       |
|-------------------------------|-------|
| 1M Tris pH 8.5 .....          | 10 ml |
| EDTA 0.5M pH 8 .....          | 1 ml  |
| SDS 10% .....                 | 2 ml  |
| 5M NaCl .....                 | 4 ml  |
| mQ-H <sub>2</sub> O to 100 ml |       |

**2.1.5.3. Bacterial culture****LB medium**

|  |      |
|--|------|
| NaCl .....                                 | 10 g |
| Bacto-Tryptone .....                       | 10 g |
| Bacterial extract .....                    | 5 g  |
| mQ-H <sub>2</sub> O to 1000 ml (pH 7.5)    |      |
| Ampicillin – final concentration 100 µg/ml |      |

**2.1.5.4. Buffers used for whole-mount *in situ* hybridization****10x TBS-T**

|                               |        |
|-------------------------------|--------|
| NaCl .....                    | 8.8 g  |
| KCl .....                     | 0.2 g  |
| 1M Tris pH 7.4 .....          | 2.5 ml |
| Tween-20 .....                | 1.5 ml |
| mQ-H <sub>2</sub> O to 100 ml |        |

*1xTBS-T is not stable at room temperature over long-term.*

**20x SSC**

|                                |         |
|--------------------------------|---------|
| NaCl .....                     | 175.2 g |
| Na-citrate .....               | 88.2 g  |
| mQ-H <sub>2</sub> O to 1000 ml |         |

**Hybridization solution** (*Store at -20°C*)

|   |        |
|---|--------|
| Formamid .....                                    | 50 ml  |
| 20xSSC .....                                      | 25 ml  |
| Heparin (100 mg/ml) .....                         | 40 µl  |
| tRNA (50 mg/ml in water)* .....                   | 100 µl |
| salmon sperm DNA (10 mg/ml)* .....                | 1 ml   |
| Tween-20 .....                                    | 150 µl |
| 1M citric acid .....                              | 6 ml   |
| mQ-H <sub>2</sub> O to 100 ml ( <b>pH 4,5-5</b> ) |        |

\*Before adding, denature heat tRNA and ssDNA at 95 °C for 10 min.

**Solution I** (*Store at -20°C*)

|                               |         |
|-------------------------------|---------|
| Formamid .....                | 125 ml  |
| SSC 20x .....                 | 62.5 ml |
| Tween-20 .....                | 375 µl  |
| mQ-H <sub>2</sub> O to 250 ml |         |

**Solution III** (*Store at -20°C*)

|                               |        |
|-------------------------------|--------|
| Formamid .....                | 125 ml |
| SSC 20x .....                 | 25 ml  |
| Tween-20 .....                | 375 µl |
| mQ-H <sub>2</sub> O to 250 ml |        |

**NTMT**

|   |         |
|---|---------|
| 5M NaCl .....                                   | 5 ml    |
| 1M Tris pH9,5 .....                             | 25 ml   |
| 1M MgCl <sub>2</sub> .....                      | 12.5 ml |
| Tween20 .....                                   | 375 µl  |
| mQ-H <sub>2</sub> O to 250 ml ( <b>pH 9.5</b> ) |         |

**2.1.5.5. Buffers for X-gal staining****X-gal** (*Store at -20°C*)

50 mg/ml in Dimethylformamide

**LacZ Fixative solution**

|                            |      |
|----------------------------|------|
| 1M MgCl <sub>2</sub> ..... | 1 ml |
| 200 mM EGTA (pH 7.3) ..... | 5 ml |
| PBS to 500 ml              |      |

*Add 40 µl of Glutaraldehyde 25% for 5 ml of LacZ Fixative*

**LacZ wash buffer**

|                                 |      |
|---------------------------------|------|
| 1% sodium deoxycholate solution | 5 ml |
| 2% NP40 (IGEPAL CA-630)         | 5 ml |
| 1M MgCl <sub>2</sub> .....      | 1 ml |
| 200 mM EGTA (pH 7.3) .....      | 5 ml |
| PBS to 500 ml                   |      |

**LacZ stain buffer**

|                                     |        |
|-------------------------------------|--------|
| 200 mM Potassium ferrocyanide ..... | 250 µl |
| 200 mM Potassium ferricyanide ..... | 250 µl |
| X-gal .....                         | 200 µl |
| LacZ Wash buffer to 10 ml           |        |

**2.1.5.6. Buffers for immunostaining****2.1.5.6.1. Immunohistochemistry on sections****DAPI (1000x)**

1 mg/ml in PBS/ 50% glycerol

**2.1.5.6.2. Whole-mount diaphragm staining****0.1M glycine**

0.7506 g of glycine in PBS

**Diaphragm Blocking Buffer**

|                                   |             |
|-----------------------------------|-------------|
| NaCl .....                        | 1.461 g     |
| BSA .....                         | 1.5 g       |
| Heat inactivated goat serum ..... | 2.5 ml      |
| Triton X .....                    | 500 $\mu$ l |
| PBS to 50 ml                      |             |

**2.1.5.6.3. Whole-mount staining of tongues****Dent's fixative**

|                |       |
|----------------|-------|
| DMSO .....     | 20 ml |
| Methanol ..... | 80 ml |

**Dent's bleach**

|  |       |
|--|-------|
| 30% H <sub>2</sub> O <sub>2</sub> (Roth) ..... | 10 ml |
| Dent's fixative .....                          | 20 ml |

**Whole-mount Blocking**

|                                   |       |
|-----------------------------------|-------|
| DMSO .....                        | 10 ml |
| Heat inactivated goat serum ..... | 5 ml  |
| PBS to 50 ml                      |       |

**BABB**

|                       |       |
|-----------------------|-------|
| Benzyl alcohol .....  | 10 ml |
| Benzyl benzoate ..... | 20 ml |

**2.2. Methods****2.2.1. Extraction and purification of nucleic acids****2.2.1.1. Isolation of plasmid DNA**

*E.coli* cells containing plasmid were cultured in sterilized LB-medium with ampicillin (100  $\mu$ g/ml) ON at 37°C. Small-scale plasmid preparation was performed using 3ml

---

LB medium of transfected *E. coli*. Isolation was performed according to alkaline lysis method (Birnboim and Doly, 1979). Large-scale plasmid preparation was performed using 250ml LB medium and Plasmid Maxi kit (Qiagen). The concentration and the purity of DNA were determined by nanodrop (Thermo scientific).

#### **2.2.1.2. Isolation of genomic DNA from mouse tissue**

Adult mice or embryos were genotyped using ear and tail biopsies or yolk sac. Tissues were lysed in 50  $\mu$ l of tail lysis buffer containing 1mg/ml proteinase K at 55°C for minimum 3h. Proteinase K was inactivated by incubation at 95°C for 10 min. Samples were diluted with 500 $\mu$ l mQ-H<sub>2</sub>O. 1  $\mu$ l of genomic DNA was used for genotyping.

#### **2.2.1.3. Polymerase chain reaction (PCR)**

Polymerase chain reaction (Saiki et al., 1985) was used to genotype the animals and to amplify cDNA fragments for cloning the *in situ* probe. Primers were designed using Oligo7 software (Molecular Biology Insights) and PCR was performed with a Biometra T3000 thermal cycler.

#### **2.1.1. Genotyping**

##### **PCR conditions and program used to genotype Tshz1-GFP allele**

Primers for WT allele:       Tshz1\_genot1\_sense  
                                  Tshz1\_genot1\_wt\_anti

Primers for mutant allele:   Tshz1\_genot1\_sense  
                                  Tshz1\_genot1\_mut\_anti

Volume of one reaction: 19  $\mu$ l + 1  $\mu$ l genomic DNA

1.5 mM MgCl<sub>2</sub>

3.5% DMSO

0.0935%  $\beta$ -mercaptoethanol

0.5 mM dNTPs (Invitex)

12.5% sucrose

0.146% (NH<sub>4</sub>)<sub>2</sub>SO<sub>4</sub>

0.0042% Cresol Red

4  $\mu$ M of each primer

0.22  $\mu$ l Taq polymerase (Invitrogen)

Program:

|      |          |       |
|------|----------|-------|
| 94°C | 4 min    | } 35x |
| 95°C | 30 s     |       |
| 55°C | 30 s     |       |
| 72°C | 1 min    |       |
| 72°C | 7 min    |       |
| 15°C | $\infty$ |       |

### PCR conditions and program used to genotype Tshz1 $\Delta$ allele

Primers: Flox\_homotyping\_sense 5'

Flox\_alistai\_an 5'

Volume of one reaction: 19  $\mu$ l + 1  $\mu$ l genomic DNA

1.5 mM MgCl<sub>2</sub>

3.5% DMSO

0.0935%  $\beta$ -mercaptoethanol

0.5 mM dNTPs (Invitex)

12.5% sucrose

0.146% (NH<sub>4</sub>)<sub>2</sub>SO<sub>4</sub>

0.0042% Cresol Red

1  $\mu$ M of each primer

0.22  $\mu$ l Taq polymerase (Invitrogen)

Program:

|      |       |       |
|------|-------|-------|
| 94°C | 4 min |       |
| 95°C | 30 s  | } 35x |
| 55°C | 30 s  |       |
| 72°C | 1 min |       |
| 72°C | 7 min |       |
| 15°C | ∞     |       |

### PCR conditions and program used to genotype Tshz1<sup>lox</sup> allele

Primers: Tshz1F\_homo\_up  
Flox\_recomb\_anti

For one reaction (Volume: 19 µl + 1 µl genomic DNA)

|                                  |           |
|----------------------------------|-----------|
| 10X reaction buffer (Invitrogen) | 2 µl      |
| 50mM MgCl <sub>2</sub>           | 0.8 µl    |
| 5mM dNTP                         | 1 µl      |
| 4µM primer                       | 1 µl each |
| Taq polymerase (Invitrogen)      | 0.133 µl  |
| mQ-H <sub>2</sub> O              | 13.1 µl   |

Program:

|      |       |       |
|------|-------|-------|
| 94°C | 1 min |       |
| 94°C | 45 s  | } 35x |
| 65°C | 30 s  |       |
| 72°C | 1 min |       |
| 72°C | 5 min |       |
| 15°C | ∞     |       |

### PCR conditions and program used to genotype Olig2<sup>Cre/+</sup> allele

Primers: Cre new 1  
Cre new 2

Volume of one reaction: 19  $\mu$ l + 1  $\mu$ l genomic DNA

1.5 mM MgCl<sub>2</sub>

3.5% DMSO

0.0935%  $\beta$ -mercaptoethanol

0.5 mM dNTPs (Invitex)

12.5% sucrose

0.146% (NH<sub>4</sub>)<sub>2</sub>SO<sub>4</sub>

0.0042% Cresol Red

1  $\mu$ M of each primer

0.22  $\mu$ l Taq polymerase (Invitrogen)

Program:

|      |          |       |
|------|----------|-------|
| 94°C | 4 min    | } 35x |
| 95°C | 30 s     |       |
| 55°C | 30 s     |       |
| 72°C | 1 min    |       |
| 72°C | 7 min    |       |
| 15°C | $\infty$ |       |

### PCR conditions and program used to genotype *Mapt*<sup>tm2Arbr</sup> (SAM) allele

Primers for WT allele: SAM\_wt\_up  
SAM\_wt\_lw

Primers for mutant allele: SAM\_mut\_fw  
SAM\_mut\_rev

Volume of one reaction: 19  $\mu$ l + 1  $\mu$ l genomic DNA

1.5 mM MgCl<sub>2</sub>

3.5% DMSO

0.0935%  $\beta$ -mercaptoethanol

0.5 mM dNTPs (Invitex)

12.5% sucrose

0.146% (NH<sub>4</sub>)<sub>2</sub>SO<sub>4</sub>

0.0042% Cresol Red

4  $\mu$ M of each primer

0.22  $\mu$ l Taq polymerase (Invitrogen)

Program:

|      |       |       |
|------|-------|-------|
| 94°C | 4 min | } 35x |
| 95°C | 30 s  |       |
| 55°C | 30 s  |       |
| 72°C | 1 min |       |
| 72°C | 7 min |       |
| 15°C | ∞     |       |

### PCR conditions and program used to genotype Hb9<sup>GFP</sup> allele

Primers:                   GFP 1  
                                  GFP 2

Volume of one reaction: 19 µl + 1 µl genomic DNA

1.5 mM MgCl<sub>2</sub>

3.5% DMSO

0.0935% β-mercaptoethanol

0.5 mM dNTPs (Invitex)

12.5% sucrose

0.146% (NH<sub>4</sub>)<sub>2</sub>SO<sub>4</sub>

0.0042% Cresol Red

4 µM of each primer

0.22 µl Taq polymerase (Invitrogen)

Program:

|      |       |       |
|------|-------|-------|
| 94°C | 4 min | } 35x |
| 95°C | 30 s  |       |
| 55°C | 30 s  |       |
| 72°C | 1 min |       |
| 72°C | 7 min |       |
| 15°C | ∞     |       |

### PCR conditions and program used to genotype Rosa26R-LacZ allele

Primers:                   LacZ a  
                                  LacZ b

For one reaction (Volume: 19  $\mu$ l + 1  $\mu$ l genomic DNA)

|  |                |
|--|----------------|
| 10X reaction buffer (Invitrogen) ..... | 2 $\mu$ l      |
| 50mM MgCl <sub>2</sub> .....           | 1.2 $\mu$ l    |
| 5mM dNTP .....                         | 1 $\mu$ l      |
| 4 $\mu$ M primer .....                 | 1 $\mu$ l each |
| Taq polymerase (Invitrogen) .....      | 0.133 $\mu$ l  |
| mQ-H <sub>2</sub> O .....              | 12.8 $\mu$ l   |

Program:

|      |          |       |
|------|----------|-------|
| 94°C | 35 s     | } 38x |
| 65°C | 30 s     |       |
| 72°C | 45 s     |       |
| 15°C | $\infty$ |       |

### 2.2.2. Generation of riboprobes for *in situ* hybridization

A specific DNA fragment of *Tshz1* gene was cloned into pGEM-T Easy plasmid by Dr. A. Garratt. I electroporated the plasmid into electrocompetent *E. Coli* bacteria for amplification (see §2.2.1.1). 5  $\mu$ g of plasmid was linearized with the restriction enzyme *SpeI* (restriction site: ACTAGT) at 37°C in 1h. *In vitro* transcription of the antisense probe was performed using DIG-RNA labeling kit according to manufacturer's instructions (Roche) with the T7 RNA polymerase. 500 ng of plasmid was transcribed at 37°C in 2h. Labeled cRNA was purified using RNeasy Mini Protocol (Qiagen) and eluted in 50  $\mu$ l mQ-H<sub>2</sub>O. The probes were stored in 50% formamide at -80°C.

### 2.2.3. Whole-mount *in situ* hybridization

Whole mount *in situ* hybridization was performed following the core protocol from Cepko/Tabin lab. All steps were performed in a glass tube under agitation.

Embryos were dissected in ice-cold PBS. Ventricles of the brain were pierced with a fine needle and dorsal spinal cord was opened with a scalpel (E10.5-11.5). At E12.5, internal organs were additionally removed. For embryos older than E12.5, only the spinal cord and hindbrain were kept for staining.

Embryos were then fixed overnight in PFA 4% at 4°C. The next day, embryos were washed 2 times for 10 min in PBT. Then, embryos were dehydrated through a series of methanol baths at 4°C (25%, 50%, 75%, 100% methanol in PBT for 15 min each and then 1h in 100% methanol). Embryos were bleached 1h at -20°C in methanol/H<sub>2</sub>O<sub>2</sub> 30% (4:1) and kept at -20°C in 100% methanol.

The first day of the whole-mount *in situ* hybridization *per se*, embryos were rehydrated (75%, 50%, 25% methanol in PBT, for 20 min each) and washed twice for 20 min in PBT. Next, embryos were permeated for 30 minutes with proteinase K (20 µg/mL). Samples were post-fixed with 4% PFA/0.2% glutaraldehyde (20 min at RT). They were equilibrated for 15 min at RT, and pre-hybridized at 65°C between 1 and 3h, in hybridization solution. Embryos were incubated overnight at 65°C in 3 ml of fresh hybridization solution with 12 µl of denatured DIG-labelled Tshz1 riboprobes. Denaturation of the probe was done at 80°C for 10 min, and the probe was then placed on ice for 1 min.

The following day, unattached probes were removed by several washing steps. First, embryos were washed twice for 40 min at 65°C with solution I. Then, they were washed 3 times for 1h at 62°C with solution III. Embryos were washed 3 times for 15 min in 1x TBS-T and blocked for 1h in 20% heat inactivated goat serum in TBS-T. Embryos were then incubated ON with the antibody, anti-DIG fragments (Fab) conjugated with the alkaline phosphatase (AP). The antibody solution was prepared as follows: a small amount of embryo powder was heat-inactivated in 4ml of TBS-T for 30 min at 65°C and spin down. The pellet was added to a solution containing 500 µl of TBS-T/ 5% goat serum and 1 µl of DIG antibody and incubated for 1h at 4°C. This solution was spin down and the supernatant was diluted 4 times with TBS-T / 5% goat serum.

The third day was dedicated to the removal of excess of Fab antibody. Embryos were washed numerous times in TBS-T at RT (3 times for 15 min and then 12 times for 40 min) and at 4°C overnight.

The last day, embryos were washed twice in freshly made NTMT for 45 min. The colorimetric reaction was performed in the dark with 10.5 µl of NBT and 10.5 µl of BCIP in 3 ml of NTMT. When, the desired coloration was obtained, staining was stopped by 3 washings in PBS/EDTA 1mM. Embryos were afterwards post-fixed in 4%

---

PFA (2 hours, RT). Embryos were sometimes embedded in 20% gelatin/PBS. The block was fixed 24h in 4% PFA prior to vibratome sectioning (thickness: 35  $\mu$ m, Leica VT1000S).

#### **2.2.4. Dissection and fixation of mouse tissue**

Mouse tissues were dissected in ice-cold PBS and were fixed at 4°C in 4% paraformaldehyde (PFA) for one to three hours, depending on tissue and age (Table 4). At earlier stages (E10.5 until E16.5), head and bodies were fixed. For older animals, the head without skin and the spinal cord with vertebrae were fixed. Vertebrae were cut open after fixation. Tissues were then washed 3 times in PBS and cryoprotected in 30% sucrose at 4°C overnight prior to embedding in OCT compound (Sakura).

For whole-mount preparation of tongue/ lower jaw and diaphragm, head and trunk were fixed, respectively and washed in PBS. More precise dissection was performed after fixation.

#### **2.2.5. Preparation of frozen sections**

Frozen tissues were cut on a cryostat (Microtom HM560, Walldorf) at the thickness indicated in Table 4. The sections were collected alternatively on 4 or 6 glass slides (Marienfeld) and dried 1h at 37°C. Slides were stored at -80°C.

**Table 4 | Fixation and cutting of several mouse tissues**

| Tissue               | Age         | Fixation time | Thickness of cutting |
|----------------------|-------------|---------------|----------------------|
| Head                 | E10.5-E12.5 | 45 min        | 12 $\mu$ m           |
|                      | E16.5       | 1 h 30 min    | 14 $\mu$ m           |
|                      | P0.5        | 2 h           | 16 mm                |
| Spinal cord          | E10.5-E12.5 | 45 min        | 12 $\mu$ m           |
|                      | E16.5       | 1 h 30min     | 16 $\mu$ m           |
|                      | P0.5        | 2 h           | 18 $\mu$ m           |
| Tongue/<br>lower jaw | P0.5        | Overnight     |                      |
| Diaphragm            | P0.5        | 2 h           |                      |

### 2.2.6. Hematoxylin-eosin staining

Hematoxylin-eosin (HE) stain was performed at RT. 12  $\mu$ m-thick cryosections of the oral cavity were dried overnight at 37°C, then post-fixed in 4% PFA for 10 min. Sections were washed with tap water and stained 9 min with Weigert's iron hematoxylin (Sigma-Aldrich). Sections became blue. Slides were then washed 3 times with tap water, shortly dipped in a fresh Ethanol/1%HCL solution. Sections turned red. Next sections were washed 5 min under running tap water and became blue again. Sections were stained with eosin Y (40 s), then dehydrated through successive baths of 70%, 80% and 96% ethanol for (15 s; 60 s; 60 s), isopropanol (60 s) and xylol (15 s). Sections were dried and mounted with Entellan new (Millipore).

Hematoxylin-eosin stains nuclei in dark blue, cytoplasm in pink, muscles fibers in dark pink and blood cells in red.

### **2.2.7. X-gal staining**

Whole embryos (E12.5) or central nervous system and intestines (E16.5) were dissected in ice-cold PBS. All the steps of X-Gal staining were performed at room temperature under agitation.

Embryos/ tissues were fixed for 15 min in LacZ fixative solution + 0.2% glutaraldehyde and then washed 3 times for 10 min in LacZ wash buffer. Staining was performed in the dark in freshly prepared LacZ stain solution for 30 min to overnight. When the desired coloration was reached, staining was stopped by extensive PBS washing and fixed in 4% PFA.

### **2.2.8. Immunocytochemistry on section**

Prior to staining, slides were dried 2h at 37°C. Sections were rehydrated for 15 min in PBS and permeabilized in PBX (2 washes of 10 min) in Coplin jar. In order to perform blocking and staining with smaller volume of solutions, sections were circled with a water-repellent pen (Dako Pen). Non-specific binding sites were saturated with 10% horse serum in PBX for at least 1h at room temperature on horizontal slides. Primary antibodies were incubated overnight at 4°C in 10% horse serum in PBX. Slides were incubated for 1h30 with secondary antibodies coupled with Cy2, Cy3 or Cy5 and DAPI (Roche) at RT. Following additional washing steps in PBX, slides were covered with Shandon Immuno-mount (Thermo Scientific).

When Tshz1 antibody was used, staining was done using the M.O.M. (mouse on mouse) kit (Vector Laboratories) according to the manufacturer's instructions.

### **2.2.9. Whole-mount diaphragm staining**

The protocol for staining whole-mount diaphragm was adapted from the protocol described in Lin et al., 2001.

After dissection and fixation, diaphragm preparations were incubated in 0.1M Glycine in PBS for 1 hour at RT. Diaphragms were permeabilized in 0.5% Triton X-100 in PBS (2 washes of 5 min, at RT). Unspecific antibody binding was prevented by 90

min incubation in Diaphragm Blocking solution (prior to overnight incubation with primary antibody (rat  $\alpha$ -GFP or chicken  $\alpha$ -NF200) in Diaphragm Blocking solution. Next, diaphragms were extensively washed (3 times 75 min) in 0.5% Triton X-100 in PBS. They were incubated 2 hours in Diaphragm Blocking solution with Bungarotoxin conjugated with Alexa Fluor-555 (Invitrogen) and with Fluor- or HRP-coupled (horseradish peroxidase) secondary antibodies. After several additional washes in 0.5% Triton X-100 in PBS, diaphragms were either directly mounted in Immuno-mount (Thermo Scientific) or after colorimetric reaction with DAB (Vector Laboratories) (for HRP-coupled antibodies) according to manufacturer's instructions.

#### **2.2.10. Whole-mount tongue staining**

Whole-mount tongue and lower jaw staining were performed following a protocol established by Dr. Igor Adameyko. All steps were performed in glass tubes with rotation.

After fixation with 4% PFA, samples were bleached 24h in Dent's Bleach at 4°C. The next day, tongue/lower jaw preparations were washed (5 times for 10 min) in 100% methanol. Tongues were fixed in Dent's Fixative for 24h at 4°C and could be stored in Dent's fixative until staining.

The first day of the staining, tongue preparations were washed in PBS: 3 times for 10 min at 4°C and then, 3 times for 20 min at room temperature. Tongues were incubated 5 days at RT with chicken  $\alpha$ -NF200 antibody in Whole-mount Blocking + 0.025% sodium azide.

Next tongue preparations were washed 6 times for 30 min with PBX and incubated for 2 days incubation with Alexa Fluor 555- coupled secondary antibody in Whole-mount Blocking + 0.025% sodium azide at room temperature in the dark.

Finally, samples were extensively washed in PBX (6 times, 30 min) and dehydrated in methanol. Tongue preparations could be kept in 100% methanol at -20°C until imaging. Prior to imaging, tissues were cleared in BABB for 5 min. Tongues were returned to methanol for long-term storage.

### 2.2.11. Imaging and analysis

#### 2.2.11.1. Imaging of *in situ* hybridization, X-gal and HE staining

Imaging of whole-mount *in situ* hybridization and X-gal staining was performed with a Leica MZ16 binocular microscope topped with a Leica DFC95 camera. Blue background was obtained using agarose coated petri dish.

Imaging of vibratome sections of *in situ* hybridization and Hematoxylin-Eosin staining was performed with a Zeiss ApoTome.2 microscope using direct light. Stitching of the picture was done in Adobe Photoshop.

#### 2.2.11.2. Confocal imaging

Fluorescent immunostainings were photographed with a LSM 700 confocal microscope using a 20x objective.

#### 2.2.11.3. Counting of motor neuronal populations

For characterization of *Tshz1* expression, counts were done unilaterally on every sixth sections (hypoglossal nucleus and phrenic motor column) or on four sections along the motor column (lateral and medial motor column).

For *Tshz1*<sup>MNΔ</sup> and control animals, motor neurons were counted on serial sections, collected alternatively on 4 slides. One slide was stained and every section containing nXII, phrenic or lumbar LMC MNs were imaged and counted (bilaterally for nXII and phrenic MNS, unilaterally for LMC neurons). Counts were plotted to assess the total number of motor neuron per nucleus.

For the comparison of different groups of data, a t-test (Excel) was used. The differences were considered statistically significant when  $p < 0.05$ (\*) and very significant when  $p < 0.01$ (\*\*). The average values were plotted and errors bars represented the standard deviation.

#### **2.2.11.4. Branching analysis**

Analysis of the branching of the dorsal branch of the phrenic nerve was performed on Z-stack image of whole mount diaphragm. Tracing were done using the Image J plugin, simple neurite tracer. Raw data were processed in an Excel file designed by Dr Cyril Chéret, a post-doctorant researcher from the laboratory. The amount of branches of different orders and their length were then assessed.

The width of the endplate band, visualized by the BTX staining, was quantified to assess innervation of the ventral diaphragm. The same grid was added to every image and the width of the endplate was measured for each square and averaged.

### 3. Results

#### 3.1. *Tshz1* expression in motor neurons

*Tshz1* expression in the central nervous system (CNS) is only documented in the forebrain and olfactory bulb (Caubit et al., 2000; Caubit et al., 2005; Ragancokova et al., 2014). Therefore, I investigated the expression of *Tshz1* during embryonic development in the hindbrain and in the spinal cord, particularly in motor neurons, using *in situ* hybridization and a *Tshz1*<sup>GFP</sup> allele.

##### 3.1.1. RNA expression of *Tshz1*

I first assessed the expression pattern of *Tshz1* mRNA by whole-mount *in situ* hybridization of entire embryos (E10.5 until E12.5) or isolated CNS (E14.5 and E18.5; Fig. 3.1).

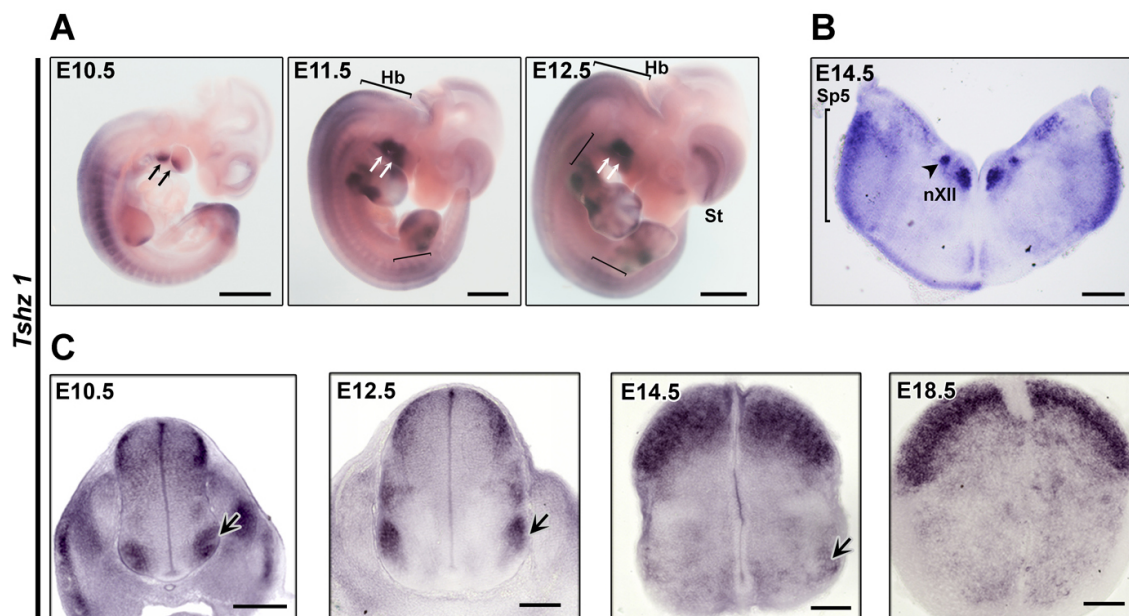


**Figure 3.1 | *Tshz1* expression during mouse development**

(A) *Tshz1* transcripts were detected by whole-mount *in situ* hybridization in embryos at E10.5, E11.5 and E12.5. *Tshz1* is expressed in branchial arches (arrows in A), limb buds, the spinal cord and starting from E11.5 in the hindbrain (Hb) and striatum (St). In the ventral spinal cord, the territory of motor neurons, *Tshz1* transcripts are detected only at limb levels (brackets).

**(B)** Hindbrain nuclei expressing *Tshz1* were assessed by whole-mount *in situ* hybridization at E14.5. *Tshz1* transcripts are detected in trigeminal (Sp5) and hypoglossal nuclei (nXII) as well as in an unknown group of neurons indicated by an arrowhead. **(C)** Whole-mount *in situ* hybridization of the spinal cord at different embryonic stages reveals that dorsal expression of *Tshz1* starts at E10.5 and increases in intensity during development. In the ventral spinal cord, *Tshz1* transcripts are detected in the MN territory (arrow) at limb level only at E10.5 and E12.5. This expression is transient and declines between E14.5 and E18.5. Scale bar in A: 1 mm; scale bar in B: 400  $\mu$ m; scale bar in C: 100  $\mu$ m.

At E10.5, I observed expression of *Tshz1* in the first and second branchial arches, in somites, limb buds and the spinal cord (Fig. 3.1A). The expression of *Tshz1* in branchial arches persisted at E11.5 and E12.5. *Tshz1* expression in limb buds narrowed to interdigital areas at E12.5. *Tshz1* transcripts were expressed in the dorsal spinal cord on all axial levels at E10.5, E11.5 and E12.5; but in the ventral spinal cord only on limb levels at E11.5 and E12.5. *Tshz1* expression extended to the brain at E11.5. This expression, particularly in the hindbrain and striatum, increased at E12.5.

I investigated which hindbrain nuclei express *Tshz1* using coronal sections of E14.5 brains (Fig. 3.1B). A strong expression of *Tshz1* was detected in the sensory neurons of the spinal trigeminal nucleus (Sp5) located in the lateral brainstem. In the caudal hindbrain near the midline, *Tshz1* transcripts were detected in the somatic motor neurons of the hypoglossal nucleus (nXII). *Tshz1* was additionally strongly expressed by unidentified neurons, which were located nearby the hypoglossal nucleus.

*Tshz1* expression in the spinal cord was dynamically regulated (Fig. 3.1C). At E10.5, *Tshz1* transcripts were detected in subpopulations of dorsally and ventrally located neurons. In accordance with the expression observed by whole-mount *in situ* hybridization, *Tshz1* was expressed on all axial levels of the dorsal spinal cord but in ventral neurons only on limb levels. During development, the ventral expression of *Tshz1* decreased and was not longer detected after E14.5. In contrast, expression levels in dorsal spinal neurons increased at later developmental stages (i.e. E14.5 and E18.5).

### 3.1.2. Analysis of *Tshz1* expression in motor neurons

I used, for further experiments, immunohistology to study the expression of *Tshz1* in motor neuronal subpopulations of the brainstem and spinal cord during embryonic development (Fig. 3.2-3.4). To identify *Tshz1*-expressing cells, I used heterozygous mice from a *Tshz1*<sup>GFP</sup> strain generated previously in the laboratory (Ragancokova et al., 2014). In the hindbrain and spinal cord, MNs are produced from a restricted ventral ventricular zone starting at E9.5, which is called the motor neuron progenitor domain (pMN). Progenitor cells that will give rise to motor neurons express the transcription factor *Olig2*. Postmitotic MNs express the transcription factor *Isl1* and switch off *Olig2* expression.

In the brainstem, I focused on two motor neuronal populations: the somatic MNs of the hypoglossal nucleus and branchiomotor MNs of the dorsal motor nucleus of the vagus (subsequently called vagal MNs). These nuclei, located in the caudal hindbrain, are adjacent to each other and can be distinguished by the fact that they express different transcription factors. Branchiomotor and somatic MNs both express *Isl1*, but only branchiomotor neurons express *Phox2b*. Therefore, hypoglossal MNs are *Isl1*<sup>+</sup>/*Phox2b*<sup>-</sup>, whereas the neighboring vagal MNs are *Isl1*<sup>+</sup>/*Phox2b*<sup>+</sup> (Fig. 3.2B). At E12.5, *Tshz1* co-localizes with the postmitotic *Isl1*<sup>+</sup> neurons of the hypoglossal nucleus, but is never expressed in *Olig2*<sup>+</sup> motor neuron progenitors (Fig. 3.2C). I quantified every sixth section of the entire hypoglossal nucleus of three animals at E12.5, E15.5 and P0.5. I established that 85% ( $\pm 1\%$ ) of *Isl1*<sup>+</sup> hypoglossal MNs were expressing *Tshz1* at E12.5 (Fig. 3.2D). *Tshz1* expression in hypoglossal MNs persisted during development, and 66% ( $\pm 1\%$ ) of E15.5 hypoglossal MNs and 71% ( $\pm 7\%$ ) of P0.5 MNs expressed *Tshz1*. *Tshz1* expression, at E15.5 and P0.5, was restricted to subdomains of the hypoglossal nucleus as summarized in Figure 3.2E. Rostrally, *Tshz1*-expressing MNs located in the ventro-lateral part of the nucleus. In the central part of the nucleus, all MNs were expressing *Tshz1*, and at the caudal hypoglossal nucleus, *Tshz1* was expressed strongly in dorso-medial MNs and at lower levels in other caudal hypoglossal MNs. Topographical organization of MNs in the hypoglossal nucleus has been reported (Aldes, 1995; McLoon and Andrade, 2013), and the observed distribution suggested that *Tshz1* is expressed only in MNs innervating specific tongue muscles. I could not detect *Tshz1* expression at E15.5 or P0.5 in *Isl1*<sup>+</sup>/*Phox2b*<sup>+</sup> vagal MNs (Fig. 3.2B). *Tshz1* was in addition

expressed in *Phox2b*/*Isl1*- neurons at E14.5 and P0.5 that were not analyzed further.

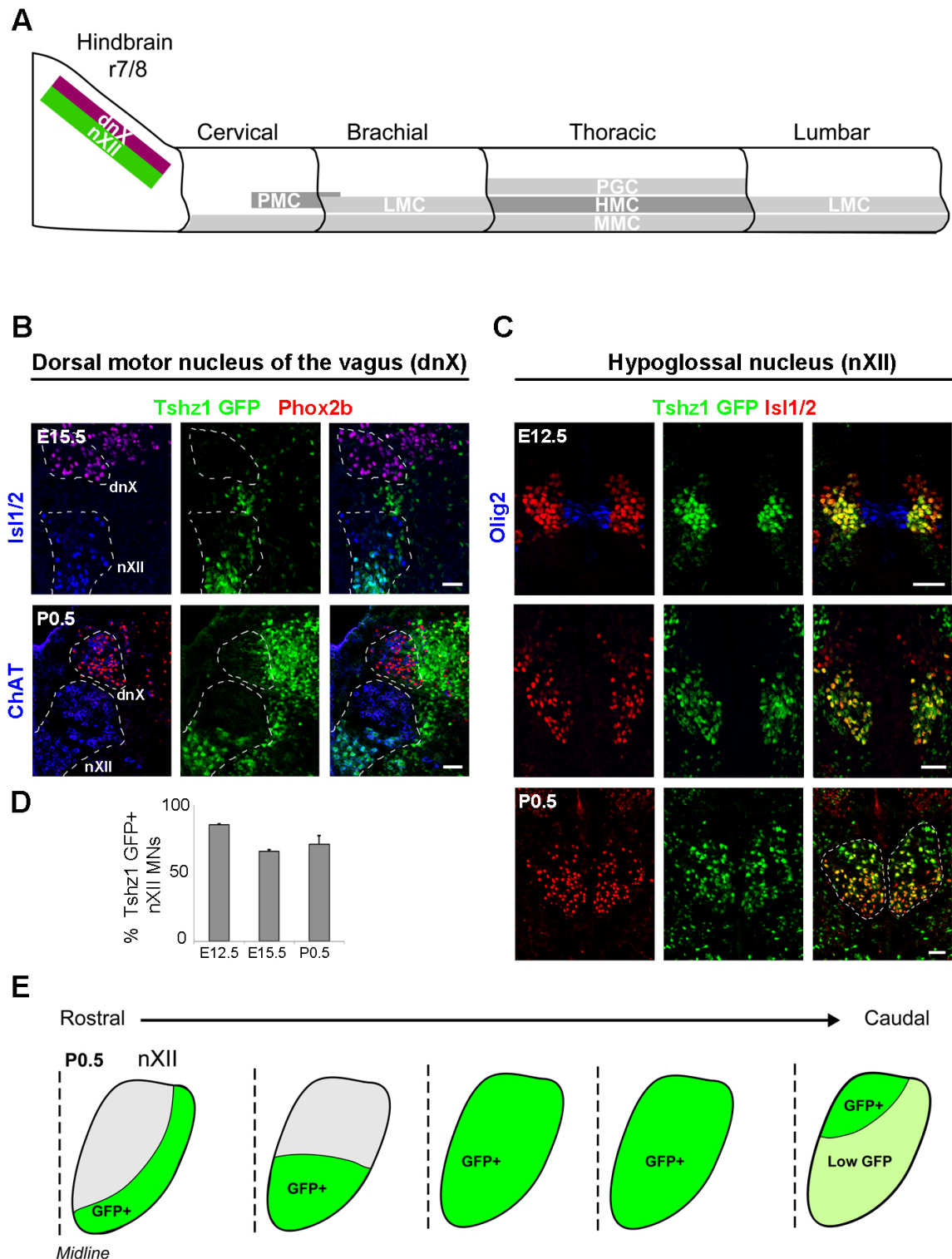


**Figure 3.2 | *Tshz1* expression in hindbrain motor neurons during development**

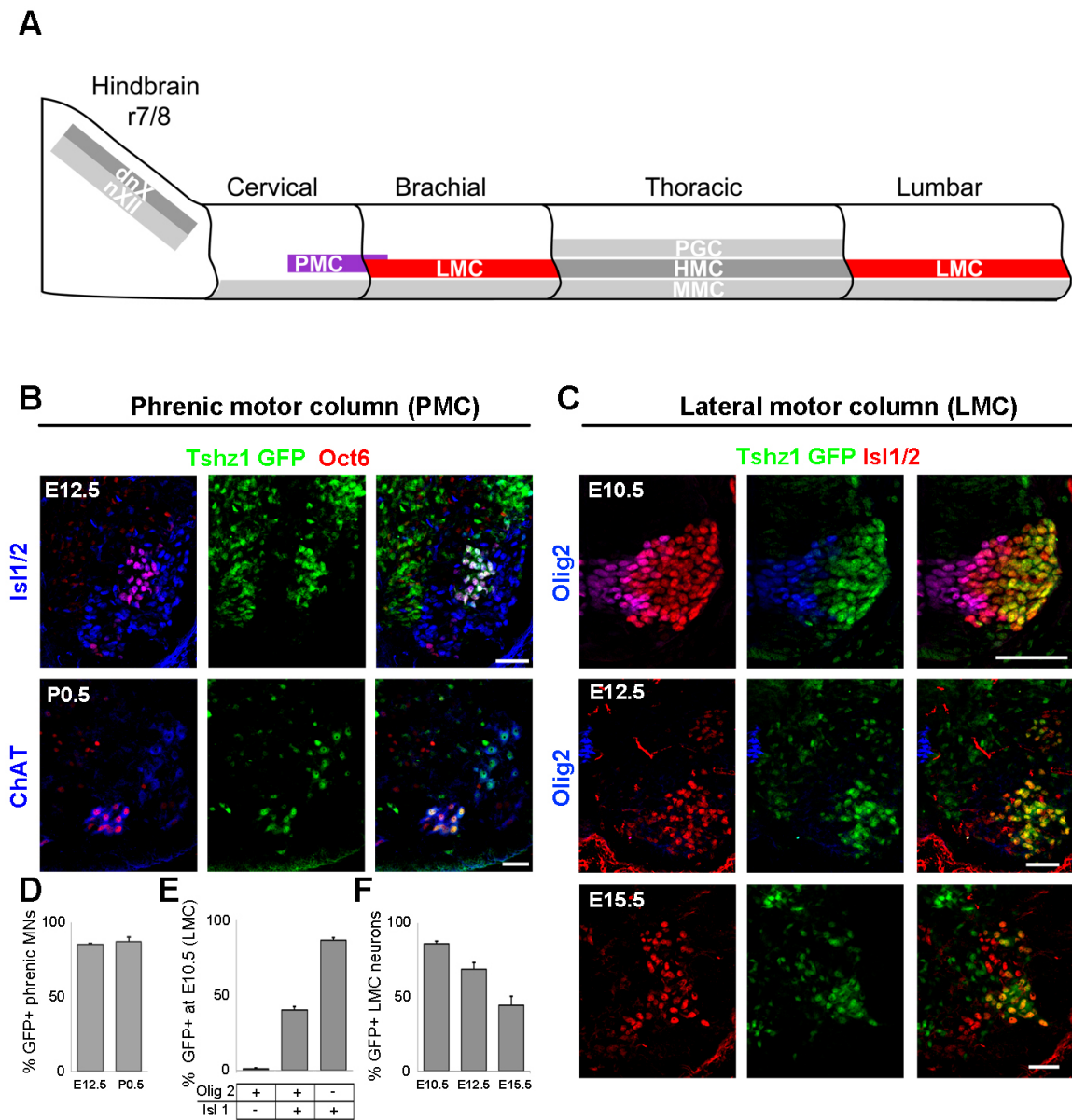
(A) Schematic representation of motor neuron columns in the brainstem and the spinal cord. Purple and green indicate the dorsal motor nucleus of the vagus (dnX) and the hypoglossal

nucleus (nXII), respectively; both nuclei are located in rhombomere 7/8 of the hindbrain. **(B)** Vagal MNs correspond to branchiomotor MNs (i.e. innervate derivatives of branchial arches) and express *Isl1*, *ChAT* and *Phox2b*. In vagal MNs, GFP expressed from the *Tshz1*<sup>GFP</sup> allele is neither detected at E15.5 nor at P0.5. Somatic hypoglossal neurons express *Tshz1*-GFP, *Isl1* and *ChAT* but not *Phox2b*. Note that unidentified *Isl1*-/*ChAT*-/*Phox2b*- neighboring neurons strongly express *Tshz1*-GFP. **(C, D)** *Tshz1* is expressed by 86%, 66% and 71% of all *Isl1*+ hypoglossal motor neurons at E12.5, E15.5 and P0.5, respectively. **(E)** At E15.5 and P0.5, *Tshz1* is not expressed in hypoglossal MNs on all axial levels. In the rostral nucleus, *Tshz1* is expressed only in ventral MNs. In the center of the nucleus, *Tshz1* is expressed in all MNs, and in the caudal nucleus, *Tshz1* is strongly expressed dorsally and at lower levels ventrally. Scale bar: 50  $\mu$ m. Data are represented as mean  $\pm$  SD.

I then analyzed *Tshz1* expression in the spinal cord. Phrenic motor neurons that innervate the diaphragm reside in the ventral horn of the cervical spinal cord (C3 to C5 level). In addition to *Isl1*, these neurons express *choline acetyltransferase (ChAT)* and the transcription factor *Oct6* (also known as *Scip* and *POU3F1*). I analyzed *Tshz1* expression in the phrenic motor column at E12.5 and at P0.5 (Fig. 3.3B) and quantified GFP expression, from the *Tshz1*<sup>GFP</sup> allele, in *Isl1*+/*Oct6*+ (E12.5) or *ChAT*+/*Oct6*+ (P0.5) phrenic MNs on every sixth section of the phrenic motor column of three different animals. *Tshz1* was expressed in 85% ( $\pm$ 0.5%) and 87% ( $\pm$ 3%) of phrenic MNs at E12.5 and P0.5, respectively (Fig. 3.3D).

MNs innervating fore- and hindlimb muscles cluster to form the lateral motor column (LMC) of the brachial and the lumbar spinal cord, respectively. The LMC is located, as its name indicates, in the lateral part of the ventral spinal cord. At E10.5, all postmitotic MNs express *Isl1*, but at later stages some MNs downregulate *Isl1*. I considered all *Isl1*+ MNs at limb levels to correspond to LMC neurons. Immunohistological stainings revealed three neuronal populations in the ventral spinal cord: *Olig2*+/*Isl1*- cells, located near the midline that corresponded to motor neuron progenitors; *Olig2*-/*Isl1*+ cells, located laterally, that were postmitotic motor neurons; and *Olig2*+/*Isl1*+ cells, located in between the previous cell populations, that corresponded to differentiating motor neurons (Fig. 3.3C). Motor neurons were born near the midline of the progenitor domain and then migrated laterally while they differentiated. *Tshz1* was never expressed in MN progenitors. Its expression was switched on after *Isl1* starts to be expressed. 86% ( $\pm$ 2%) of postmitotic MNs express *Tshz1* (Fig. 3.3E). In addition, low GFP expression was found in 40% ( $\pm$ 2%) of differentiating MNs. Thus, *Tshz1* expression initiated during early motor neuronal differentiation. *Tshz1* expression in postmitotic motor neurons of the LMC was transient (Fig. 3.3C,F). At E10.5, 86% of LMC MNs were *Tshz1*+. At E12.5, *Tshz1*

was still expressed in 69% ( $\pm 4\%$ ) of LMC neurons. Finally, at E15.5, only 44% ( $\pm 6\%$ ) of LMC neurons expressed *Tshz1* (Fig. 3.3F).



in 40% of differentiating MN (Olig2+/Isl1+). At E10.5, 86% of postmitotic MNs (Isl1+/Olig2-) express *Tshz1* at limb level. **(C, F)** *Tshz1* expression in postmitotic motor neurons of the LMC decreases to 69% at E12.5 and to 44% at E15.5. Scale bar: 50  $\mu$ m. Data are represented as mean  $\pm$  SD.

MNs cluster according to their innervation target and form motor columns that express the same set of transcription factors. An extensive literature describes these different motor columns in the ventral spinal cord at E12.5 (Dasen and Jessell, 2009; Garcia and Jessell, 2008; Rouso et al., 2008). Thus, I decided to analyze more precisely expression of *Tshz1* in the different motor columns along the spinal cord at E12.5 (Fig. 3.4). MN populations can be distinguished according to the axial level and by differential expression of the transcription factors *Isl1*, *Foxp1* and *Lhx3*. I performed co-immunohistological staining with antibodies that detect GFP, from *Tshz1*<sup>GFP</sup> allele, *Isl1/2*, and *Foxp1* as well as antibodies that detect GFP, *Isl1/2* and *Lhx3*. I used sections from three different *Tshz1*<sup>GFP/+</sup> E12.5 embryos to perform the staining, and counted four non-adjacent sections per axial level to evaluate the proportion of GFP+ MNs. In the brachial spinal cord, three motor neuron populations are present: (1) the LMCI (lateral motor column, lateral) characterized by *Isl1* and *Foxp1* expression that innervates dorsal muscles of the forelimbs; (2) the LMCm (lateral motor column, medial) characterized by *Foxp1* expression and *Isl1* absence that innervates ventral muscles of the forelimbs; and (3) the medial motor column (MMC) expressing *Isl1* and *Lhx3* that innervates axial muscles (Fig. 3.4A,B). 74% and 69% of LMCm and LMCI populations, respectively, expressed high levels of *Tshz1* (Fig. 3.4C,E). In the rostral part of the brachial spinal cord, almost all LMCI neurons were GFP+ whereas in the caudal part, the proportion of GFP+ MNs dropped to 50%. Low levels of *Tshz1* were expressed in 11% of MMC MNs of the brachial spinal cord (Fig. 3.4D,E).

The thoracic spinal cord possesses three different motor neuronal populations: (1) the medial motor column (MMC), expressing *Lhx3* and *Isl1* and innervating the axial muscles, is present on all axial levels, (2) the hypaxial motor column (HMC) expressing *Isl1* and innervating the body wall muscles, and (3) the preganglionic column (PGC) MNs that express low level of *Isl1* and *Foxp1* and innervate the sympathetic ganglia chain (Fig. 3.4A,F). As mentioned above, *Tshz1* was not expressed in the ventral spinal cord at thoracic level. Neuronal counts indicated that less than 5% of PGC and 10% of HMC neurons expressed low levels of *Tshz1*; none of the *Lhx3*+ MMC neurons expressed *Tshz1* (Fig. 3.4G,H,I).

At lumbar levels the ventral spinal cord is organized similarly to brachial levels. Three motor columns are present: LMCm and LMCI innervating the dorsal and ventral hindlimbs, respectively, as well as the MMC (Fig. 3.4J). *Tshz1* expression in these MN populations was similar but not identical to the one observed in the brachial spinal cord (Fig. 3.4K,L). 17% of MMC neurons expressed low levels of *Tshz1*. The expression of *Tshz1* in LMCI and LMCm was more dissimilar than at brachial level, and 75% of LMCI MNs but only 57% of LMCm neurons were GFP+ (Fig. 3.4M).

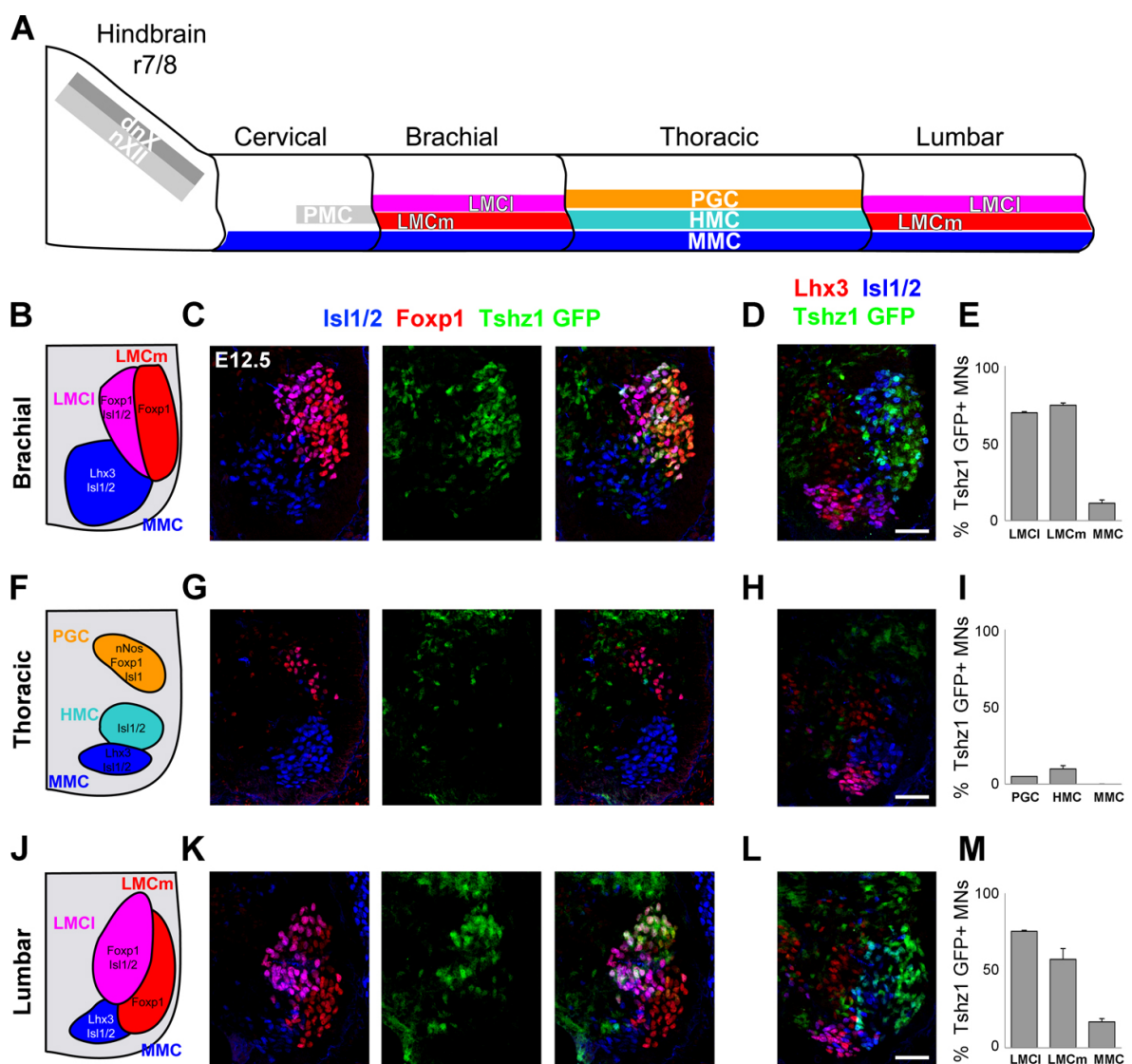


**Figure 3.4 | *Tshz1* expression in several motor neuron pools along the spinal cord at E12.5**

**(A)** Schematic representation of motor neuron populations in the brainstem and the spinal cord. Shown are in dark blue: medial motor column (MMC), pink: lateral motor column lateral

(LMCI), red: lateral motor column medial (LMCm), yellow: preganglionic column (PGC) and light blue: hypaxial motor column (HMC). **(B-E)** On brachial level, LMCI, LMCm and MMC motor neurons are present and can be distinguished at E12.5 by differential expression of transcription factors. LMCI: *Foxp1+Isl1+/Lhx3-*; LMCm: *Foxp1+Isl1-/Lhx3-*; MMC: *Foxp1-/Isl1+/Lhx3+*. *Tshz1* is expressed by 69% of LMCI, 74% of LMCm and 11% of MMC neurons. **(F-I)** On thoracic level, PGC (*Foxp1+Isl1+/Lhx3-*), HMC (*Foxp1-/Isl1+/Lhx3-*) and MMC (*Foxp1-/Isl1+/Lhx3+*) neurons are present. *Tshz1* is expressed at low levels and I detected GFP driven by the *Tshz1* locus only in 5% of PGC and 10% of HMC neurons. **(J-M)** On lumbar levels, the motor neuron populations are similar to the ones observed on brachial levels (LMCI, LMCm and MMC). *Tshz1* is expressed by 75% of LMCI, 57% of LMCm and 17% of MMC neurons. Scale bar: 50  $\mu$ m. Data are represented as mean  $\pm$  SD.

## 3.2. Mutation of *Tshz1* in motor neurons leads to neonatal lethality

### 3.2.1. Conditional mutation of *Tshz1* in motor neurons using *Olig2*<sup>Cre</sup> allele

Molecular mechanisms that determine neuronal variability are incompletely understood, and motor neuron development provides a model to understand how this variability can arise during development. The *Tshz1* expression pattern indicates that this factor might play a role in development of specific subtypes of motor neurons. We took advantage of the Cre-lox recombination technology to mutate *Tshz1* specifically in somatic MNs to investigate this further. We used *Tshz1*<sup>fllox</sup> mice, in which exon 2 of the *Tshz1* gene is flanked by *loxP* sites, that had been generated by a former PhD student in the laboratory, Dr. Elena Rocca (Ragancokova et al., 2014). We introduced the *Olig2*<sup>Cre</sup> allele in the *Tshz1*<sup>fllox</sup> mutant background (*Olig2*<sup>tm1(cre)Tmj</sup>; Dessaud et al. 2007). I verified the specificity of the *Olig2*<sup>Cre</sup>-dependent recombination using an inducible *Rosa26R-LacZ* reporter allele (*Gt(ROSA)26Sor*<sup>tm1Sor</sup>; Soriano 1999) (Fig. 3.5). To assess recombination, I analyzed the distribution of the  $\beta$ -galactosidase enzyme (the protein product of *LacZ*) using its substrate X-gal to generate a colored product at E12.5 (Fig. 3.5A) and at E16.5 (Fig. 3.5B); the protein is only expressed after recombination has occurred. At E12.5, X-gal staining was found in the ventral spinal cord, the ventral hindbrain and the forebrain. I did not detect it outside of the central nervous system (Fig. 3.5A). At E16.5, I performed X-gal staining on whole-mount spinal cords, brain and intestine (Fig. 3.5B). In the hindbrain and spinal cord, X-gal staining was detected near the midline (pMN domain) and in several ventral populations of neurons that correspond

to the different motor neuron subtypes. I did not detect X-gal staining in the intestine (Fig. 3.5B). X-gal staining revealed that *Olig2<sup>Cre</sup>* induced recombination in the ventral PMN domain of the hindbrain and spinal cord, and in MNs that derive from these progenitors.

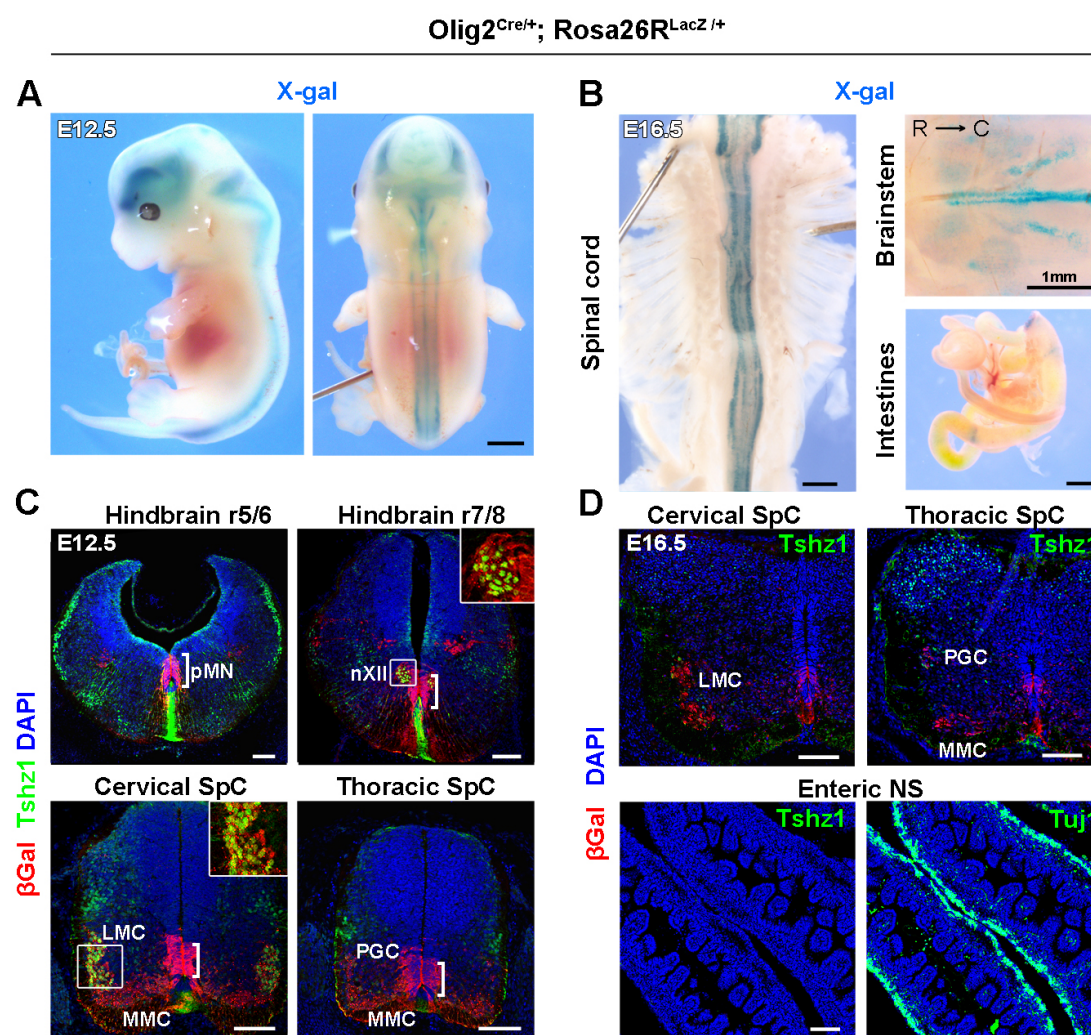


**Figure 3.5 | *Olig2<sup>Cre</sup>* recombination pattern**

Embryos carrying one *Olig2<sup>Cre</sup>* allele and an inducible *Rosa26R-LacZ* reporter allele were stained for LacZ expression using X-gal; **(A)** X-gal staining was performed at E12.5 on the entire embryo, **(B)** and on isolated spinal cord, brain and intestine obtained from E16.5 mice. Strong X-gal staining was detected in the hindbrain, as well as in the ventro-lateral spinal cord and near the midline. Note that no LacZ expression was observed in the intestine. Immunohistological detection of  $\beta$ -galactosidase ( $\beta$ -Gal, red in the figure) and Tshz1 (green) at E12.5 **(C)** and E16.5 **(D)** in *Olig2<sup>Cre/+</sup>; Rosa26R<sup>LacZ/+</sup>* mice demonstrates that Tshz1 protein is expressed in neuronal cell populations that have undergone Cre-dependent recombination.  $\beta$ -galactosidase is strongly expressed in the pMN domain (bracket) and derivative postmitotic MNs (nXII, LMC, MMC and PGC) in the hindbrain and the spinal cord. In the hindbrain, only

hypoglossal MNs (nXII) co-express *Tshz1* and  $\beta$ -galactosidase. In the spinal cord, motor neurons of the lateral motor column (LMC) co-express *Tshz1* and  $\beta$ -galactosidase and will therefore be affected by *Olig2<sup>Cre</sup>* dependent mutation of *Tshz1*. The enteric nervous system (Tuj1+), located in the intestines, does neither express  $\beta$ -galactosidase nor *Tshz1*. Scale bar in A, C: 1 mm; scale bar in B, D: 100  $\mu$ m.

I intended to define which cell populations might be affected by *Tshz1* mutation upon *Olig2<sup>Cre</sup>* induced conditional recombination. I performed immunohistological analysis of  $\beta$ -galactosidase and *Tshz1* at E12.5 (Fig. 3.5C) and E16.5 (Fig. 3.5D) in *Olig2<sup>Cre/+</sup>; Rosa26R<sup>LacZ/+</sup>* mice. Immunostainings confirmed  $\beta$ -galactosidase expression, upon *Olig2<sup>Cre</sup>* driven recombination, in the ventral pMN domain of the hindbrain and spinal cord, and in MNs that derived from these progenitors, as well as oligodendrocytes that were generated in late development from the pMN domain. At E12.5, postmitotic motor neurons of the hypoglossal nucleus in the hindbrain co-expressed *Tshz1* and  $\beta$ -galactosidase. In the spinal cord, *Olig2<sup>Cre</sup>* induced recombination in all motor neuronal populations and all MNs expressed  $\beta$ -galactosidase, but *Tshz1* was expressed only in LMC neurons (Fig. 3.5C). At E16.5, immunohistological analyses of  $\beta$ -galactosidase and *Tshz1* also confirmed the specificity of recombination in somatic motor neurons. Neither  $\beta$ -galactosidase nor *Tshz1* expression was detected in the Tuj1+ neurons of the enteric nervous system located in the intestine (Fig. 3.5D).

### 3.2.2. *Tshz1<sup>MN $\Delta$</sup>* mutants die on the first day after birth

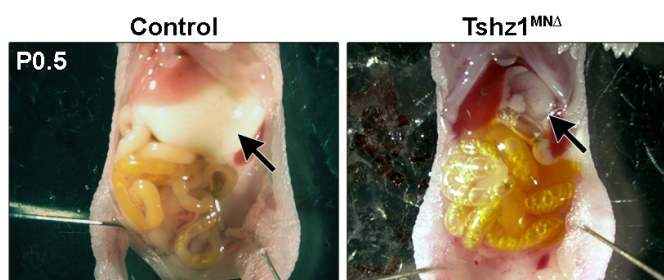
I used conditional mutation in somatic motor neurons (*Olig2<sup>Cre/+</sup>; Tshz1<sup>flox/ $\Delta$</sup>* , subsequently called *Tshz1<sup>MN $\Delta$</sup>* ) to examine the role of *Tshz1* during motor neuronal development. Such mice were generated from the following matings: *Olig2<sup>Cre/+</sup>; Tshz1 <sup>$\Delta$ /+</sup>* x *Tshz1<sup>flox/flox</sup>*. Additionally, we introduced the *Hb9-GFP* reporter transgene (Tg(Hlxb9-GFP)1Tmj; Wichterle et al. 2002) to visualize MNs and their projections.

*Tshz1<sup>MN $\Delta$</sup>*  mutant animals were born at normal Mendelian ratio. However, none of the *Tshz1<sup>MN $\Delta$</sup>*  pups survived beyond P0.5 and *Tshz1<sup>MN $\Delta$</sup>*  mice were not found when animals were genotyped two weeks after birth (Table 5).

Table 5 | *Tshz1*<sup>MNΔ</sup> mice were born and subsequently died

|  | At birth  |            | 2 weeks old |           |
|--|-----------|------------|-------------|-----------|
|  | Number    | Percent    | Number      | Percent   |
| <i>Tshz1</i> <sup>flox/+</sup>                                     | 23        | 24%        | 17          | 37%       |
| <i>Tshz1</i> <sup>flox/Δ</sup>                                     | 22        | 23%        | 12          | 26%       |
| <i>Olig2</i> <sup>Cre/+</sup> ; <i>Tshz1</i> <sup>flox/+</sup>     | 23        | 24%        | 17          | 37%       |
| <b><i>Olig2</i><sup>Cre/+</sup>; <i>Tshz1</i><sup>flox/Δ</sup></b> | <b>27</b> | <b>28%</b> | <b>0</b>    | <b>0%</b> |
|  | 95        |            | 46          |           |

At P0.5, *Tshz1*<sup>MNΔ</sup> pups had no milk in the stomach. Dissection of the abdominal cavity revealed that intestines of *Tshz1*<sup>MNΔ</sup> pups were filled with air (aerophagia). In addition, *Tshz1*<sup>MNΔ</sup> pups displayed respiratory distress: they were slightly cyanotic and gasped. I observed that *Tshz1*<sup>MNΔ</sup> animals died six to seven hours after birth (Fig. 3.6).

Figure 3.6 | *Tshz1*<sup>MNΔ</sup> animals do not feed and display aerophagia

*Tshz1*<sup>MNΔ</sup> mutant pups have no milk in their stomach (arrow), and their intestine is full of air bubbles.

### 3.2.3. *Tshz1*<sup>MNΔ</sup> mutants do not have malformation of the oral cavity

*Tshz1* total knock-out mice (*Tshz1*<sup>NULL</sup>) do not survive beyond the first day of birth and exhibit a similar phenotype to *Tshz1*<sup>MNΔ</sup> pups at P0.5 (Core et al. 2007, personal observation). Indeed, *Tshz1*<sup>NULL</sup> pups do not feed, gasp and display an even more severe aerophagia than *Tshz1*<sup>MNΔ</sup> pups. Coré and her colleagues attributed the aerophagia to malformations of the oral cavity of *Tshz1*<sup>NULL</sup> pups. The soft palate,

which separates the naso- and oropharynx, is absent; and the epiglottis, which closes the trachea and directs food in the esophagus during swallowing, is flattened in *Tshz1*<sup>NULL</sup> pups.

I expected that the *Olig2*<sup>Cre</sup> driven recombination is specific to somatic motor neurons and that oral cavity malformations should not occur in *Tshz1*<sup>MNΔ</sup> animals. I verified the integrity of oral cavity at P0.5, using hematoxylin-eosin staining on coronal and sagittal sections of at least three mutants and three littermate controls (Fig. 3.7). Histological analysis showed no absence or deformation of the soft palate and the epiglottis, and for instance the palate was not shortened in *Tshz1*<sup>MNΔ</sup> animals. Thus, aerophagia and inability to feed were expected to be the result of a motor neuron specific dysfunction.

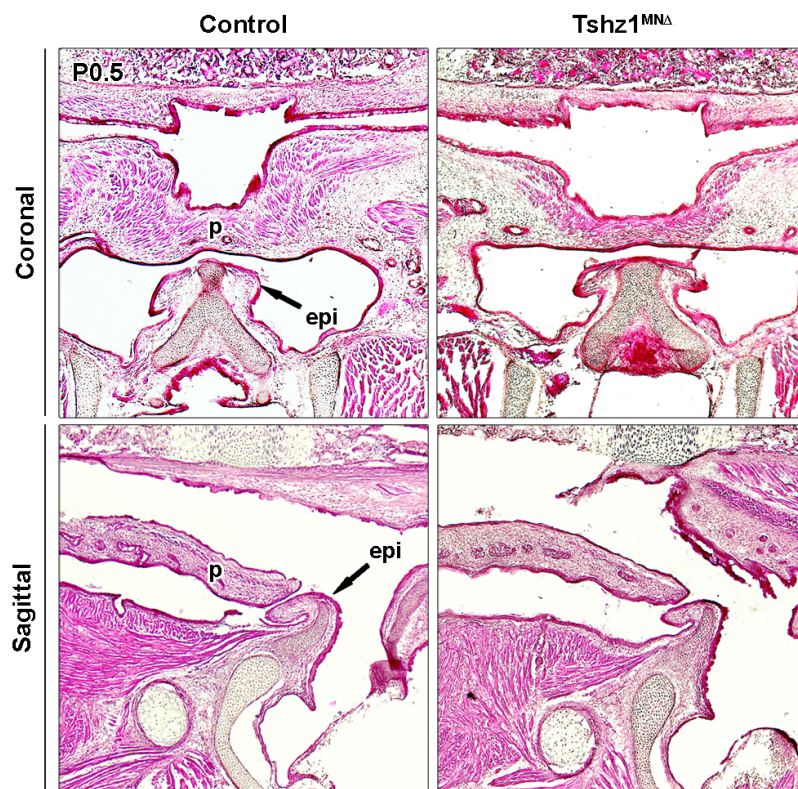


**Figure 3.7 | *Tshz1*<sup>MNΔ</sup> animals have an intact oral cavity**

Histological analysis of the oral cavity (hematoxylin-eosin staining) of *Tshz1*<sup>MNΔ</sup> and control mice. Coronal sections show that the soft palate (p, which is the posterior palate) and the epiglottis (epi) are present and intact. Sagittal sections confirmed that the palate had an appropriate length in *Tshz1*<sup>MNΔ</sup> animals.

### 3.2.4. The hypoglossal nucleus is smaller and hypoglossal nerve branching is impaired in *Tshz1*<sup>MNΔ</sup> mutants

Surgical impairment of hypoglossal nerves that innervate the tongue muscles was shown to prevent feeding (Fujita et al., 2006; Fukushima et al., 2014). Expression data emphasize that *Tshz1* is strongly and persistently expressed in motor neuronal subpopulations of the hypoglossal nucleus. Therefore, I performed immunohistological staining of Isl1 and ChAT at different developmental stages to define whether the hypoglossal motor neurons were present in correct numbers in *Tshz1*<sup>MNΔ</sup> animals (Fig. 3.8).

At E12.5, hypoglossal MNs are still being generated. Postmitotic MNs express *Isl1* and have characteristic euchromatic nuclei (pale DAPI staining with a few brighter spots). I counted Isl1+ MNs, bilaterally, on every fourth section along the entire nucleus for at least three animals per genotype (Fig. 3.8A). At E12.5, I did not observe any difference in MN numbers between *Tshz1*<sup>MNΔ</sup> animals and controls. This indicates that MNs of the hypoglossal nucleus were generated in correct number.

During normal fetal development, half of motor neurons generated undergo apoptosis, i.e. programmed cell death (Dekkers et al., 2013; Yamamoto and Henderson, 1999). A functional neuromuscular junction requires one muscle fiber to be innervated by only one motor axon, and MNs that did not contact or that contacted an already innervated muscle fiber, are eliminated by apoptosis. I defined the overall number of hypoglossal motor neurons and the number of apoptotic MNs at E14.5 in *Tshz1*<sup>MNΔ</sup> animals and littermates (Fig. 3.8B). I counted bilaterally Isl1+ motor neurons in the hypoglossal nuclei on every fourth section from at least 3 animals per genotype. In addition, apoptosis was assessed by an antibody detecting the active form of caspase-3. I found a 20% reduction in the number of hypoglossal MNs in *Tshz1*<sup>MNΔ</sup> animals compared to their littermates (5785 ± 236 vs 4596 ± 374). In addition, I observed a 2.3 fold increase of apoptotic hypoglossal MNs at E14.5 in *Tshz1*<sup>MNΔ</sup> animals.

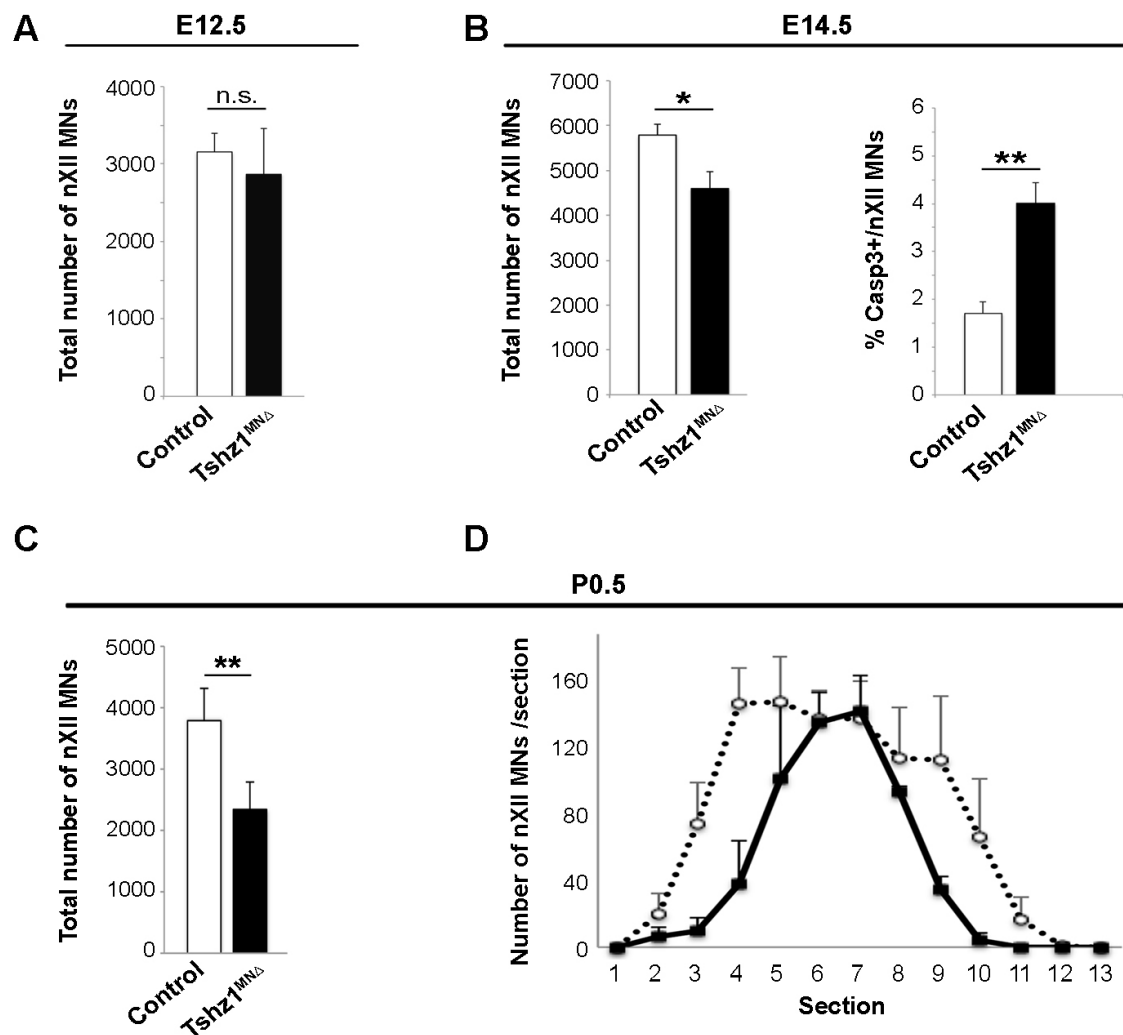


**Figure 3.8 | Reduced numbers of motor neurons in the hypoglossal nucleus of *Tshz1*<sup>MNΔ</sup> mutants**

Hypoglossal motor neurons were detected using Isl1 (E12.5 and E14.5) and ChAT (P0.5) antibodies and quantified. **(A)** Quantification of hypoglossal MNs at E12.5 revealed that they were generated in equivalent numbers in *Tshz1*<sup>MNΔ</sup> and control animals. **(B)** At E14.5, the number of hypoglossal MNs is decreased by 20% and increased numbers of MNs co-expressed the active form of caspase-3, a marker of apoptotic cells, in *Tshz1*<sup>MNΔ</sup> mice. **(C)** At P0.5, the number of hypoglossal MNs was decreased by 40% in *Tshz1*<sup>MNΔ</sup> animals. **(D)** Because of this, the hypoglossal nucleus was shortened along the antero-posterior axis. Data are represented as mean  $\pm$  SD. (t-test, \*\*  $p < 0.01$ , \*  $p < 0.05$ , n.s. not significant)

Finally, I investigated the number of hypoglossal motor neurons at birth (P0.5) (Fig. 3.8C,D). At P0.5, hypoglossal MNs express *ChAT* and have characteristic euchromatic nuclei. These neurons do not express the transcription factor *Phox2b* and can thus be distinguished from neighboring vagal motor neurons. I counted ChAT+/Phox2b- neurons on serial sections (bilateral counting on every fourth

section). This showed a reduction of 38% in the number of hypoglossal motor neurons at P0.5 in *Tshz1<sup>MNA</sup>* animals ( $3788 \pm 531$  vs  $2353 \pm 425$ ) (Fig. 3.8C). The motor neuron loss was more pronounced at P0.5 than E14.5 (38% versus 20%), suggesting that it was progressive during development. I observed that although the maximal number of hypoglossal motor neurons per section was comparable in *Tshz1<sup>MNA</sup>* and control mice, the motor column was shortened in the anterior-posterior axis in *Tshz1<sup>MNA</sup>* mice (Fig. 3.8D).

These results demonstrate that hypoglossal MNs of *Tshz1<sup>MNA</sup>* animals were generated in normal number (E12.5), but increased numbers were undergoing apoptosis (E14.5), which resulted in a 40% reduction of motor neurons in the hypoglossal nucleus at birth.

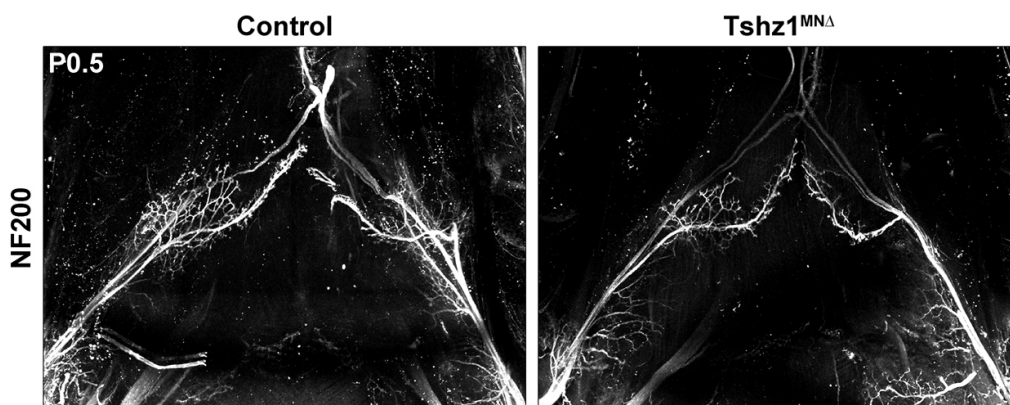


**Figure 3.9 | Hypoglossal nerve branching is disrupted in *Tshz1<sup>MNA</sup>* animals**

The hypoglossal nerve innervating the tongue was visualized by whole-mount immunostaining with neurofilament NF200 antibody. Hypoglossal nerves of *Tshz1<sup>MNA</sup>* animals were thinner and displayed a less complex arborization than hypoglossal nerves of control animals.

I asked whether the reduction in the number of hypoglossal motor neurons led to a defect in tongue innervation at P0.5. I used whole-mount immunostaining of neurofilament protein, NF200, in tongue and lower jaw preparations and imaged tongue innervation with a confocal microscope (Fig. 3.9). Hypoglossal nerves in *Tshz1<sup>MNA</sup>* animals appeared thinner than in littermate controls. Additionally, hypoglossal nerves in *Tshz1<sup>MNA</sup>* animals displayed reduced branching. These results

suggest that the impaired feeding and aerophagia observed in *Tshz1*<sup>MNΔ</sup> animals may result from the hypoglossal nucleus and efferent hypoglossal nerve impairment.

### 3.2.5. The phrenic motor column is reduced and phrenic nerve branching is impaired in *Tshz1*<sup>MNΔ</sup> mutants

*Tshz1*<sup>MNΔ</sup> animals gasped and showed respiratory distress. I therefore also analyzed phrenic MNs that control breathing and that express *Tshz1* strongly and persistently (Fig. 3.10-3.13). Axons of phrenic MNs exit the ventral spinal cord and innervate the diaphragm.

At E12.5, phrenic motor neurons are born and can be distinguished from other MNs at the same axial level because they locate between MNs of the lateral and medial motor column, and express *Oct6*. I counted *Isl1*+/*Oct6*+ phrenic MNs in *Tshz1*<sup>MNΔ</sup> and littermate embryos (Fig. 3.10A). At E12.5, I did not observe any difference in phrenic motor neuron counts. Thus, phrenic motor neurons were generated in correct numbers in *Tshz1*<sup>MNΔ</sup> animals.

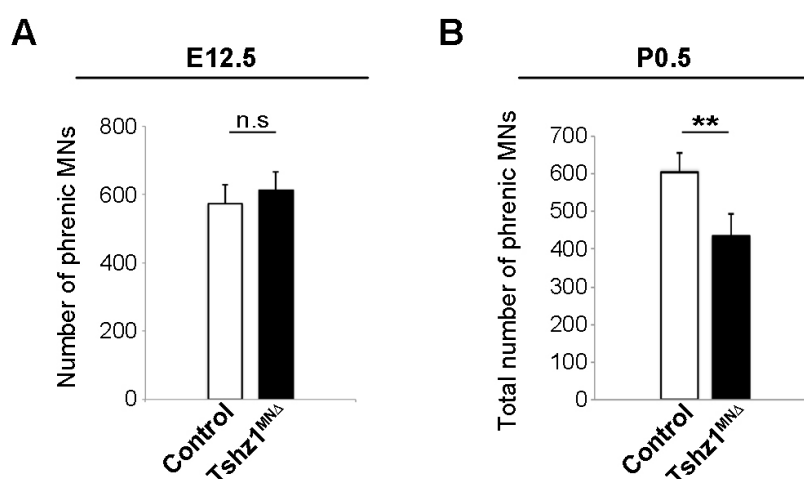


**Figure 3.10 | Phrenic MNs of *Tshz1*<sup>MNΔ</sup> animals are reduced in numbers**

Quantification of phrenic motor neurons that were identified using *Isl1* and *Oct6* antibodies at E12.5 (A), and *ChAT* and *Oct6* antibodies at P0.5 (B). Note that similar numbers of phrenic MNs exist in *Tshz1*<sup>MNΔ</sup> and control animals at E12.5, but at P0.5 the number of phrenic MNs was reduced in *Tshz1*<sup>MNΔ</sup> animals. Data are represented as mean  $\pm$  SD. (t-test, \*\*  $p < 0.01$ , \*  $p < 0.05$ , n.s. not significant)

I investigated whether neurons in the phrenic motor column are present in correct numbers at later stages. I performed co-immunostainings with ChAT (marker of all MNs) and Oct6 (specific marker of phrenic MNs at C3-C5 axial level) antibodies and counted ChAT+/Oct6+ phrenic motor neurons bilaterally on every fourth section at P0.5 (Fig. 3.10B). The number of phrenic MNs was reduced by 28% in *Tshz1*<sup>MNΔ</sup> animals compare to littermates. This result indicates that, similarly to hypoglossal MNs, phrenic MNs were generated in correct numbers (E12.5), but subsequently die which resulted in the reduction of their numbers at P0.5.

Next I examined whether the innervation of the diaphragm by the phrenic nerve was modified. I visualized phrenic nerves using an inducible indicator mouse line that expressed a *Tau-GFP* transgene (*Mapt*<sup>tm2Arbr</sup>; Hippenmeyer et al. 2005) and performed an immunodetection of GFP on diaphragm preparations (Fig. 3.11). The diaphragm innervation pattern is variable in different individuals (personal observations, Laskowski et al. 1991). Overall, phrenic nerves of *Tshz1*<sup>MNΔ</sup> animals were less stained and thus appeared thinner than phrenic nerves in control littermates. In addition, they exhibited a less complex terminal arborization (Fig. 3.11). This is reminiscent of the morphological changes observed in hypoglossal nerves.

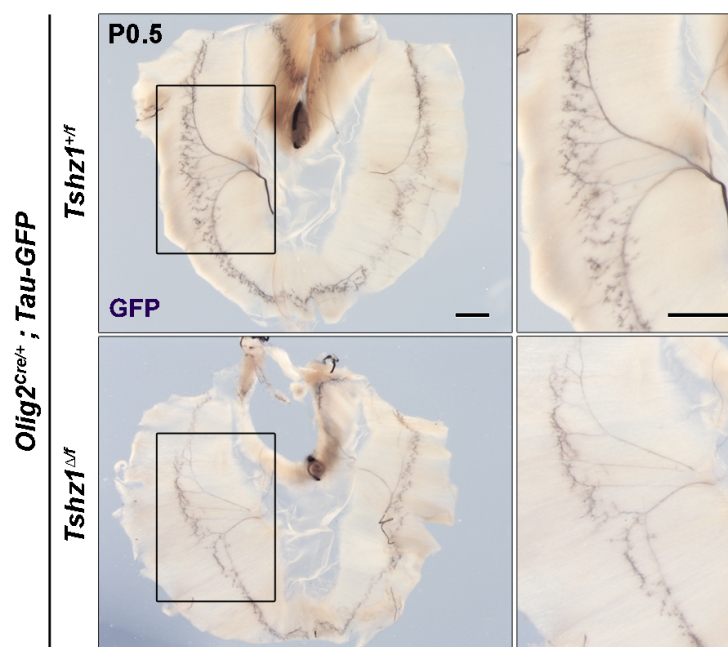


**Figure 3.11 | Disrupted arborization of phrenic MNs in *Tshz1*<sup>MNΔ</sup> animals**

Mice expressing *Tau-GFP* in an inducible manner in MNs were used to visualize phrenic nerves. Phrenic nerves of *Tshz1*<sup>MNΔ</sup> animals had a weaker staining than controls and thus

appeared thinner. Additionally, higher magnification (right panel) of the dorsal branch revealed a change in arborization. Scale bar: 1 mm.

To investigate the diaphragm innervation more precisely, I switched to the *Hb9-GFP* allele (Tg(Hlxb9-GFP)1Tmj; Wichterle et al. 2002) that allowed visualization of terminal branches (Fig. 3.12, 3.13). I did immunohistochemistry stainings on diaphragm preparations using an anti-GFP antibody to increase the intensity of signal. Additionally, I visualized neuromuscular junctions using a snake toxin,  $\alpha$ -bungarotoxin (BTX), which binds irreversibly to nicotinic receptors of acetylcholine on postsynaptic muscle fibers. When reaching the diaphragm, the phrenic nerve divides into three branches: one ventral, one dorsal and one innervating the crus. Innervation patterns differ for each branch, so I analyzed them separately.

I first analyzed the complex arborization of the dorsal branch of the right side of the diaphragm (Fig. 3.12A). Hence, I traced the Hb9-GFP+ nerve with the ImageJ plugin simple neurite tracer. Tracings were done on Z-stack confocal images and raw data were processed using an excel file designed by Dr. Cyril Chéret, a postdoctoral researcher from the laboratory. I defined the primary branch as the dorsal branch of the right phrenic nerve, secondary (order 2) branches to originate from the primary branch and tertiary (order 3) to originate from secondary branches. Phrenic innervation of the diaphragm varies among individual animals and therefore differences between arborization of the phrenic nerve of *Tshz1<sup>MNΔ</sup>* mutants and littermate controls were difficult to quantify. Altogether, tracing analysis validated a mild disorganization of the branching pattern of *Tshz1<sup>MNΔ</sup>* phrenic nerves. The number of larger branches (secondary, tertiary) was decreased in *Tshz1<sup>MNΔ</sup>* phrenic nerves. On the other hand, the number of thinner branches (order 5 to order 7) was increased (Fig. 3.12B). Moreover, the length of the branches was increased in *Tshz1<sup>MNΔ</sup>* animals (Fig. 3.12C) suggesting a precocious defasciculation of motor axons. The length difference between branches of *Tshz1<sup>MNΔ</sup>* and control animals was more pronounced for larger branches (order 2 to order 4). Early defasciculation of the nerve and disorganization of the innervation could reflect a reduction in the number of motor neurons (Huettl et al., 2011; Lin et al., 2000).

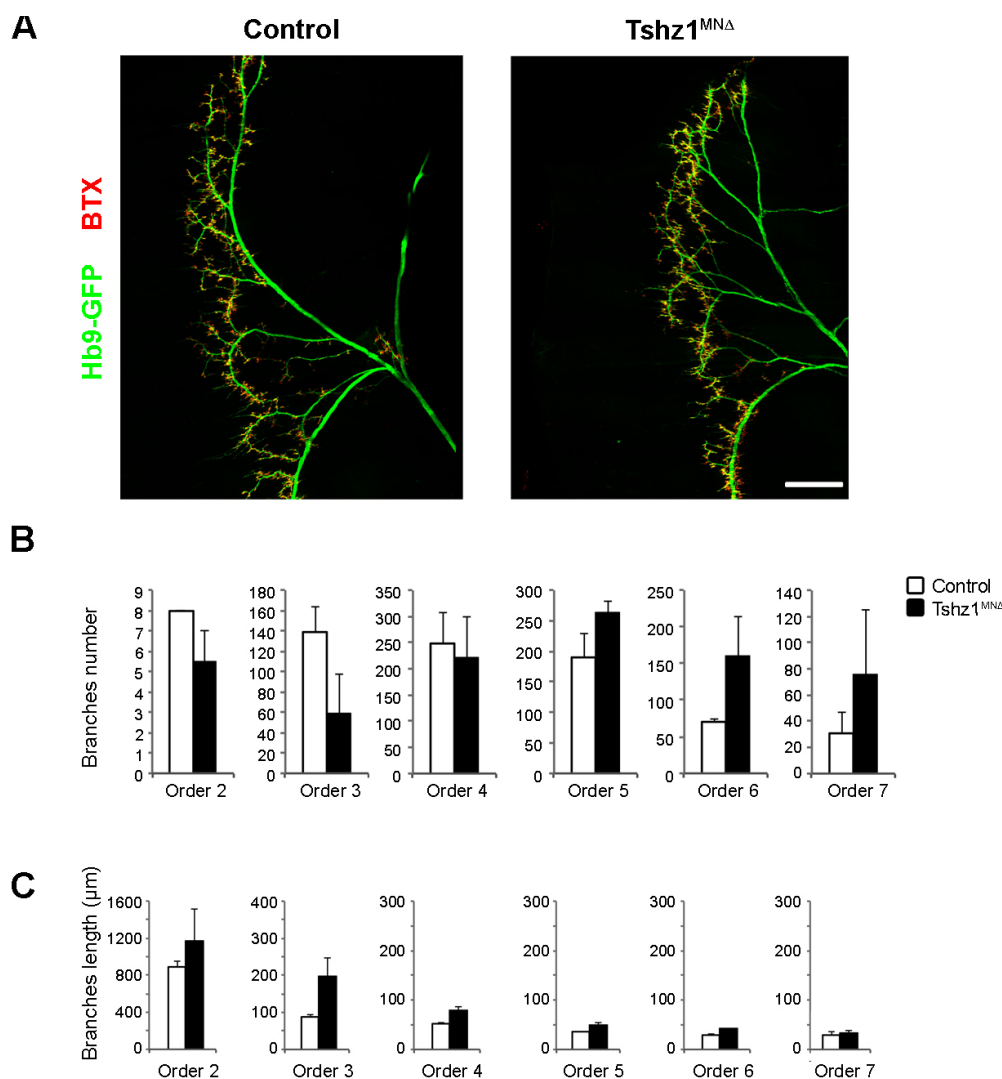


**Figure 3.12 | Branching analysis of the dorsal branch of the right phrenic nerve showed an early defasciculation in *Tshz1*<sup>MNA</sup> animals**

(A) To assess terminal branching of the phrenic nerve, the *Hb9-GFP* allele was used and combined with  $\alpha$ -bungarotoxin staining (BTX). Phrenic nerve is green and BTX is red in the pictures. (B) Quantification of the branching of the dorsal branch of the phrenic nerve revealed a reduction in larger branches (order 2/3) and an increase of higher order branches (order 5/6/7) in *Tshz1*<sup>MNA</sup> animals. (C) In addition, there was an overall elongation of branches length in *Tshz1*<sup>MNA</sup> animals. Scale bar: 500  $\mu$ m. Data are represented as mean  $\pm$  SD.

The ventral branch of the phrenic nerve displays a less complex branching than the dorsal branch. Numerous short secondary branches originate from the ventral branch and do not ramify much. Therefore, I assessed the innervation of the ventral diaphragm by measuring the width of the endplate band that was visualized by  $\alpha$ -bungarotoxin staining (Fig. 3.13A). Width of endplate band was reduced by 32% in *Tshz1*<sup>MNA</sup> compare to control animals ( $248 \pm 12 \mu$ m vs  $168 \pm 38 \mu$ m) (Fig. 3.13B).

Endplate width reduction reflected a shortening of the secondary branches of the ventral phrenic nerve. Altogether, the analysis of the phrenic nerve in *Tshz1<sup>MNΔ</sup>* animals indicated an impaired and reduced branching, which may contribute to the observed breathing problem.

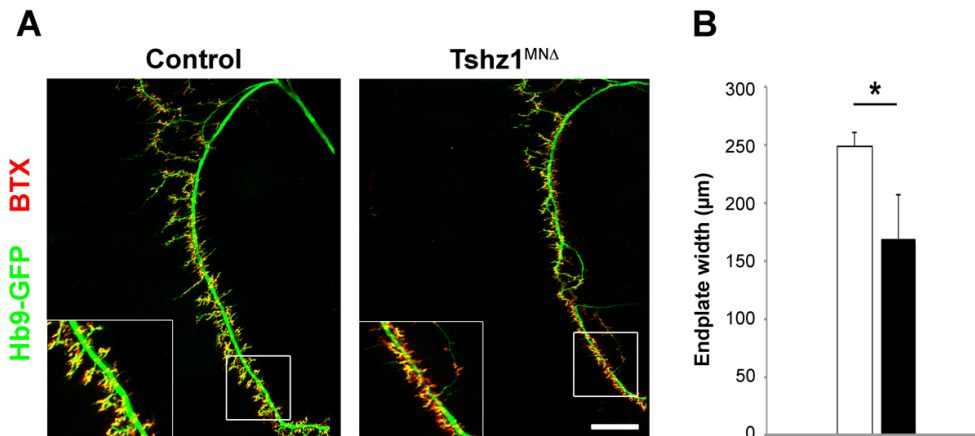


**Figure 3.13 | Endplate width of ventral branch of phrenic nerve in *Tshz1<sup>MNΔ</sup>* animals**

Ventral branch innervation was assessed using *Hb9-GFP allele* (green) and  $\alpha$ -bungarotoxin staining (BTX, red) (A); the width of the endplate was quantified (B). *Tshz1<sup>MNΔ</sup>* animals have a reduced endplate width (32% less than controls). Scale bar: 500  $\mu$ m. Data are represented as mean  $\pm$  SD. (t-test, \*  $p < 0.05$ )

### 3.2.6. Other motor columns are not affected in *Tshz1<sup>MNΔ</sup>* mutants

*Tshz1<sup>MNΔ</sup>* animals did not exhibit a general impairment of motor behavior at birth, and the animals moved and crawled. Expression data indicated that *Tshz1* was transiently expressed in lateral motor columns in the brachial and lumbar spinal cord, which innervate fore- and hindlimbs respectively. Thus, I tested whether these motor columns were affected by the *Tshz1* mutation at P0.5 (Fig. 3.14).

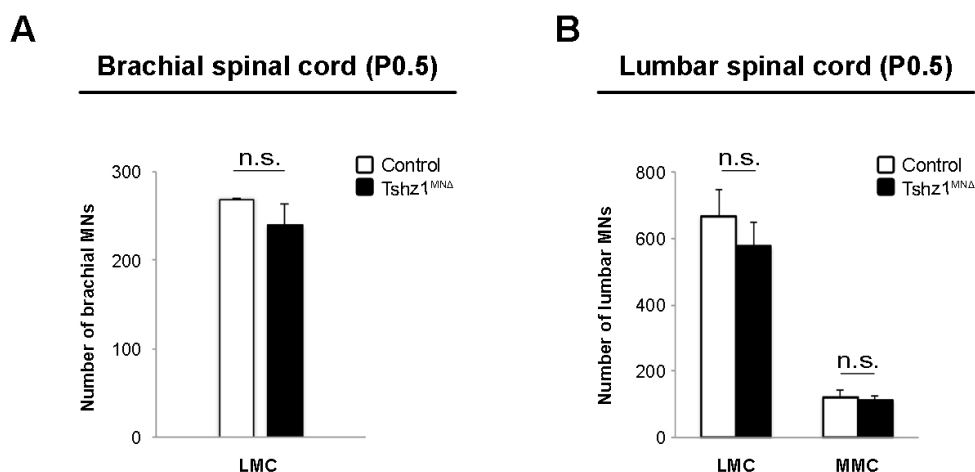


**Figure 3.14 | Analysis of lateral (LMC) and medial motor column (MMC) neurons in *Tshz1<sup>MNΔ</sup>* animals**

Motor neurons of the lateral (LMC) and medial (MMC) motor columns were visualized by immunohistochemistry using ChAT antibody at P0.5. **(A)** In the cervical spinal cord, LMC neurons were counted on serial sections at the phrenic motor column level. Counts showed no difference in LMC MN number between *Tshz1<sup>MNΔ</sup>* and control animals. **(B)** In the lumbar spinal cord, both LMC and MMC neurons were counted. Motor neuron number was similar for *Tshz1<sup>MNΔ</sup>* and control animals for both motor columns. Data are represented as mean  $\pm$  SD. (t-test, n.s. not significant)

Immunohistological analysis of the brachial and lumbar spinal cord allowed visualization of motor neurons by detection of ChAT and characteristic euchromatic nuclei. I counted motor neurons at P0.5 on every fourth section of at least three animals per genotype in the lateral and medial motor columns. In brachial spinal cord, I did not observe a difference in the number of LMC neurons in *Tshz1<sup>MNΔ</sup>* and control animals (Fig. 3.14A). In lumbar spinal cord, I could not detect any difference in MN numbers, neither in the medial nor lateral motor column, between *Tshz1<sup>MNΔ</sup>* and control animals (Fig. 3.14B). My results indicated that the *Tshz1* mutation leads to deficits that are specific for hypoglossal and phrenic motor neurons.

## 4. Discussion

Somatic motor neurons control the contraction of striated muscles. All somatic motor neurons derive from *Olig2*<sup>+</sup> pMN precursors, and settle ventrally in the brainstem and spinal cord. However, somatic motor neurons are diverse: MNs cluster into molecularly distinct motor columns according to the group of muscles they innervate. In addition, MNs that innervate a unique muscle cluster into motor pools and express specific markers (Dasen et al., 2005; Sürmeli et al., 2011). Motor neurons provide a good model to study molecular mechanisms involved in the generation of neuronal diversity during development, because the pools can be identified anatomically, and their output (i.e. axons innervating muscle and the control of muscle contraction) can be easily visualized and recorded.

The *teashirt* gene family of zinc finger transcription factors has been shown to control the specification of several cell types. Teashirt proteins interact with other transcription factors and components of signaling pathways (e.g. *Hox* genes, Wingless/Wnt pathway). In mice, the *Tshz1* gene is strongly expressed in the central nervous system (Caubit et al., 2000) and is required for neuroblast differentiation in the olfactory bulb (Ragancokova et al., 2014). However, its expression and function in motor neurons has not been analyzed. I show here that specific motor neuron populations in the hindbrain and spinal cord express *Tshz1* during development (i.e. hypoglossal, phrenic and lateral motor column MNs). I used conditional mutation of *Tshz1* in somatic motor neurons using the *Olig2*<sup>Cre</sup> allele to demonstrate that *Tshz1* expression in these neurons is required for normal breathing and feeding. *Tshz1* is necessary for survival of hypoglossal and phrenic motor neurons and for correct branching of their axons.

### 4.1. Identification of *Tshz1*-expressing motor neurons

Somatic motor neurons start to arise at E9.5 from the *Olig2*<sup>+</sup> pMN progenitor domain in the ventral hindbrain and spinal cord. When progenitors become postmitotic, they switch on the expression of the transcription factor *Isl1* and switch off the expression of *Olig2*. I performed a triple immunodetection of *Olig2*, *Isl1* and GFP (expressed from a *Tshz1*<sup>GFP</sup> allele) at E10.5. I found that *Tshz1* expression was switched on during development in motor neurons after *Isl1* expression initiated, but was detected

only in MN subpopulations in brachial and lumbar spinal cord as well as defined MNs of the hindbrain.

The identity of motor neurons is essentially defined by their columnar identity: MNs located in the same motor column express the same molecular markers, settle at a stereotypical position in the neural tube, and extend their axons towards the same group of muscles in the periphery. At a specific position along the rostro-caudal axis, columnar identity of MNs can easily be assessed by molecular markers that have been described previously by others (Jessell, 2000; Rousso et al., 2008).

Hypoglossal motor neurons of the hindbrain locate to rhombomeres 7/8 and express *Isl1*, *ChAT* but not *Phox2b*. I detected *Tshz1* expression between E12.5-P0.5 in rhombomeres 7/8, and the *Tshz1*<sup>+</sup> neurons co-expressed *Isl1*, *ChAT* but not *Phox2b*. Thus, subpopulations of hypoglossal motor neurons persistently expressed *Tshz1*. The hypoglossal nerve innervates seven of the eight tongue muscles, and motor neurons innervating a unique muscle (i.e. a motor pool) cluster at a stereotypic position in the hypoglossal nucleus. The myotopic organization in the hypoglossal nucleus has been partially described (Aldes, 1995; Dobbins and Feldman, 1995; McClung and Goldberg, 2002). The distribution of the *Tshz1*<sup>+</sup> neurons in the ventro-lateral hypoglossal nucleus at rostral and median levels indicates these correspond to MNs that innervate the genioglossus extrinsic muscle (Aldes, 1995). Other *Tshz1*-expressing MNs of the hypoglossal nucleus could not be linked to specific motor pools since their anatomical position has not been described. However, their location in the nucleus (illustrated in Fig. 3.2E) indicates that they correspond to neurons innervating intrinsic retrusor and protrusor muscles, and an extrinsic retrusor muscle (cf. Aldes, 1995).

In the cervical spinal cord at C3-C5 levels, phrenic MNs that innervate the diaphragm locate between MNs of the medial and lateral motor columns and express *Isl1*, *ChAT* and *Oct6* (Philippidou et al., 2012). I found that these phrenic MNs persistently expressed *Tshz1* between E12.5 and P0.5.

Finally, in the brachial and lumbar spinal cord, MNs, which innervate the ventral and dorsal limb muscles, locate to the medial (LMCm) and lateral (LMCl) motor column, respectively. *Tshz1* was expressed in both motor columns at brachial and lumbar levels at E12.5, but was expressed transiently in these columns. In summary, I detected persistent *Tshz1* expression in hypoglossal and phrenic MNs, and transient expression in spinal MNs that innervate the limbs. Interestingly, the changes in

development in *Tshz1* mutants were restricted to those MNs that express the factor persistently, i.e. hypoglossal and phrenic MNs.

#### **4.2. *Tshz1* expression in motor neurons is required for feeding and normal breathing**

To understand the function of *Tshz1* in somatic motor neurons, I induced a loss-of-function mutation of *Tshz1* in these neurons using recombination with the *Olig2<sup>Cre</sup>* allele (*Tshz1<sup>MNΔ</sup>*). The use of a *Rosa26R-LacZ* reporter allele confirmed that *Olig2<sup>Cre</sup>* induces recombination only in the central but not the peripheral nervous system. In particular, recombination was introduced in pMN progenitors and their derivatives (MNs and oligodendrocytes) in the hindbrain and spinal cord. *Tshz1* is not expressed in the oligodendrocyte lineage (Dr. Alistair Garratt, personal communication). Therefore, the conditional *Tshz1* mutation can be expected to impinge only on the development of somatic motor neurons.

My observations of newborn animals revealed that *Tshz1<sup>MNΔ</sup>* animals had no milk in their stomach and thus they did not feed. In addition, I observed that they displayed aerophagia (i.e. air in the gastrointestinal tract) and exhibited respiratory distresses reflected in slight cyanosis and gasping. General motor coordination appeared not to be impaired and the newborn *Tshz1<sup>MNΔ</sup>* mutant animals were able to move and crawl. The *Tshz1<sup>MNΔ</sup>* mice died six to seven hours after birth, apparently due to feeding and breathing impairments. The behavioral phenotypes in *Tshz1<sup>MNΔ</sup>* mutants were reminiscent of the ones observed in *Tshz1* null-mutants (*Tshz1<sup>NULL</sup>*). *Tshz1<sup>NULL</sup>* mice did not feed, gasped and their intestines were filled with air bubbles (Coré et al., 2007). However, the aerophagia and the absence of feeding were imputed to malformations of the oral cavity of *Tshz1<sup>NULL</sup>* mice that displayed an absence of the soft palate and malformation of the epiglottis. The soft palate contains muscles and separates the naso- and oropharynx. These two regions are connected during breathing, but the soft palate separates them during swallowing. The epiglottis, a cartilage structure, prevents food and liquid entry into the trachea during swallowing and allows the passage of air through the larynx. *Tshz1* was expressed in the branchial arches but neither in the soft palate nor in the epiglottis. The authors suggested that the oral phenotype was a consequence of the absence of *Tshz1* in the branchial arches that generate the epiglottis and soft palate (Coré et al., 2007).

My data indicate that the absence of feeding and the aerophagia resulted mostly from motor neuron specific deficits, and are not caused by malformation of the oral cavity. My analysis of the *Olig2<sup>Cre/+</sup>; Rosa26R-LacZ* reporter animals demonstrated that recombination did not occur in branchial arches or their derivatives. Furthermore, the histological analyses that I performed demonstrated that the oral cavity of *Tshz1<sup>MNΔ</sup>* animals remained intact.

Accumulation of air in the intestine can be associated with other developmental defects than a cleft palate. For instance, ankyglossia, a congenital malformation that decreases the mobility of the tip of the tongue caused by an unusually short membrane that connects the tongue to the floor of the mouth, was observed in LGR5 mutant mice and was reported to lead to aerophagia (Morita et al., 2004). Thus, changes in tongue mobility can cause such a phenotype.

#### **4.1. *Tshz1* is necessary for survival of hypoglossal motor neurons and correct innervation of the tongue**

Tongue muscles are crucial during breathing and feeding behaviors. During breathing, tongue position and its stiffness allow to keep the airways open (McLoon and Andrade, 2013). The contraction of tongue protruders (i.e. genioglossus, transversus and verticalis tongue muscles) widens the opening of the pharynx. The genioglossus muscle, which is the main protrusive muscle, has a tonic activity that regulates the basal size of the pharynx opening, and a phasic activity (brief and intense) that counterbalances the negative pressures generated by the diaphragm and its contractions during inspiration (Edwards and White, 2011; Fregosi, 2011; McLoon and Andrade, 2013). Tongue retrusors are inactive during normal breathing, but they are crucial for swallowing (McLoon and Andrade, 2013). Various tongue muscles participate in suckling behavior: (1) pups voluntarily protrude their tongue on the nipple (genioglossus muscle); (2) then apply an upward pressure or stroke to the nipple that forces milk excretion (styloglossus and verticalis muscle); (3) finally, they move the bolus/milk toward the back of the tongue to trigger swallowing (intrinsic and hyoglossus muscles) (McLoon and Andrade, 2013).

All tongue muscles, except the palatoglossus, are innervated by the hypoglossal nerve (cranial nerve XII). The hypoglossal nerve divides into a medial and a lateral

branch that innervate protrusive and retrusive muscles, respectively. Studies on neonatal rats established that the innervation of tongue muscles by the hypoglossal nerve is critical for life. Indeed, pups that had a bilateral resection of hypoglossal nerves (either at trunk, medial branch or lateral branch level) failed to suckle milk and did not survive. Unilateral impairments of the medial or lateral hypoglossal nerves led to variable survival rates and revealed that the medial branch of the hypoglossal nerve that innervates protrusive muscles is the most important for milk intake (Fujita et al., 2006; Fukushima et al., 2014). Thus, tongue mobility and feeding deficits can be associated with malfunction of the hypoglossal nerve, and I propose that the morphological changes of the hypoglossal nerve observed in *Tshz1<sup>MNΔ</sup>* mutants might account for their changed behavior.

I examined the integrity of the hypoglossal nucleus of *Tshz1<sup>MNΔ</sup>* mice at different development stages. My data indicate that hypoglossal motor neurons were born in normal number, but many died subsequently by apoptosis. This resulted in a 40% reduction of the number of hypoglossal MNs at P0.5. My results did not reveal whether the hypoglossal MNs that died belonged to specific motor pools, or whether they were located in specific areas of the hypoglossal nucleus.

The death of hypoglossal motor neurons resulted in a thinning of the hypoglossal nerve and, in addition, its branching pattern was changed. It remains unclear whether the branching deficit in *Tshz1<sup>MNΔ</sup>* animals was due to the changed MN numbers or whether *Tshz1* directly controls axonal branching. Nevertheless, the overall reduction of MN numbers in the hypoglossal nucleus and the aberrant patterning of the hypoglossal nerve could explain aerophagia and lack of feeding observed in *Tshz1<sup>MNΔ</sup>* mice.

#### **4.2. *Tshz1* is necessary for the survival of phrenic motor neurons and correct diaphragm innervation**

The diaphragm is a key muscle in breathing. Inspiration is triggered by contraction of the diaphragm, which expands the thoracic cavity and leads to an influx of air into the lung. Expiration occurs when the diaphragm relaxes and the air is passively exhaled. The phrenic nerve innervates the diaphragm and controls its contraction. Several mutant mice (e.g. *Hb9* mutant, *Hox5* mutant) that lack phrenic motor neurons display

a complete absence of innervation of the diaphragm and are unable to inflate their lungs at birth (Philippidou et al., 2012; Yang et al., 2001). I observed that phrenic MNs were reduced in numbers in *Tshz1*<sup>MNΔ</sup> mutants, which might explain the fact that these animals inflated their lungs, but displayed respiratory distress and gasped. I propose that a moderate impairment of the diaphragm innervation could explain this phenotype. In addition, other functional deficits in phrenic MN functions might exist that could contribute to a breathing problem.

During development, motor axons aggregate in bundles and grow toward their target. They defasciculate when they reach the muscle, form smaller axon bundles and, finally, individual axons contact muscle fibers (M Landgraf, Bossing, Technau, & Bate, 1997; Matthias Landgraf, Baylies, & Bate, 1999; Sanes, Reh, & Harris, 2011). Early defasciculation of the nerve can lead to changes in its branching pattern (Huettl et al., 2011; Lin et al., 2000). Defasciculation and branching of the phrenic nerve can be visualized, and branches of the phrenic nerve are well spread over the diaphragm, which allows their tracing and the quantification of branching. My data indicate that phrenic motor neurons were born in correct numbers in *Tshz1*<sup>MNΔ</sup> mutants, but compared to control mice increased numbers died at later stages due to apoptosis (approximately 30% decrease). Differences in the arborization of the phrenic nerve between *Tshz1*<sup>MNΔ</sup> and control animals were difficult to quantify due to variability among individual mice (cf. Laskowski et al., 1991). Analysis of the branching pattern revealed a reduced number of secondary and tertiary branches, increased numbers of higher order branches and longer branches. This suggested that defasciculation of the phrenic nerve into individual motor axons happened prematurely in *Tshz1*<sup>MNΔ</sup> mice. My findings did not allow me to conclude whether branching deficits are indirectly caused by the reduced number of phrenic MNs, or whether *Tshz1* directly functions during nerve defasciculation and axonal branching. Overall, the reduction of phrenic motor neuron numbers and the aberrant branching pattern could explain the respiratory distress and gasps observed in *Tshz1*<sup>MNΔ</sup> mice.

### 4.3. Specific role of *Tshz1* in hypoglossal and phrenic motor neurons

During development, *Tshz1* was expressed by motor neurons of the hypoglossal nucleus and in phrenic and lateral motor columns. However, the *Tshz1* mutation did not affect these motor neuron types in the same manner. *Tshz1*<sup>MNΔ</sup> animals exhibited reduced numbers in hypoglossal and phrenic MNs but survival of MNs of the lateral motor column in the spinal cord was not affected. In addition, the absence of obvious behavioral changes – the mutant animals moved and crawled like the control littermates – indicates that motor neurons of the lateral motor column that control limb movement were functioning. Manfroid and her colleagues previously showed that mouse *Tshz* genes are functionally equivalent, i.e. expression of any of the three mouse *Tshz* rescued the loss-of-function of the *Drosophila Tsh* gene (Manfroid et al., 2004). Expression of *Tshz2* and *Tshz3* in motor neurons has not been assessed. Overlapping expression of the *Tshz* genes in the lateral motor column, but not hypoglossal and phrenic MNs might therefore contribute to the specificity of the observed *Tshz1* phenotype.

In *Drosophila*, Tsh protein interacts with the Hox protein Sex combs reduced, which is the homologue of *Hoxa5* in mouse. In mice, several *Hox* genes have been implicated in the specification of motor neurons. *Hoxa5* and *Hoxc5* are required for phrenic motor neurons, while *Hox6* and *Hox10* are necessary for brachial and lumbar spinal LMC motor neurons, respectively. To date, no *Hox* gene was described to participate in specification of hypoglossal MNs, but *Hox4* and *Hox5* genes are expressed in rhombomere 8 (Guthrie, 2007; Philippidou and Dasen, 2013). It is possible that *Tshz1* binds to specific Hox factors and thus modulates their function during hypoglossal and phrenic motor neuron development.

### 4.4. Perspectives

In *Drosophila*, *Tsh* has been described as a transcriptional repressor that acts as a homeotic factor. Tsh directly binds to the Hox protein Sex combs reduced and to proteins of the Wingless/Armadillo signaling pathway (homologous to Wnt/ $\beta$ -catenin in mouse) (Alexandre et al., 1996; Fasano et al., 1991; Gallet et al.; Röder et al., 1992; Saller et al., 2002; Taghli-Lamalle et al., 2007; Waltzer et al., 2001). Mouse

---

*Tshz* genes are able to rescue a loss-of-function of *Tsh* in *Drosophila*, suggesting that molecular mechanisms of *Tshz* function are conserved during evolution. Therefore, analysis of *Tshz1* target genes might reveal signaling pathways important during motor neuron development.

The motor neuron populations affected by the *Tshz1* mutation are small. Therefore, a detailed molecular analysis of the *Tshz1* function that relies on isolated motor neurons would be fastidious and would require tissue from many animals. I plan to use in the future embryonic stem cell-derived MNs to define *Tshz1* target genes. Embryonic stem cells can be differentiated into motor neurons, and a phrenic identity can be induced by expression of *Hoxa5* and *Oct6* (Machado et al., 2014). Embryonic stem cells that express *Hoxa5* and *Oct6* in an inducible manner were generated in the laboratory of Dr. Lieberam (King's College, London), and I will use them to mutate *Tshz1* using the CRISPR/Cas9 technology (Ran et al., 2013). Comparison of the transcriptome of WT and *Tshz1*<sup>-/-</sup> motor neurons will define *Tshz1* targets, and might unravel functionally important interaction partners during phrenic MN development.

## 5. Summary

Motor neurons (MNs) relay between the central nervous system and muscles, and eventually trigger muscle contraction. Motor neurons cluster in the brainstem and spinal cord according to the target muscles they are innervating. *Tshz1*, a member of the *teashirt* zinc finger family of transcription factors, is strongly expressed in the central nervous system of the mouse during development and adulthood. However, *Tshz1* expression and function during motor neuron development had not been addressed.

I defined the precise spatio-temporal expression pattern of *Tshz1* in hindbrain and spinal motor neurons using *in situ* hybridization and immunological detection of GFP that was expressed from a *Tshz1<sup>GFP</sup>* allele. *Tshz1* was expressed exclusively by postmitotic somatic motor neurons. Hypoglossal and phrenic MNs expressed *Tshz1* strongly and persistently, and MNs of the lateral motor columns in the cervical and lumbar spinal cord expressed *Tshz1* transiently.

Next, I generated mice that lack *Tshz1* specifically in somatic motor neurons (*Olig2<sup>Cre/+</sup>; Tshz1<sup>flox/Δ</sup>*, subsequently called *Tshz1<sup>MNΔ</sup>*). *Tshz1<sup>MNΔ</sup>* pups were born in Mendelian ratio but died on the day of birth. *Tshz1<sup>MNΔ</sup>* pups had no milk in their stomach, air in their gastrointestinal tract and they gasped and were mildly cyanotic. I assessed the integrity of several motor nuclei/columns in *Tshz1<sup>MNΔ</sup>* animals by staining and counting MNs in the hindbrain and spinal cord. Interestingly, the number of motor neurons in the hypoglossal nucleus and in the phrenic motor column, which innervate tongue muscles and the diaphragm, respectively, was reduced at birth. Motor neurons in both nuclei were born in correct number but increased numbers died subsequently by apoptosis. Labeling of the nerves (neurofilament NF200 staining and *Hb9<sup>GFP</sup>* allele) revealed that hypoglossal and phrenic nerves both displayed aberrant branching patterns. The numbers of spinal motor neuronal populations were unaffected by *Tshz1* mutation. Altogether, my results demonstrate that *Tshz1* is required for survival of specific motor neuron subtypes and for the branching of their efferent nerves. I propose that the deficits in these motor neurons cause the changes in feeding and breathing behaviors that are observed in *Tshz1<sup>MNΔ</sup>* mutants.

## 6. Zusammenfassung

Motoneurone sind eine Schaltstelle zwischen dem Zentralnervensystem und der Muskulatur und können die Muskelkontraktion auslösen. Motoneurone sind topologisch organisiert, d.h. sie sind in Gruppen im Hirnstamm und Rückenmark lokalisiert und jede der Gruppen innerviert einen bestimmten Muskel. *Tshz1*, ein Mitglied der *teashirt* Familie von Zinkfinger Transkriptionsfaktoren, wird im Zentralnervensystem der Maus während der Entwicklung und im adulten Stadium stark ausgeprägt. Die Expression und Funktion von *Tshz1* während der Entwicklung der Motoneurone war bisher nicht untersucht worden.

Zuerst habe ich das genaue räumlich-zeitliche Expressionsmuster von *Tshz1* in Motoneuronen des Rhombenzephalons und des Rückenmarks definiert. *Tshz1* ist ausschließlich in postmitotischen somatischen Motoneuronen exprimiert: Motoneurone der hypoglossalen und phrenischen Nerven im Rhombenzephalon bzw. zervikalen Rückenmark exprimieren *Tshz1* stark und persistent. Motoneurone der lateralen Motorsäule im zervikalen und lumbalen Rückenmark exprimieren *Tshz1* transient.

Anschließend haben ich *Tshz1* mutante Mäuse generiert, in denen *Tshz1* spezifisch in somatischen Motoneuronen mutiert wurde (*Olig2*<sup>Cre/+</sup>; *Tshz1*<sup>flox/Δ</sup> Tiere, die im weiteren *Tshz1*<sup>MNΔ</sup> genannt werden). *Tshz1*<sup>MNΔ</sup> Jungtiere wurden im erwarteten mendelschen Verhältnis geboren, starben aber noch am Tag der Geburt. *Tshz1*<sup>MNΔ</sup> Jungtiere hatten keine Milch im Magen und Luft im gastrointestinalen Trakt. Außerdem zeigten sie Schnappatmung und eine bläuliche Körperfarbe. Ich analysierte die Integrität mehrerer Kerne und Säulen von Motoneuronen im Rhombenzephalon und Rückenmark von *Tshz1*<sup>MNΔ</sup> Tieren, in dem ich Motoneurone anfärbte und ihre Anzahl bestimmte. Die Anzahl der Motoneurone im Nucleus hypoglossus und Nucleus phrenicus, welche die Muskeln der Zunge beziehungsweise des Zwerchfells innervieren, waren zum Zeitpunkt der Geburt reduziert. Motoneurone beider Kerne/Säulen wurden in korrekter Anzahl angelegt und starben anschließend. Die Anfärbung der Nerven (Neurofilament NF200 Färbung und *Hb9*<sup>GFP</sup> Allel) zeigte, dass sowohl hypoglossale als auch phrenische Nerven ein verändertes Verzweigungsmuster aufwiesen. Andere Motoneuronpopulationen (laterale Motorsäule des zervikalen und lumbalen Rückenmarks) waren durch die Mutation von *Tshz1* nicht beeinträchtigt.

Zusammen demonstrieren meine Ergebnisse, dass *Tshz1* für das Überleben von spezifischen Subtypen von Motoneuronen notwendig ist und die korrekte Innervation/Verzweigung der entsprechenden efferenten Nerven moduliert. Ich schlage vor, dass die Veränderungen im Säuge- und Atmungsverhalten von *Tshz1* mutanten Tieren durch die Fehlbildung der hypoglossalen und phrenischen Nerven verursacht wird.

---

## 7. References

- Alaynick, W. A., Jessell, T. M. and Pfaff, S. L.** (2011). SnapShot: spinal cord development. *Cell* **146**, 178–178.e1.
- Aldes, L. D.** (1995). Subcompartmental organization of the ventral (protrusor) compartment in the hypoglossal nucleus of the rat. *J. Comp. Neurol.* **353**, 89–108.
- Alexandre, E., Graba, Y., Fasano, L., Gallet, A., Perrin, L., De Zulueta, P., Pradel, J., Kerridge, S. and Jacq, B.** (1996). The Drosophila teashirt homeotic protein is a DNA-binding protein and modulo, a HOM-C regulated modifier of variegation, is a likely candidate for being a direct target gene. *Mech. Dev.* **59**, 191–204.
- Bianchi, A. L., Denavit-Saubié, M. and Champagnat, J.** (1995). Central control of breathing in mammals: neuronal circuitry, membrane properties, and neurotransmitters. *Physiol. Rev.* **75**, 1–45.
- Birnboim, H. C. and Doly, J.** (1979). A rapid alkaline extraction procedure for screening recombinant plasmid DNA. *Nucleic Acids Res.* **7**, 1513–23.
- Bloch-Gallego, E.** (2015). Mechanisms controlling neuromuscular junction stability. *Cell. Mol. Life Sci.* **72**, 1029–43.
- Bonanomi, D. and Pfaff, S. L.** (2010). Motor axon pathfinding. *Cold Spring Harb. Perspect. Biol.* **2**, a001735.
- Briscoe, J. and Ericson, J.** (2001). Specification of neuronal fates in the ventral neural tube. *Curr. Opin. Neurobiol.* **11**, 43–9.
- Burden, S. J.** (1998). The formation of neuromuscular synapses. *Genes Dev.* **12**, 133–148.
- Burgess, R. W., Jucius, T. J. and Ackerman, S. L.** (2006). Motor axon guidance of the mammalian trochlear and phrenic nerves: dependence on the netrin receptor *Unc5c* and modifier loci. *J. Neurosci.* **26**, 5756–66.

- 
- Caubit, X., Core, N., Boned, A., Kerridge, S., Djabali, M. and Fasano, L.** (2000). Vertebrate orthologues of the *Drosophila* region-specific patterning gene *teashirt*. *Mech Dev* **91**, 445–448.
- Caubit, X., Tiveron, M.-C., Cremer, H. and Fasano, L.** (2005). Expression patterns of the three *Teashirt*-related genes define specific boundaries in the developing and postnatal mouse forebrain. *J. Comp. Neurol.* **486**, 76–88.
- Caubit, X., Lye, C. M., Martin, E., Coré, N., Long, D. A., Vola, C., Jenkins, D., Garratt, A. N., Skaer, H., Woolf, A. S., et al.** (2008). *Teashirt 3* is necessary for ureteral smooth muscle differentiation downstream of SHH and BMP4. *Development* **135**, 3301–10.
- Caubit, X., Thoby-Brisson, M., Voituren, N., Filippi, P., Bévengut, M., Faralli, H., Zanella, S., Fortin, G., Hilaire, G. and Fasano, L.** (2010). *Teashirt 3* regulates development of neurons involved in both respiratory rhythm and airflow control. *J. Neurosci.* **30**, 9465–76.
- Cohen, M., Briscoe, J. and Blassberg, R.** (2013). Morphogen interpretation: the transcriptional logic of neural tube patterning. *Curr. Opin. Genet. Dev.* **23**, 423–8.
- Conte, F., Oti, M., Dixon, J., Carels, C. E. L., Rubini, M. and Zhou, H.** (2015). Systematic analysis of copy number variants of a large cohort of orofacial cleft patients identifies candidate genes for orofacial clefts. *Hum. Genet.*
- Cordes, S. P.** (2001). Molecular genetics of cranial nerve development in mouse. *Nat. Rev. Neurosci.* **2**, 611–23.
- Coré, N., Caubit, X., Metchat, A., Boned, A., Djabali, M. and Fasano, L.** (2007). *Tshz1* is required for axial skeleton, soft palate and middle ear development in mice. *Dev Biol* **308**, 407–420.
- Cowan, W. M., Jessell, T. M. and Zipursky, S. L.** (1997). *Molecular and Cellular Approaches to Neural Development*. Oxford University Press.
- Dasen, J. S. and Jessell, T. M.** (2009). Hox networks and the origins of motor neuron diversity. *Curr Top Dev Biol* **88**, 169–200.
- Dasen, J. S., Liu, J.-P. and Jessell, T. M.** (2003). Motor neuron columnar fate imposed by sequential phases of Hox-c activity. *Nature* **425**, 926–33.

- 
- Dasen, J. S., Tice, B. C., Brenner-Morton, S. and Jessell, T. M.** (2005). A Hox regulatory network establishes motor neuron pool identity and target-muscle connectivity. *Cell* **123**, 477–91.
- de Zulueta, P., Alexandre, E., Jacq, B. and Kerridge, S.** (1994). Homeotic complex and teashirt genes co-operate to establish trunk segmental identities in *Drosophila*. *Development* **120**, 2287–96.
- Dekkers, M. P. J., Nikolettou, V. and Barde, Y.-A.** (2013). Cell biology in neuroscience: Death of developing neurons: new insights and implications for connectivity. *J. Cell Biol.* **203**, 385–93.
- Dessaud, E., Yang, L. L., Hill, K., Cox, B., Ulloa, F., Ribeiro, A., Mynett, A., Novitsch, B. G. and Briscoe, J.** (2007). Interpretation of the sonic hedgehog morphogen gradient by a temporal adaptation mechanism. *Nature* **450**, 717–20.
- Dessaud, E., McMahon, A. P. and Briscoe, J.** (2008). Pattern formation in the vertebrate neural tube: a sonic hedgehog morphogen-regulated transcriptional network. *Development* **135**, 2489–2503.
- Dias, J. M., Alekseenko, Z., Applequist, J. M. and Ericson, J.** (2014). Tgfb signaling regulates temporal neurogenesis and potency of neural stem cells in the CNS. *Neuron* **84**, 927–39.
- Dobbins, E. G. and Feldman, J. L.** (1995). Differential innervation of protruder and retractor muscles of the tongue in rat. *J. Comp. Neurol.* **357**, 376–94.
- Edwards, B. A. and White, D. P.** (2011). Control of the pharyngeal musculature during wakefulness and sleep: implications in normal controls and sleep apnea. *Head Neck* **33 Suppl 1**, S37–45.
- Erkner, A., Gallet, A., Angelats, C., Fasano, L. and Kerridge, S.** (1999). The role of Teashirt in proximal leg development in *Drosophila*: ectopic Teashirt expression reveals different cell behaviours in ventral and dorsal domains. *Dev. Biol.* **215**, 221–32.
- Faralli, H., Martin, E., Coré, N., Liu, Q.-C., Filippi, P., Dilworth, F. J., Caubit, X. and Fasano, L.** (2011). Teashirt-3, a novel regulator of muscle differentiation, associates with BRG1-associated factor 57 (BAF57) to inhibit myogenin gene expression. *J. Biol. Chem.* **286**, 23498–510.

- Fasano, L., Roder, L., Core, N., Alexandre, E., Vola, C., Jacq, B. and Kerridge, S.** (1991). The gene teashirt is required for the development of *Drosophila* embryonic trunk segments and encodes a protein with widely spaced zinc finger motifs. *Cell* **64**, 63–79.
- Feenstra, I., Vissers, L. E. L. M., Pennings, R. J. E., Nillessen, W., Pfundt, R., Kunst, H. P., Admiraal, R. J., Veltman, J. A., van Ravenswaaij-Arts, C. M. A., Brunner, H. G., et al.** (2011). Disruption of teashirt zinc finger homeobox 1 is associated with congenital aural atresia in humans. *Am. J. Hum. Genet.* **89**, 813–9.
- Fregosi, R. F.** (2011). Respiratory related control of hypoglossal motoneurons--knowing what we do not know. *Respir. Physiol. Neurobiol.* **179**, 43–7.
- Fujita, K., Yokouchi, K., Fukuyama, T., Fukushima, N., Kawagishi, K. and Moriizumi, T.** (2006). Effects of hypoglossal and facial nerve injuries on milk-suckling. *Int J Dev Neurosci* **24**, 29–34.
- Fukushima, N., Yokouchi, K., Kawagishi, K., Kakegawa, A., Sumitomo, N., Karasawa, M. and Moriizumi, T.** (2014). Quantitative analysis of survival of hypoglossal neurons in neonatally nerve-injured rats: Correlation with milk intake. *Arch Oral Biol* **59**, 616–620.
- Gallet, A., Erkner, A., Charroux, B., Fasano, L. and Kerridge, S.** Trunk-specific modulation of wingless signalling in *Drosophila* by teashirt binding to armadillo. *Curr. Biol.* **8**, 893–902.
- Gallet, A., Angelats, C., Erkner, A., Charroux, B., Fasano, L. and Kerridge, S.** (1999). The C-terminal domain of armadillo binds to hypophosphorylated teashirt to modulate wingless signalling in *Drosophila*. *EMBO J.* **18**, 2208–17.
- Garcia, N. V. D. M. and Jessell, T. M.** (2008). Early Motor Neuron Pool Identity and Muscle Nerve Trajectory Defined by Postmitotic Restrictions in Nkx6.1 Activity. *Neuron* **57**, 217–231.
- Garcia, A. J., Zanella, S., Koch, H., Doi, A. and Ramirez, J.-M.** (2011). Chapter 3--networks within networks: the neuronal control of breathing. *Prog. Brain Res.* **188**, 31–50.

- 
- Gaufo, G. O., Thomas, K. R. and Capecchi, M. R.** (2003). Hox3 genes coordinate mechanisms of genetic suppression and activation in the generation of branchial and somatic motoneurons. *Development* **130**, 5191–201.
- Goulding, M.** (2009). Circuits controlling vertebrate locomotion: moving in a new direction. *Nat. Rev. Neurosci.* **10**, 507–18.
- Gouti, M., Metzis, V. and Briscoe, J.** (2015). The route to spinal cord cell types: a tale of signals and switches. *Trends Genet.* **31**, 282–9.
- Guthrie, S.** (2007). Patterning and axon guidance of cranial motor neurons. *Nat Rev Neurosci* **8**, 859–871.
- Harland, R.** (2000). Neural induction. *Curr. Opin. Genet. Dev.* **10**, 357–362.
- Helms, A. W. and Johnson, J. E.** (2003). Specification of dorsal spinal cord interneurons. *Curr. Opin. Neurobiol.* **13**, 42–9.
- Hippenmeyer, S., Vrieseling, E., Sigrist, M., Portmann, T., Laengle, C., Ladle, D. R. and Arber, S.** (2005). A developmental switch in the response of DRG neurons to ETS transcription factor signaling. *PLoS Biol* **3**, e159.
- Hua, Z. L., Smallwood, P. M. and Nathans, J.** (2013). Frizzled3 controls axonal development in distinct populations of cranial and spinal motor neurons. *Elife* **2**, e01482.
- Huetli, R.-E., Soellner, H., Bianchi, E., Novitch, B. G. and Huber, A. B.** (2011). Npn-1 contributes to axon-axon interactions that differentially control sensory and motor innervation of the limb. *PLoS Biol.* **9**, e1001020.
- Jessell, T. M.** (2000). Neuronal specification in the spinal cord: inductive signals and transcriptional codes. *Nat. Rev. Genet.* **1**, 20–9.
- Kanning, K. C., Kaplan, A. and Henderson, C. E.** (2010). Motor neuron diversity in development and disease. *Annu. Rev. Neurosci.* **33**, 409–40.
- Kiehn, O.** (2006). LOCOMOTOR CIRCUITS IN THE MAMMALIAN SPINAL CORD.
- Kühl, M.** (2003). *Wnt Signaling in Development*. Springer Science & Business Media.

- 
- Laskowski, M. B., Norton, A. S. and Berger, P. K.** (1991). Branching patterns of the rat phrenic nerve during development and reinnervation. *Exp. Neurol.* **113**, 212–20.
- Lieberam, I., Agalliu, D., Nagasawa, T., Ericson, J. and Jessell, T. M.** (2005). A Cxcl12-CXCR4 chemokine signaling pathway defines the initial trajectory of mammalian motor axons. *Neuron* **47**, 667–79.
- Lin, W., Sanchez, H. B., Deerinck, T., Morris, J. K., Ellisman, M. and Lee, K. F.** (2000). Aberrant development of motor axons and neuromuscular synapses in erbB2-deficient mice. *Proc. Natl. Acad. Sci. U. S. A.* **97**, 1299–304.
- Lin, W., Burgess, R. W., Dominguez, B., Pfaff, S. L., Sanes, J. R. and Lee, K. F.** (2001). Distinct roles of nerve and muscle in postsynaptic differentiation of the neuromuscular synapse. *Nature* **410**, 1057–64.
- Lowe, A. A.** (1980). The neural regulation of tongue movements. *Prog Neurobiol* **15**, 295–344.
- Machado, C. B., Kanning, K. C., Kreis, P., Stevenson, D., Crossley, M., Nowak, M., Iacovino, M., Kyba, M., Chambers, D., Blanc, E., et al.** (2014). Reconstruction of phrenic neuron identity in embryonic stem cell-derived motor neurons. *Development* **141**, 784–94.
- Manfroid, I., Caubit, X., Kerridge, S. and Fasano, L.** (2004). Three putative murine Teashirt orthologues specify trunk structures in *Drosophila* in the same way as the *Drosophila* teashirt gene. *Development* **131**, 1065–1073.
- Martin, E., Caubit, X., Airik, R., Vola, C., Fatmi, A., Kispert, A. and Fasano, L.** (2013). TSHZ3 and SOX9 regulate the timing of smooth muscle cell differentiation in the ureter by reducing myocardin activity. *PLoS One* **8**, e63721.
- Mathies, L. D., Kerridge, S. and Scott, M. P.** (1994). Role of the teashirt gene in *Drosophila* midgut morphogenesis: secreted proteins mediate the action of homeotic genes. *Development* **120**, 2799–809.
- McClung, J. R. and Goldberg, S. J.** (2002). Organization of the hypoglossal motoneurons that innervate the horizontal and oblique components of the genioglossus muscle in the rat. *Brain Res.* **950**, 321–324.

- 
- McLoon, L. K. and Andrade, F. eds.** (2013). *Craniofacial Muscles; Chapter 12*. New York, NY: Springer New York.
- Morita, H., Mazerbourg, S., Bouley, D. M., Luo, C.-W., Kawamura, K., Kuwabara, Y., Baribault, H., Tian, H. and Hsueh, A. J. W.** (2004). Neonatal lethality of LGR5 null mice is associated with ankyloglossia and gastrointestinal distension. *Mol. Cell. Biol.* **24**, 9736–43.
- Pan, D. and Rubin, G. M.** (1998). Targeted expression of teashirt induces ectopic eyes in *Drosophila*. *Proc. Natl. Acad. Sci. U. S. A.* **95**, 15508–12.
- Philippidou, P. and Dasen, J. S.** (2013). Hox Genes: Choreographers in Neural Development, Architects of Circuit Organization. *Neuron* **80**, 12–34.
- Philippidou, P., Walsh, C. M., Aubin, J., Jeannotte, L. and Dasen, J. S.** (2012). Sustained Hox5 gene activity is required for respiratory motor neuron development. *Nat. Neurosci.*
- Ragancokova, D., Rocca, E., Oonk, A. M., Schulz, H., Rohde, E., Bednarsch, J., Feenstra, I., Pennings, R. J., Wende, H. and Garratt, A. N.** (2014). TSHZ1-dependent gene regulation is essential for olfactory bulb development and olfaction. *J Clin Invest* **124**, 1214–1227.
- Ran, F. A., Hsu, P. D., Wright, J., Agarwala, V., Scott, D. a and Zhang, F.** (2013). Genome engineering using the CRISPR-Cas9 system. *Nat. Protoc.* **8**, 2281–308.
- Raum, J. C., Soleimanpour, S. A., Groff, D. N., Coré, N., Fasano, L., Garratt, A. N., Dai, C., Powers, A. C. and Stoffers, D. A.** (2015). Tshz1 Regulates Pancreatic  $\beta$ -Cell Maturation. *Diabetes* **64**, 2905–2914.
- Röder, L., Vola, C. and Kerridge, S.** (1992). The role of the teashirt gene in trunk segmental identity in *Drosophila*. *Development* **115**, 1017–33.
- Rousso, D. L., Gaber, Z. B., Wellik, D., Morrissey, E. E. and Novitch, B. G.** (2008). Coordinated actions of the forkhead protein Foxp1 and Hox proteins in the columnar organization of spinal motor neurons. *Neuron* **59**, 226–40.

- 
- Saiki, R., Scharf, S., Faloona, F., Mullis, K., Horn, G., Erlich, H. and Arnheim, N.** (1985). Enzymatic amplification of beta-globin genomic sequences and restriction site analysis for diagnosis of sickle cell anemia. *Science* (80- ). **230**, 1350–1354.
- Saller, E., Kelley, A. and Bienz, M.** (2002). The transcriptional repressor Brinker antagonizes Wingless signaling. *Genes Dev.* **16**, 1828–38.
- Santos, J. S., Fonseca, N. A., Vieira, C. P., Vieira, J. and Casares, F.** (2010). Phylogeny of the teashirt-related zinc finger (tshz) gene family and analysis of the developmental expression of tshz2 and tshz3b in the zebrafish. *Dev. Dyn.* **239**, 1010–8.
- Soriano, P.** (1999). Generalized lacZ expression with the ROSA26 Cre reporter strain. *Nat. Genet.* **21**, 70–1.
- Sürmeli, G., Akay, T., Ippolito, G. C., Tucker, P. W. and Jessell, T. M.** (2011). Patterns of spinal sensory-motor connectivity prescribed by a dorsoventral positional template. *Cell* **147**, 653–65.
- Taghli-Lamalle, O., Gallet, A., Leroy, F., Malapert, P., Vola, C., Kerridge, S. and Fasano, L.** (2007). Direct interaction between Teashirt and Sex combs reduced proteins, via Tsh's acidic domain, is essential for specifying the identity of the prothorax in *Drosophila*. *Dev. Biol.* **307**, 142–51.
- Waltzer, L., Vandel, L. and Bienz, M.** (2001). Teashirt is required for transcriptional repression mediated by high Wingless levels. *EMBO J.* **20**, 137–45.
- Wichterle, H., Lieberam, I., Porter, J. A. and Jessell, T. M.** (2002). Directed differentiation of embryonic stem cells into motor neurons. *Cell* **110**, 385–397.
- Wu, H., Xiong, W. C. and Mei, L.** (2010). To build a synapse: signaling pathways in neuromuscular junction assembly. *Development* **137**, 1017–33.
- Yamamoto, Y. and Henderson, C. E.** (1999). Patterns of programmed cell death in populations of developing spinal motoneurons in chicken, mouse, and rat. *Dev. Biol.* **214**, 60–71.

- 
- Yang, X., Arber, S., William, C., Li, L., Tanabe, Y., Jessell, T. M., Birchmeier, C. and Burden, S. J.** (2001). Patterning of muscle acetylcholine receptor gene expression in the absence of motor innervation. *Neuron* **30**, 399–410.

## **8. Eidesstattliche Erklärung**

Hiermit versichere ich, die vorliegende Dissertation selbstständig und ohne unerlaubte Hilfe angefertigt zu haben.

Bei der Verfassung der Dissertation wurden keine anderen als die im Text angegebenen Quellen und Hilfsmittel verwendet.

Ein Promotionsverfahren wurde zu keinem früheren Zeitpunkt an einer anderen Hochschule oder bei einem anderen Fachbereich beantragt.

Berlin, den 21.12.2015

Charlotte Chaimowicz